國立臺灣大學醫學院藥理學研究所

博士論文

Graduate Institute of Pharmacology

College of Medicine

National Taiwan University

Doctoral Dissertation

探討 vincristine-vorinostat 合併使用與

微管抑制劑 MPT0B392 之抗癌機轉

及 eIF4E binding protein 1 在癌症中的重要性

Anticancer mechanisms of vincristine-vorinostat combination

and a tubulin-binding agent MPT0B392,

and the role of eIF4E binding protein 1 in cancer patients

趙敏吾

Min-Wu Chao

指導老師：鄧哲明 博士，潘秀玲 博士

Advisor：Che-Ming Teng, Ph.D., Shiow-Lin Pan, Ph.D.

中華民國 104 年 7 月

July 2015

# Contents

# 國立臺灣大學博士學位論文
# 口試委員會審定書

探討 vincristine-vorinostat 合併使用

與微管抑制劑 MPT0B392 之抗癌作用機轉

及 eIF4E binding protein 1 在癌症中的重要性

Acticancer mechanisms of vincristine-vorinostat combination

and a tubulin-binding agent MPT0B392,

and the role of eIF4E binding protein 1 in cancer patients

本論文係趙敏吾君（D98443001）在國立臺灣大學藥理學研究所完成之博士學位論文，於民國 104 年 7 月 17 日承下列考試委員審查通過及口試及格，特此證明

口試委員：　　　_鄧哲明_____（指導教授）

　　　　　　　　_陸青吟_____（指導教授）

　　　　　　　　_顏茂雄_____

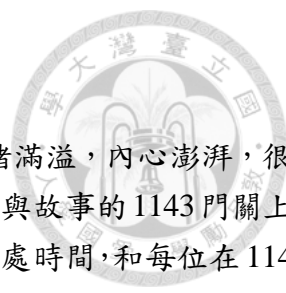　　　　　　　　_楊春茂_____

　　　　　　　　_黃德富_____

　　　　　　　　_蕭哲志_____


所　　長：　　　_林琬琬_____

I

# 致謝

　　當口試進行到最後致謝時，所有八年在實驗室的各種回憶和情緒滿溢，內心澎湃，很高興能替 鄧哲明老師在臺灣大學的學術生涯畫下完美句點，將充滿回憶與故事的 1143 門關上。這八年待在實驗室的時間很長，長過在家休息的時間，長過與家人的相處時間，和每位在 1143、1149、1151 成長茁壯的學長學姊學弟學妹們都有過深刻的情感，有歡笑、有淚水、有一起奮鬥與努力的痕跡。每一天都感謝著 鄧哲明老師當初的選擇，讓我有機會在老師的庇護下無止盡的學習，學習著老師處事的寬大胸襟，學習著老師對生技產業的熱忱，學習著老師對後輩的不吝提攜，因為老師的支持與鼓勵，讓我在美國兩年裡不論是視野或是心境上都趨成熟且斬獲甚多。感謝老師一輩子的心靈支柱-美麗大方的師母，謝謝貼心及細心的您對我們呵護備至，從親手做的鳳梨酥與小禮物，到費心的挑選相框，裝載著我們一幅幅幸福的笑臉。感謝充滿著自信、開朗與樂觀的阿潘學姊，從我小碩一拉拔到博士班畢業，您總是能把在實驗中迷惘且載浮載沉的我一把拉起，給予我強大的信心，繼續努力向前。感謝美國俄亥俄州大學的 陳慶士老師，因為您的教導和啟發，讓我在兩年裡得到許多寶貴的經驗與思考能力。感謝北醫大 劉景平老師與 鄭雅雯老師，對於本篇論文都給予極大的幫助。感謝各位口試委員 顏茂雄老師、 黃德富老師、 楊春茂老師和 蕭哲志老師的不吝指教，讓本論文能更臻完善。

　　感謝藥理所的所有師長們，因為有您們的指導與訓練，才有更出色的我。最親切所辦公室的梁姐姐和沈姐姐，謝謝您們的幫忙和叮嚀，讓我順利的完成每個階段性任務。謝謝永遠是 1143 台柱的雅玲學姊，學姐乾脆俐落且剛正不阿的處事精神，使實驗室一切井然有序，除了讓我毫無後顧之憂的研究也是我們牡羊座的最佳典範，最後一起在 1143 的日子，有種相依為命之感。謝謝美麗又幸福的姿璇學姊，正努力學習妳那豁達的人生觀與聰明的完成每件事的態度。外表優雅卻個性調皮的婕妤學姐，謝謝妳的巧手，讓實驗室電腦周邊所有問題迎刃而解。謝謝士維學長的耳提面命，我會努力走出自己的小圈圈，多和校友們聯誼，拓展自己的眼界。感謝劉董的愛之深責之切，總是能一針見血的突破我的盲點。聰明且對研究充滿熱忱的輝隆學長，謝謝你在實驗方向與思考的提點以及在美國時辛苦開車帶著我們東奔西跑。感謝細心又貼心的岸祈學姊，妳送的乳木油陪我度過嚴寒又乾燥的 OSU 冬天，與妳聊天總是能讓我有不同的思考模式。謝謝刀子口豆腐心的思穎學姊，希望常常放空的我能夠像妳一樣永遠的心思敏捷，祝妳在玩樂天堂的加州一切都好。感謝帶我入門的俊翰學長，最喜歡看你細心且仔細地做著每個實驗，讓我學習專注在每個實驗的小細節上。美全學姊爽朗又幽默的說話方式與聰穎的處事態度，有一種讓人無法離開視線的魔力，學姊和學長間的成熟互動也一直是情緒性的我努力看齊的目標。謝謝從碩士班起就是我最佳 msn 好友張 cc，陪伴我度過許多情緒起伏的日子，幫助我解決實驗的煩惱，懷念一起八卦的日子，無法習慣沒有妳在的 1143，有妳在真好！最親愛的賴清清相好，很高興認識妳這聰慧的親密好友，對於我們天馬行空假設性的問題，永遠有說不完的話題，想念妳真誠的擁抱。謝謝心思細膩的小白常和我分享妳心裡深層的感受，希望我們能夠為彼此都帶來正面力量。說話永遠溫柔的王之之，

希望妳能早日達成做貴婦醫師娘的夢想，相信聰明卻謙虛的佑維，一定能夠實現妳的願望，祝你們永遠幸福快樂！想念我的牡羊座好夥伴耙子，活潑率真卻感性的妳總是能把每件事整理的有條不紊，好懷念妳的長手長腳，豐富的肢體語言。感謝在美國努力的憶萩，因為有妳盡心盡力的熱心幫忙，一次又一次解決我們在美國遭遇的困難，想念小銀載著我們遊遍美國大小州的美好時光。謝謝好脾氣又無止盡付出的瀚立，包容我和杜奶奶的任性，常常讓妳處在一個尷尬的局面，還是很懷念美國住在一起的時光，一起出門，一起回家，一起煮飯，一起分享心情，是永遠不會忘的回憶。外表和個性衝突卻哭點很低的鍾珺，超級欣賞有原則的妳，不因外在環境而妥協的輕易改變自己。謝謝嘴巴永遠抹著蜜糖的小精明雅琪，總是在妳的話裡找到自信。單純卻有想法的惠暄，相信喜歡解決困難的妳，可以完成妳在美國的驕傲。謝謝熱情又好客的土雞城小開嘉華，看似愛玩的你卻有份孝順的心思。超級認真無比的俊瑋和子涵，謝謝你們最後這一年的陪伴，讓實驗室不再孤單。謝謝曾陪著我一起擠在 1151 桌子上的瑞陵和情色界三八天后琪琪，我們永遠是美食的追尋者。感謝一直為實驗室及動物實驗默默付出的助理們：優雅卻搞笑的楊 Demi，美麗又溫和的 Anita，甜到無法直視的幸蓉，文靜卻有想法的思淨，屁股愛搖來搖去偽靦腆的于傑，最最可愛的怡琳，沒有你們的幫助就不會有這篇完整的論文。謝謝串門子的阮惇惇，想念我們一起聊天運動的日子。

感謝在美國實驗室的大家：熱心的筱菁學姊，替我們解決許多不論是生活上或是實驗上遇到的窘境和瓶頸。神手志謙，真的沒有你做不出的實驗，請受小女子一拜。無私奉獻且無心機的羿如學姊，宛如大姊姊般的照顧著大家。聲音溫柔卻堅定的明臻學姊，謝謝妳探索美食和實驗上的建議。謝謝柏廷，願意開著車帶大家東奔西跑。喜歡和裕洲宥庭夫婦聊運動，聊美食，聊韓劇，期待你們每一次的回臺之聚。愛耍帥的俊升，和你的革命情感一直都在！謝謝恩旗、柏政和 Sam 在生化技術和動物實驗上的幫助。瑋凌、家憲、santoshi 和張老師，美國生活因你們而精彩！謝謝一直陪伴在我身邊的好朋友們，你們的默默加油，使我能夠順利完成學位。

最後，感謝一直給予支持鼓勵和無條件付出的最親愛家人們，謝謝你們以寬容的心體諒我，只為了讓我毫無保留的追求理想，成為我最堅強的後盾。謝謝一輩子的知己-皇儒，九年來時時刻刻在身旁的守護，陪我走過每個酸甜苦辣的日子，分享我的喜怒哀樂，研究的生活因為有你而不孤單。

謹以最誠摯與感恩的心，獻上此篇論文給所有關心與愛護我的每一位予以惠存，因為有您們，才有今天的我，謝謝！

# Abbreviations

| | |
|---|---|
| 4E-BP1 | 4E-binding protein 1 |
| Ac-Histone | Acetylated Histone 3 |
| Ac-α-tubulin | Acetylated-α-tubulin |
| AML | Acute myeloid leukemia |
| ALL | Acute lymphoblastic leukemia |
| Bcl-2 | B cell lymphoma-2 |
| Bcl-xl | B-cell lymphoma-extra large |
| Bid | BH3 interacting domain death agonist |
| DMSO | Dimethyl sulfoxide |
| DTT | Dithiothreitol |
| ECL | Enhanced chemiluminescene |
| eIF | Eukaryotic initiation factors |
| ELISA | Enzyme-linked immunosorbent assay |
| FBS | Fetal bovine serum |
| HDAC | Histone deacetylase |
| HIF | Hypoxia-inducible factor |
| HRE | Hypoxia responsive element |
| HUVEC | Human umbilical vein endothelial cell |
| IgG | Immunoglobulin |
| IRES | Internal ribosome entry site |
| JNK | c-Jun N-teminal kinase |
| MAPK | Mitogen-activated protein kinase |
| Mcl-1 | Myeloid cell leukemia sequence 1 |
| MPM2 | Mitotic phosphoprotein monoclonal-2 |
| MTT | 3-（4,5-Dimethylthiazol-2-yl）-2,5-diphenyl-tetrazolium |
| mTOR | The mammalian target of rapamycin |
| mRNA | Messenger ribonucleic acid |
| p70S6K | Ribosome protein s6 kinase |
| PARP | Poly (ADP-ribose) polymerase |
| PBS | Phosphate-buffered saline |
| P-gp | P-glycoprotein |

| | |
|---|---|
| PI | Propidium iodide |
| PMSF | Phenylmethane sulphonyl fluoride |
| PVDF | Polyvinylidene defluoride |
| SAHA | Suberanilohydroxamic acid (vorinostat) |
| S.C | Subcutaneous |
| SCID | Severe combined immunodeficient |
| SDS | Sodium dodecyl sulphate |
| TEMED | N, N, N, N, tetramethylethylene diamine |
| Tris | Tris-（hydroxymethyl）aminomethane |
| qRT-PCR | quantitative reverse-transcriptase polymerase chain reaction |

# 中文摘要

目前最新的世界衛生組織統計，癌症是世界上致死率與發病率的主要原因之一，在 2012 年有八百二十萬的人口死於癌症相關疾病，且預測在未來的 20 年裡，新的案例會以每年成長 57% 的速率增加。而且根據台灣衛生福利部的統計結果，在過去的三十年裡，癌症在台灣的十大死因中始終位於首位。尋求理想的合併療法以降低抗癌藥物的毒性和減少抗藥性的產生，發展新的小分子藥物來改善目前臨床上抗癌藥物使用的瓶頸，以及建立重要的癌症預後因子並根據其研發新穎的分子標拔藥物一直是治療癌症的最終目標。在此篇論文中，我們將研究 (1) vincristine 和 vorinostat 合併使用在人類急性淋巴性白血病的作用機轉，(2) 探討 MPT0B392 在人類急性白血病中的抗癌機轉，和 (3) 評估 eIF4E binding protein 1 (4E-BP1) 對於人類大腸直腸癌在臨床上的重要性。

Vincristine 是一種傳統的微管抑制劑，在臨床上常用於治療急性淋巴性白血病的合併療法中；vorinostat，俗稱 SAHA，是第一個被 FDA 認可使用在 T 細胞淋巴瘤的廣泛型組織蛋白去乙醯酶抑制劑 (HDAC inhibitor)。在此論文的第一部分中，我們將著重 vincristine 和 vorinostat 合併使用之抗白血病機轉探討，由實驗結果發現當合併使用 vincristine 和 vorinostat 後使得白血病細胞加成性的停留在 $G_2M$ 期，並隨之明顯地累積在 $subG_1$ 期；低濃度的 vincristine 會影響微管的動態平衡，在加入 vorinostat 之後會增加此現象，主要是因為 vorinostat 會藉由抑制 HDAC6 的活性因而促進微管蛋白的乙醯化進而使得微管的動態平衡改變；且在當我們併用 vincristine 和 HDAC6 專一性抑制劑 (tubastatin A 和 Acy1215) 也觀察到此加成的現象。除此之外，vincristine-vorinostat 的合併使用在小鼠體內異種移植的動物實驗中也具有較佳

的療效且耐受性良好。根據這些結果，合併使用微管抑制劑和組織蛋白去乙醯酶抑制劑可以做為臨床上治療急性淋巴性白血病的基礎概念。

在第二部分中，我們探討一個全新可口服的 quinoline 衍生物-MPT0B392 (B392) 在急性白血病的抗癌機轉。B392 會使得人類急性白血球細胞滯留在 $G_2M$ 期，但最終還是會進行細胞凋亡，從小鼠異體移植的切片染色得知，投與 B392 會增加 cleavage-caspase 3 的表現。B392 也會抑制微管的聚合作用，並且不會影響 P-gp 的活性，同時會活化 mitotic spindle checkpoint 以及 c-Jun-N-terminal-kinase (JNK)，而 JNK 的磷酸化會進一步流失粒線體的膜電位以及各種 caspases 的活化和 PARP cleavage。另外，我們也發現 B392 在對 sirolimus (mTOR 抑制劑) 具有抗性的細胞中會增強 sirolimus 的細胞毒性。因此，由以上結果可知，不論是單獨使用或是合併療法，B392 是個具有發展潛力的抗白血病藥物。

4E-BP1 (eIF4E binding protein 1) 在 cap-dependent 以及 cap-independent 轉譯的路徑中扮演著關鍵的調控角色，也因此控制了蛋白質的生合成。在第三部分，我們認為 4E-BP1 在大腸直腸癌中是個重要的預後因子。在人類大腸直腸癌細胞株與癌化的組織中 4E-BP1 蛋白質的表現量遠高於正常的大腸細胞株和組織，且藉由分析臨床病人的病理參數發現 4E-BP1 蛋白的表現量與疾病進程具有統計上的相關性。在缺氧的情況下，4E-BP1 在 cap-independent 轉譯過程中更顯重要；此外，cryptopleurine 衍生物 YXM110 也已被證實會藉由抑制 4E-BP1 的表現來達到腫瘤抑制作用，因此，我們更進一步去研究在缺氧情況下 YXM110 抑制蛋白質生合成的情況。由結果得知，YXM110 可以經由抑制 HIF-1α 蛋白的表現進而調控 VEGF 的轉錄。總結來說，4E-BP1 在大腸直腸癌物中是具有前瞻性的預測指標，而 YXM110 則具有潛力研發成新的標靶抗癌藥物。

此篇論文中，我們探討了不同方向的抗癌治療策略，包括: vincristine 和 vorinostat 的合併療法，MPT0B392 單一化學療法和確立 4E-BP1 為新的預後因子，希冀這些結果與發現能夠實際應用於臨床上。

# Abstract

Cancer is the leading causes of mortality and morbidity worldwide with approximately 8.2 million cancer related deaths in 2012 and is expected that annual new cases will rise 57% within the next two decades as reported by World Health Worldwide. According to the statistics from Taiwan's Ministry of Health and Welfare, cancer has taken the first position in causes of death in Taiwan in the past three decades. Searching for the optimal combination therapeutic approaches to decrease drugs toxicities and resistance, developing novel small molecular agents to improve current treatments and identifying the important prognostic factors to design the targeted therapies are our ultimate goals of eliminating cancers. In this thesis, we investigated (1) the effect of vincristine-vorinostat combination on human acute lymphoblastic leukemia (ALL), (2) the mechanism underlying anticancer activity of MPT0B392 on human acute leukemia and (3) the clinical importance of eIF4E binding protein 1 (4E-BP1) on human colorectal cancer (CRC).

Vincristine, a traditional microtubule-depolymerizing agent, is one of combination chemotherapy drugs used in treatment of ALL; vorinostat, also called SAHA, was the first approved pan-HDAC inhibitor for T cell lymphoma. In the first study, we investigated the vincristine and vorinostat combined effect and the underlying antileukemic mechanism. Our data showed that combination of vincristine and vorinostat induced cells arrest synergistically in the $G_2M$ phase, following by obviously accumulation in the subG1 phase. Low concentration of vincristine caused microtubule dynamic changes, and this phenomenon was enhanced by co-incubated with vorinostat, which inhibited HDAC6, causing tubulin acetylation, also leading to microtubule

4

instabilities. This result was consistent with vincristine in combination with HDAC6 inhibitors, tubastatin A and Acy1215. *In vivo* xenografting experiments corroborated the *in vitro* activity and tolerability of the combination. Based on these findings, the combination of microtubule depolymerizing agents and HDAC inhibitors can provide the basis of clinical treatment for ALL.

In the second study, we elucidated the underlying mechanisms of a novel quinoline derivative, MTP0B392 (B392), which was specially designed for oral administration. B392 induced acute leukemic cells arrest in the $G_2M$ phase and ultimately led to apoptosis, which was corroborated by the observation of cleavaged-caspase 3 by immunohistochemistry staining in B392-treated groups of xenograft experiments. B392 also suppressed microtubule polymerization with less susceptibility to P-gp activity, activated mitotic spindle checkpoint as well as caused activation of c-Jun-N-terminal-kinase (JNK), which further contributing to mitochondrial membrane potential loss, caspases and PARP cleavages. Furthermore, B392 had an ability to enhance the cyototoxicity of sirolimus (mTOR inhibitor) in the sirolimus-resistant cells. Our results suggest that B392 is a potential antileukemic drug that could be applied in mono- and combination therapy.

4E-BP1 (eIF4E binding protein 1) is a key regulator in cap-dependent and independent translation, thereby controlling protein synthesis. In the third study, we identified 4E-BP1 as an important prognostic factor in CRC. We found that the protein expression level of 4E-BP1 was more abundant in colorectal cancer cell lines and patients' tissues when compared to normal colon cell line and tissues. By the analysis of clinical patients' pathological parameters, 4E-BP1 expression has statically correlation with disease progression. Under hypoxia, 4E-BP1 is thought to be a crucial factor for cap-independent translation. Additionally, YMX-110, a cryptopleurine derivative, led

to tumor suppression by deletion of 4E-BP1. Thus, the inhibition of protein synthesis by YXM110 in hypoxic condition was further evaluated. Our data show that YXM110 decreased hypoxia-inducible factor 1α (HIF-1α)–regulated vascular endothelial growth factor (VEGF) expression translationally. In sum, these observations indicate that 4E-BP1 is a promising predicted marker in CRC.

In this thesis, we studied different aspects of anticancer therapeutics, including vincristine-vorinostat combination therapy, MPT0B392 mono-chemotherapy and identifying a new prognostic factor, 4E-BP1, excepting that these findings could be applied in clinical studies.
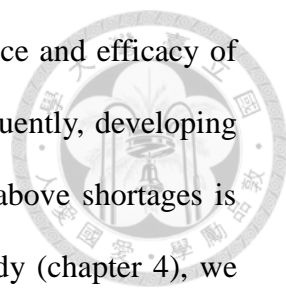
# Chapter 1 Introduction

## 1-1　Research Motivation and Aim

Cancer has been the leading cause of death in worldwide. According to recent reports from Taiwan's Ministry of Health and Welfare, mortality rate of cancer is as high as 29 %, about one person per four people death from cancer on average, and this rate is growing gradually but there is no sexual difference in the death rate. Moreover, the leading cause of death among adults over the age of 25 is cancer. Therefore we are still trying to find better therapeutic strategies to fight cancers.

Leukemia, the most common blood cancer, occupies the sixth place of incidence and mortality in male and female and the cases increase in the recent years. For children, the most common malignancies in childhood are leukemia at home and abroad. The guiding principles of leukemia treatment are bone marrow transplantation and/or the treatment of adjuvant therapy such as chemotherapy or radiation therapy. But chemotherapy always has dosage-dependent, serious and unbearable side effects. In addition, the formation of leukemia is not only caused by one oncogene (heterogeneity), but cancer cells often change their survival ways or initiate a new niche for their growth, such as metastasis or drug resistance, to adapt to the microenvironment instead. Therefore combination therapy is a good therapeutic strategy to decrease high dosage caused side effect and drug resistance. In my first study (chapter 3), we assessed the combination effect of vincristine and vorinostat, which were both approved for clinical usage, in acute lymphoblastic leukemia *in vitro* and *in vivo*.

Chemotherapy, such as microtubule binding agents, is still essential in treatment

of heterogenetic and complex leukemia. Side effects, drug resistance and efficacy of clinical chemo-drugs are obstacles for leukemia treatment. Consequently, developing a new potent microtubule binding drug which can overcome the above shortages is also an attractive option for anticancer therapy. In my second study (chapter 4), we cooperated with the medical chemistry team of Dr. Jing-Ping Liou (Taipei Medical University), who developed MTP0B392 and further confirmed its potent anti-leukemic cells effect *in vitro* and *in vivo*. Moreover, we also evaluated the toxicity of MPT0B392 and its efficacy on P-gp overexpressed cell line, which was resistant to vincristine.

In addition to combination therapy and improved chemotherapy, identifying a prognostic marker and developing specific targeted therapy is another therapeutic strategy against tumor. Many targeted therapies have been successfully used in clinical and responded well, including erlotinib against EGFR mutation non-small lung cancer, sorafenib against advanced hepatocellular carcinoma, and trastuzumab against Her2 positive breast cancer. Colorectal cancer is the third most common cancer in the world and its standard treatment protocol is surgical resection and accompanying multiple combination chemotherapy. In my third study (chapter 5), we discussed the importance of eIF4E binding protein 1 (4E-BP1) in colorectal cancer. Furthermore, YXM110, synthesized by the group of Dr. Kuo Hsiung Lee (Eshelman School of Pharmacy, University of North Carolina at Chapel Hill, NC, USA) and previously demonstrated a strong anticancer activity, dramatically suppressed 4E-BP1 expression. We considered that YXM110 might be a promising targeted therapy for colorectal cancer.

# 1-2 Literature Review

**Leukemia**

Leukemia is a form of blood cancer that causes an abnormal production of white blood cells in the blood or bone marrow. It is a complex disease with many types and subtypes that can be grouped into acute and chronic types depending on the course of the disease. Leukemia also is classified as myeloid or lymphoblastic. Myeloid leukemia is abnormal in granulocytes, monocytes, red blood cells, and platelets. Abnormalities of B cells and T cells are characteristics of lymphoblastic leukemia. In general, the causes of leukemia are multi-factorial. The exact etiology of leukemia is still unknown.

In acute leukemia, immature blood cells (blast cells) proliferate and stop differentiating, crowding out normal cells and replacing their functions with those of blast cells. These immature blast cells retain characteristics that resemble those of their sources. In ALL, the blast cells have characteristics of lymphocytes. In AML, the blast cells display characteristics of myeloid cells. If the surface antigen on the blast cells is like that of B cells, the leukemia is classified as acute B-lymphoblastic leukemia; blast cells with surface antigens like those of T cells are found in acute T-lymphoblastic leukemia. ALL often occurs in young children and is the most common childhood cancer. Without treatment, most patients with acute leukemia would live only a few months.

For treatment of ALL, a combination of vincristine, glucosteroids (prednisone, prednisolone, or dexamethasone), L-asparaginase, and anthracycline is used in remission induction. Then cytarabine, anthracycline, etoposide, and MTX are used for

9

consolidation. High-dose MTX can improve the cure rate of T-cell ALL. Approximately 20–30% of adult ALL patients who are Philadelphia chromosome positive must receive the tyrosine kinase inhibitors imatinib (Gleevec® ) or dasatinib (Sprycel® ) (Kufe and Holland 2006).
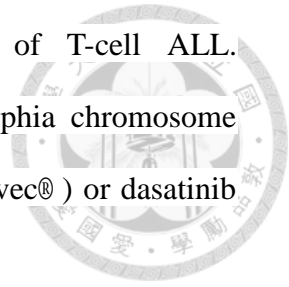
**Colorectal cancer**

Colorectal cancer (CRC) is the third most common cancer and the third leading cause of cancer related deaths worldwide (Siegel, Miller et al. 2015) (Fig.1-1). Approximately 50-60% of diagnosed CRC patients will develop metastases. Most cases of CRC are sporadic, with only a small proportion related to heredity. It has been reported that some gene mutations increase the incidence of CRC, including those of *APC* (adenomatous polyposis coli), *KRAS*, *MLH1*, *MSH2*, *TP53*, and *EGFR* (Walther, Johnstone et al. 2009). Currently, the cornerstone treatment for CRC is surgery for stage I cases, with adjuvant radiotherapy and systemic chemotherapy for stages II and III. In addition to traditional chemotherapy drugs (5-fluorouracil, irinotecan, oxaliplatin, and capecitabine), several targeted monoclonal antibodies such as bevacizumab, cetuximab, and panitumumab have been utilized in the clinic (Edwards, Chadda et al. 2012).

**Cell cycle**

The cell cycle is a series of events that occurs in cells as they grow and divide. $G_1$ is a period of preparing the cellular environment for DNA synthesis. During the S phase, DNA is synthesized. $G_2$ is the second gap of the cell cycle during which protein synthesis takes place and the cellular environment is monitored for conditions favorable for mitosis. Cell division takes place in the M phase. M phase is the shortest

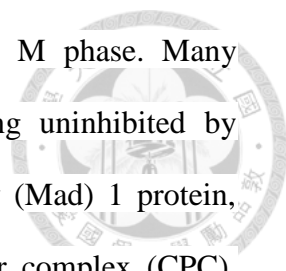phase, representing approximately 1 hour of a total cell cycle time of 24 hours.

Cell cycle checkpoints are critical monitoring mechanisms in the progression and completion of the cell cycle. Three key checkpoints are included in the total cell cycle. The first occurs between $G_1$ and S, and it determines whether the cell has enough growth factor for DNA synthesis. The second checkpoint, between S and $G_2$, ensures the correctness of the chromosome replication. At M phase the final checkpoint ensures that the spindle is assembled correctly and complete division is prompted.

Another mechanism for cell cycle regulation is cyclin concentration. Cyclins in the human cell cycle are lettered A, B1, D, and E. Progression from $G_1$ to S is regulated mainly by cyclins D and E. Cyclin A controls progression from S to $G_2$, and the change from $G_2$ to M is dependent on cyclin B1 activation. Cyclins form a complex with cyclin-dependent kinase (CDK), which activates CDK and regulates the progression of the cell cycle. The cyclin-CDK complex is inhibited by cyclin-dependent kinase inhibitors (Sherr and Roberts 1999).

**Mitotic phase**

As a cell begins to enter M phase from $G_2$, the CDK1 (Cdc2)/cyclin B complex must be activated. The inhibitory phosphorylation of tyrosine 15 (Tyr 15) of the complex, which is carried out by the active Cdc25C phosphatase and the phosphorylation of threonine 161 (Thr 161) of CDK1, activates the CDK1/cyclin B complex, promoting the progression from $G_2$ to M (Castedo, Perfettini et al. 2004) (Fig. 1-2).

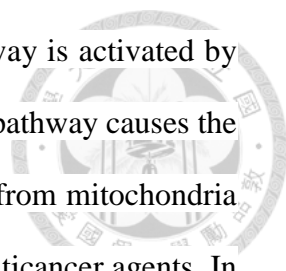Abnormal sister chromatid separation leads to genetic instability; thus, the

11

spindle assembly checkpoint (SAC) is a critical mechanism in M phase. Many proteins are involved in SAC regulation, including the budding uninhibited by benomy (Bub) 1 protein, Bub3, BubR1, mitotic arrest deficiency (Mad) 1 protein, Mad2, monopolar spindle 1 protein, and chromosomal passenger complex (CPC), which is responsible for detecting the connection between the kinetochore and the microtubule and the separation of sister chromatids (Weaver and Cleveland 2005). Many proteins compose the CPC: serine/threonine kinase aurora B, inner centromere protein, Survivin, and Borealin/DasraB. The CPC localizes to the centromere to support its attachment to the microtubule.

If a microtubule fails to connect to the centromere correctly, the SAC is activated and the CPC continues trying to repair the misconnection. On the other side, the mitotic checkpoint complex (MCC), formed by Mad2, Bub3, BubR1, and Cdc20C, inhibits anaphase-promoting complex/cyclosome, a kind of multi-subunit ubiquitin ligase, preventing the degradation of cyclin B1 and the secure centromere-microtubule connection. Thus, sister chromatids arrest the cell in metaphase without dividing, until the centromere correctly attaches to the microtubule or the tension between sister chromatids is adequate for cell division (Kang and Yu 2009) (Fig. 1-3).

**Apoptosis**

Cell death can be separated to two types, one is apoptosis, and the other is necrosis. Apoptosis is a natural cell death phenomenon and is regulated by gene or protein in order when cells are exposed to stimuli, so also called programmed cell death.

There are at least two broad pathways that lead to apoptosis, extrinsic apoptotic

pathway and intrinsic apoptotic pathway. Extrinsic apoptotic pathway is activated by the induction of death receptor. However the activation of intrinsic pathway causes the changes of mitochondria and releases some pro-apoptotic proteins from mitochondria when exposure of UV light, DNA damage, hypoxia, oncogene or anticancer agents. In both pathways, signaling results in the caspases activation. As Fas Ligand (Fas L) and TNF binds to Fas/CD95 and TNF receptor (TNFR), respectively, DSIC (death inducing signaling complex) is formed and followed by caspase 8 and caspase 3 activation, inducing cell death in the extrinsic apoptotic pathway. But in the intrinsic pathway, the mitochondria are directly influenced when the cell is explored to damage. Thus, the permeability of mitochondrial outer membrane is increased. But there is decrease in the inner membrane potential and it results in pro-apoptotic proteins releasing form mitochondria and caspase 9, 3, 6, 7 activation. Although extrinsic and intrinsic apoptosis pathways are different, they can be linked together with Bid protein. Caspase-8 activation of the extrinsic pathway initiates the mitochondrial pathway to apoptosis by cleaving the Bid to truncated Bid (tBid), which can activate the formation of mitochondrial membrane pore and loss of membrane potential as the intrinsic apoptotic pathway does (Holohan, Van Schaeybroeck et al. 2013)(Fig. 1-4).

**Bcl-2 family protein**

The intrinsic apoptotic pathway plays a critical role in apoptosis when cells are exposed to extracellular stimuli. It is regulated mainly by mitochondrial proteins such as the Bcl-2 family. This protein family has 25 members, all of which have a Bcl-2 homology (BH) domain. They are classified into 3 major subfamilies: (1) the anti-apoptotic protein subfamily, including Bcl-2, Bcl-xl, Bcl-w, Mcl-1, Bfl1/A-1, and Bcl-B; (2) the pro-apoptotic protein subfamily, including Bax, Bak, Bok; and (3) the

BH-3-only protein subfamily, such as Bik, Bad, Hrk, Bid, Bim, PUMA, NOXA, Bmf, and others, which are associated with cell apoptosis (Brunelle and Letai 2009) (Fig. 1-5).
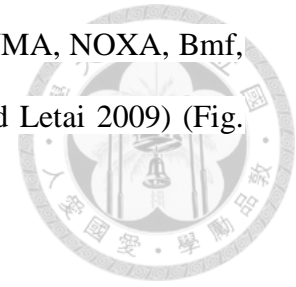
**Microtubule and tubulin-binding agents**

<u>Microtubule structure and dynamics</u>

Microtubules, a component of the cytoskeleton, are required in many cellular processes, including vesicle and organelle transportation, cellular motility, cell shape maintenance, chromosome separation, and division. Microtubules are dynamically structured polymers of α-tubulin and β-tubulin. The tubulin dimers assemble head-to-tail into linear protofilaments that form a hollow cylinder. Tubulin has 2 guanine triphosphate (GTP) binding sites, a hydrolyzable and a non-hydrolyzable site on β-tubulin and α-tubulin, respectively. The hydrolyzable site on β-tubulin binds to GTP then polymerizes to form microtubules and irreversibly dissociates to guanine diphosphate (GDP). Therefore, microtubule dynamics depends on the GTP or GDP bound to β-tubulin. If the β-tubulin binds to GTP, microtubules polymerize, but if binding to GDP occurs, microtubules depolymerize.

Microtubule dynamics plays an important role in cell division. Before cells divide, microtubule-like reticular structures spread in the cytosol. As the cell enters M phase, however, the original reticular microtubules are remodeled and assembled into mitotic spindles, which connect with chromosomes and drive chromosome separation. All of the microtubule processes described above is crucial for microtubule polymerization and depolymerization. Therefore, agents that disrupt microtubule dynamics also inhibit cell growth and division.
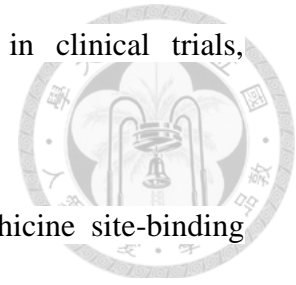
Tubulin-binding agents
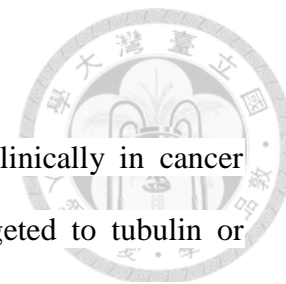
Drugs that inhibit microtubule dynamics have been used clinically in cancer treatment for more than 20 years. These agents, which are targeted to tubulin or microtubules, can increase or decrease the mass of microtubules at high concentrations, can be divided into 2 major types: microtubule-stabilizing agents and microtubule-destabilizing agents. At lower concentrations, both types affect only microtubule dynamics, inducing abnormal mitotic spindle formation and causing cell arrest in M phase and, subsequently, cell apoptosis.

Depending on their binding sites, microtubule-destabilizing agents can be classified into subtypes: vinca site-binding agents and colchicine site-binding agents. Vinca alkaloids, the major components in vinca site-binding agents such as vincristine (Oncovin®) and vinblastine (Velban®), were introduced for clinical use in 1950. Vincristine was also the first tubulin-binding agent used to treat cancer (leukemia) in 1970. Owing to their success, many semisynthesized compounds such as vindesine (Eldisine®), vinorelbine (Navelbine®), and vinflunine have also been developed. Vinca alkaloids bind to a site near the GTP binding site on β-tubulin, thus disrupting and inhibiting microtubule polymerization. In addition to vinca alkaloids, halichondrin (marine sponge Halichondria extracts), cryptophycin, hemiasterlin, and dolastains are also considered vinca site-binding agents. Among all of these agents, the best known drug is vincristine, a very potent microtubule-depolymerizing agent extracted from the leaf of *Catharanthus roseus*. Vincristine was first regarded as a immunosuppressant but was later applied to the treatment of cancer. Among various tubulin-binding agents, vincristine is the best choice for the treatment of leukemia, lymphoma, and sarcoma. Liposomal shingosomal vincristine sulfate (Marqibo®;

Tekmira), a developing new dosage form of vincristine, is in clinical trials, particularly for ALL treatment.

The other group of microtubule-destabilizing agents, colchicine site-binding agents, includes colchicine and combretastatin. These agents bind to the soluble heterodimer of α-tubulin and β-tubulin near the GTP binding site of β-tubulin and form stable structures. These structures in turn bind to the end of microtubules, thus slowing the rate at which new tubulins assemble to the end of microtubule and inhibiting microtubule polymerization. The toxicity of colchicines makes their clinical use difficult in cancer therapy. Therefore, these agents are primarily used in low concentrations as immunosuppressants in gout treatment (Risinger, Giles et al. 2009).

Microtubule-stabilizing agents consist of taxane-binding sites, epothilones, laulimalides, peloruside A, and taccalonolides. Taxane-binding agents, such as paclitaxel (*Taxus brevifolia*, Taxol® ) and docetaxel (Taxotere® , a semisynthesized compound), target β-tubulin and bind to the inside of microtubules, stabilizing the microtubule structure and enhancing the polymerization activity of microtubule. They are usually used to treat solid tumors such as lung, breast, or ovarian cancers. Epothilones are the newest microtubule-stabilizing agents being used to treat a variety of cancers, especially paclitaxel-resistant cancers (Dumontet and Jordan 2010, Loong and Yeo 2014) (Fig. 1-6; Table 1-1).

Tubulin-binding agents inhibit microtubule dynamics in the process of cell division. Thus the requirements of the SAC are not met, delaying the progression of cells from metaphase into anaphase and arresting them in M phase. If the arrest time is long (approximately 20 hours), the cells might slip from M phase or become

tetraploid and polyploid cells (Gascoigne and Taylor 2009) (Fig. 1-7). Consequently, if cells are unable to manage the stress or repair the damage, apoptosis signaling may be induced through Bcl-2 phosphorylation or JNK activation indirectly. The phosphorylation of Bcl-2 results in the loss of its apoptotic function (Mollinedo and Gajate 2003) (Fig. 1-8).

Tubulin-binding agents are already being widely used clinically for treatment of blood malignancies and solid tumors. As with other anticancer agents, however, the problems of drug resistance, neuropathy, immunosuppression, and poor solubility must be addressed. The current trends in tubulin-binding agent development are to change the dosage to improve solubility or combine these agents with other anticancer drugs to reduce toxicity and enhance activity (Mollinedo and Gajate 2003)

Tubulin binding agents and JNK

Many protein kinases including mitogen-activated protein kinase (MAPKs) have been reported to localize on or associate with microtubules, regulating pivotal roles in cell motility, survival and proliferation (Mollinedo and Gajate 2003). MAP kinase families contain three members: ERKs (Extracellular signal-regulated kinases), controlling cell survival and proliferation; JNK (c-Jun N-terminal kinases), mediating cell death and stress responses; and p38, regulating stress responses (Dhillon, Hagan et al. 2007). Tubulin binding agents have been reported that differentially regulate of MAPK kinase even in the same cancer cells (Shtil, Mandlekar et al. 1999). JNK can interact with mixed lineage kinase (MLK) and the KIF3 family of kinesin motor protein, indicating the association of JNK and microtubule (Nagata, Puls et al. 1998). It was also shown that microtubule damages induced-JNK activation is partially
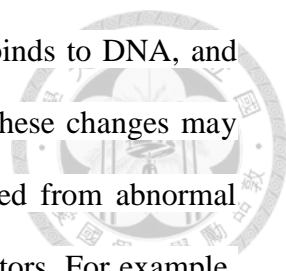
mediated by Rac, ASK1 and JNK kinas (JNKK) (Wang, Wang et al. 1998), resulting in Bcl-2 phoshorylation and followed by cell apoptosis. However, the phenomenon of JNK/pBcl2 pathway-caused cell death was different in cell types as well as tubulin targeting agents (Wang, Popp et al. 1999). Until now, the role of MAPK signaling molecular mechanisms in cell apoptosis elicited by microtubule damage is not clearly well defined and controversial.

**HDAC and HDAC inhibitor**

HDAC structure and function

HDAC, an enzyme, catalyzes the removal of the acetyl group in histones. Its function is opposite to that of histone acetyltransferase, which acetylates the lysine in histone residues. Deacetylation of the histone N-terminal lysine by HDAC results in a more compact chromatin structure that inhibits gene transcription (Laird 2005) (Fig. 1-9). The HDAC family can be divided into 4 groups according to homology, distribution, and enzyme activity: class I, including HDACs 1, 2, 3, and 8, occurs mostly in the nucleus and is widely spread throughout various cells and tissues; class II, including subclasses IIa (HDACs 4, 5, 7, and 9) and IIb (HDACs 6 and 10), often shifts between the cytosol and the nucleus. HDAC-6 has a β-tubulin deacetylase domain, so it is mediated by β-tubulin deacetylation (Hubbert, Guardiola et al. 2002); class III, including SIRTs 1–7, which require nicotinamide adenine dinucleotide coenzyme for deacetylation; and class IV, with only one member, HDAC11. The structure of this class is similar to that of classes I and II (West and Johnstone 2014)(Fig. 1-10).

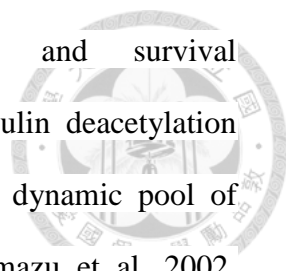Many studies have reported that abnormal fusion proteins can recruit HDAC,

leading to a kind of co-repressor that inhibits gene transcription, binds to DNA, and thus represses downstream tumor-suppressor gene transcription. These changes may lead to tumor formation. Oncogenic fusion protein is often derived from abnormal chromosomal translocation or overexpression of transcriptional factors. For example, 40% of patients with diffuse large B-cell lymphoma display B-cell lymphoma 6 overexpression. B-cell lymphoma 6 can recruit HDAC2, inhibiting cell cycle gene CDKN1A/p21 transcription. Other fusion proteins such as PML-RAR, PLZS-RAR and AML-ETO cause APL and AML through similar mechanism (Lin, Sternsdorf et al. 2001)

In addition to HDAC recruitment by oncogenetic proteins, HDAC overexpression in many cancers also has been reported. For example, HDAC1 is overexpressed in prostate (Halkidou, Gaughan et al. 2004), gastric (Choi, Kwon et al. 2001), colon, and breast cancers. HDAC2 is overexpressed in colorectal (Zhu, Martin et al. 2004), cervical, and gastric cancers. HDAC3 is overexpressed in colorectal cancer (Wilson, Byun et al. 2006), and HDAC6 is overexpressed in breast cancer (Zhang, Yamashita et al. 2004). The relationship between HDAC expression and various cancers remains unclear, but when the overexpressed HDAC is silenced, the growth of cancer cells is inhibited and apoptosis is induced. Thus, HDAC is believed to be a promising target for cancer therapy (West and Johnstone 2014)(Table 1-2).

<u>HDAC6</u>

HDAC6, which belongs to class II HDAC, predominantly locates in the cytoplasm. Therefore, HDAC6, unlike other nuclear HDACs deacetylating histone, only acetylates nonhistone proteins such α-tubulin and HSP90 *in vivo*, regulating

microtubule stabilization, cell motility, cellular stress and survival (Aldana-Masangkay and Sakamoto 2011). HDAC6-mediated tubulin deacetylation caused microtubule destabilization, controlling the stability of a dynamic pool of microtubules (Hubbert, Guardiola et al. 2002, Matsuyama, Shimazu et al. 2002, Zhang, Li et al. 2003). HDAC6 also plays a crucial role in the proteasome pathway by influencing the acetylated status of HSP90, resulting in the stabilization of client oncoproteins such as ErbB2, Bcr-abl, c-kit and FLT3, which are often overexpressed in cancers(Bots and Johnstone 2009). Furthermore, it was reported that HDAC6 is involved in aggresome pathway though its ability to bind both polyubiquitinated misfolded proteins and dynein motors (Simms-Waldrip, Rodriguez-Gonzalez et al. 2008). Many cancers have been found that overexpressed HDAC6 promotes tumorigenesis and survival. Consequently, a lot of specific HDAC6 inhibitors are under clinical trials (Kramer, Mahboobi et al. 2014).

Hstone deacetylase inhibitors

The main HDACi agents in development are natural, semisynthesized, or synthesized compounds. Depending on their structures and characteristics, they can be grouped into 6 types: short-chain fatty acids (valproic acid); hydroxamate (trichostatin A); vorinostat (suberoylanilide hydroxamic acid); panobinostat (LBH589); benzamide; cyclic tetrapeptides (depsipeptides); and electrophilic ketones. Every HDACi has its own characteristics. For example, vorinostat, trichostatin A, and panobinostat are pan-HDACi agents; however, valproic acid inhibits only class I and II HDACs, and benzamide is targeted to class Ia (West and Johnstone 2014)(Fig. 1-11). In 2006, vorinostat was approved by the FDA for cutaneous T-cell lymphoma and became the first HDACi in clinical use. Until 2015, four HDACi have been approved for cancers.

(West and Johnstone 2014)(Table 1-3).
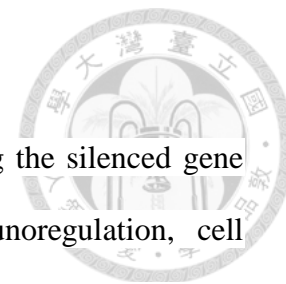
HDACi drugs cause histone hyperacetylation, thus activating the silenced gene for normal cellular function (cell cycle, angiogenesis, immunoregulation, cell apoptosis). In addition, HDACi agents have been found to target non-histone proteins as well, including protein 53 (p53), E2F1, signal transducer and activator of transcription 1, nuclear factor-κb, α-tubulin, heat shock protein (HSP) 90, and Ku 70 (Luo, Su et al. 2000, Martinez-Balbas, Bauer et al. 2000, Chen, Fischle et al. 2001). Many studies have indicated that the mechanisms of action in diverse cell lines are different even when the same HDACi is used. Similarly, distinct HDACi agents may have diverse mechanisms even in the same cell lines. Therefore, comparing the mechanism of an HDACi with a specific target (tubacin) or with that of a pan-HDACi such as vorinostat is complex (West and Johnstone 2014)(Fig. 1-10).

HDACi agents induce cell apoptosis through a variety of mechanisms. Activation of the death-receptor pathway and mitochondrial (intrinsic) death pathway, BH3-only protein and reactive oxygen species regulation, and cell cycle arrest have been reported to be involved in HDACi-mediated apoptosis. Moreover, some mechanisms are independent of gene transcription, such as those that operate through HSP90 to degrade certain oncogenetic proteins (Bcr-abl, Akt, c-Raf) and promote cell death (Bali, Pranpat et al. 2005, Bali, Pranpat et al. 2005).

The primary reason for pursuing the development of HDACi agents was their capability of causing cell differentiation by inducing p21 transcriptional activity in a p53-independent manner, thus arresting cells in $G_1/S$. Under certain conditions, however, HDACi compounds can induce cell arrest in $G_2/M$ owing to the loss of the

$G_2$ checkpoint, which causes abnormal chromosomal segregation, or the inactivation of the mitotic SAC though HDAC3 inhibition (Li, Kao et al. 2006). HDAC3 is reportedly associated with microtubule-kinetochore connecting. HDAC3 inhibition promotes aurora B kinase degradation and represses the activation of the SAC. Thus, cells start to divide with an undetected fault in microtubule disconnection with the centromere, causing aneuploidy or mitotic slippage (Eot-Houllier, Fulcrand et al. 2009).

Owing to their low toxicity and wide range of activity, HDACi agents are often combined with other anticancer drugs. Most studies have been undertaken with cell-based experiments, but many combination therapies are undergoing clinical trials, often for hematological malignancies. The current preclinical HDACi combination therapies are shown in Table 1-4 (Richon, Garcia-Vargas et al. 2009).

**mTOR pathway and inhibitor**

The mammalian target of rapamycin (mTOR) is a key serine/threonine kinase that is downstream of various signaling pathways, including phosphatidylinositol 3 kinase (PI3K)/AKT, Ras, and AMP-activated kinase (AMPK), that regulates various cellular processes required for protein synthesis, growth, and cell cycle progression and metabolism (Petroulakis, Mamane et al. 2006). mTORC1, a complex comprising mTOR and regulatory-associated protein of mTOR (raptor), is frequently deregulated in hematological malignancies (Inoki, Corradetti et al. 2005). In fact, genetic mutations, over-activated tyrosine kinase receptors, and amplification of key factors in PI3K/AKT pathways have been identified to lead to abnormal activation of mTOR signaling in leukemia (Vu and Fruman 2010) (Fig. 1-12). Thus, mTOR inhibitors were initially

developed as immunosuppressive agents; aberrant regulation of mTOR signaling was found to be important in many tumors, and thus many mTOR inhibitors were investigated in preclinical and clinical studies (Faivre, Kroemer et al. 2006). Sirolimus (rapamycin) was the first approved mTOR inhibitor used clinically as an immunosuppressive agent (Easton and Houghton 2006) (Table 1-5).
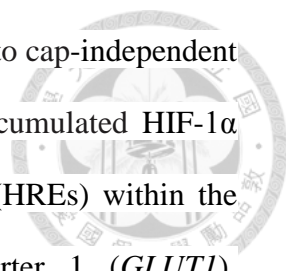
**Protein synthesis**

Protein synthesis controls cell growth, cell size maintenance, proliferation, and the survival of cancer cells (Silvera, Formenti et al. 2010). Translation phases include the rate-limiting step of initiation, the assembly of the elongation-competent 80S ribosome, and termination. Translation of mRNAs can occur in a cap-dependent and cap-independent manner. Cap-tagged mRNAs recruit eukaryotic initiation factors (eIFs), forming the eIF4F complex, composed of the following proteins: scaffolding protein eIF4G, RNA helicase eIF4A, and the cap-binding protein eIF4E (Ali, McKendrick et al. 2001). eIFs work together to initiate the translation process. However, recent studies have indicated that cap-independent translation may contribute to cancer progression. Unlike cap-dependent translation, cap-independent translation involves access to mRNAs through an internal ribosome entry site (IRES) without cap binding. Under cellular stress such as in hypoxia, cap-independent mRNAs can be translated even when cap-dependent translation is decreased (Braunstein, Karpisheva et al. 2007). Cellular mRNAs that also contain IRES elements include hypoxia-inducible factor 1α (*HIF1A*), vascular endothelial growth factor (*VEGFA*), fibroblast growth factor 2 (*FGF2*), and *BCL2*, all of which utilize a dual mechanism of initiation (cap or IRES) (Lang, Kappel et al. 2002, Sherrill, Byrd et al. 2004, Silvera, Formenti et al. 2010) (Fig 1-13).

**4E-BP1**

4E-BP1, the most common eukaryotic translation initiation factor of 4E binding proteins (4E-BPs) impacts cell proliferation, apoptosis, invasion, and metastasis. The hypophosphorylated active form of 4E-BP1, sequesters eIF4E and prevents it from binding to eIF4G, thus blocking the formation of the cap-dependent translation complex (eIF4F). 4E-BP1 also activates cap-independent translation by binding to eIF4E (Seton-Rogers 2008). It has been shown that elevated levels of 4E-BP1 and eIF4G induces hypoxia mediated inhibition of cap-dependent mRNA translation and increases the translation of mRNAs containing IRES. This leads to angiogenesis, hypoxia resistance, and survival (Braunstein, Karpisheva et al. 2007, Silvera, Formenti et al. 2010). Cap-independent translation is also highly correlated with drug resistance under hypoxic conditions (Huang, Ao et al. 2010) (Fig 1-13).

**Hypoxia**

Oxygen is necessary for cells to produce adequate amounts of ATP to support cellular metabolic activities. Hypoxic conditions are often observed within cancer tissues, due to the high proliferation rates and vascular abnormalities (Ziello, Jovin et al. 2007). Hypoxia-inducible factor-1 (HIF-1), an oxygen-sensitive transcription factor, initiates adaptive responses to changes in oxygen tension in various microenvironments (Brocato, Chervona et al. 2014). HIF-1 is a heterodimer protein complex composed of a constitutively expressed HIF-1β subunit (also called aryl hydrocarbon receptor nuclear transporter, ARNT) and a highly regulated HIF-1α subunit (Semenza 2003). The balance between protein synthesis and protein degradation determines the expression level of HIF-1α. During hypoxia, the protein

synthesis process for HIF-1α mRNA switches from cap-dependent to cap-independent (IRES-dependent) translation (Silvera, Formenti et al. 2010). Accumulated HIF-1α dimerizes with HIF-1β and binds to hypoxia-response elements (HREs) within the promoters of target genes, such as *VEGF*, glucose transporter 1 (*GLUT1*), erythropoietin (*EPO*), and nitric oxide synthase (*NOS*) (Harris 2002). HIF-1α overexpression and activation stimulates several key pathways in carcinogenesis, such as those related to angiogenesis, anaerobic glucose metabolism, dedifferentiation, and invasion (Ziello, Jovin et al. 2007). HIF-1β serves as a common binding partner for the aryl hydrocarbon receptor (AhR) as well as HIF-α subunits. HIF-1β is gerenally regarded that neither its mRNA nor protein level is affected by hypoxia. Nevertheless, increasing evidence showed that some tumor cells under low oxygen condition are able to uptregultae HIF-1β and silencing HIF-1β induces anti-tumor effects (Lang, Kappel et al. 2002, Wang, Ye et al. 2014).

**Table 1-1. Microtubule-binding agents currently in clinical practice or in development in clinical trials** (Loong and Yeo 2014)

| Mechanism of action | Type of microtubule-binding agent | Family | Compound | Clinical applications/pertinent active clinical trials |
|---|---|---|---|---|
| Microtubule destabilizing | Vinca-domain binder | Vincas | Vincristine | ALL, lymphomas, various solid tumors |
| | | | Vindesine | ALL, lymphomas, lung cancer |
| | | | Vinorelbine | Breast cancer, NSCLC |
| | | | Vinblastine | Lymphomas, various solid tumors |
| | | | Vinflunine | Bladder cancer, NSCLC, breast cancer |
| | | Halichondrin | Eribulin | Breast cancer |
| | | Maytansinoids | Mertansine ADCs | T-DM1 approved for breast cancer |
| | | Dolastatins | Brentuximab vedotin | Hodgkin's lymphoma |
| | Colchicine-domain binder | Combretastatins | Fosbretabulin | Phase I/II trials in GBM, lung, thyroid, and sarcomas |
| | | | Verubulin | |
| | | | Crinobulin | |
| | | | Ombrabulin | |
| Microtubule stabilizing | Taxol-domain binder | Taxanes | Paclitaxel | Ovarian cancer, breast cancer, NSCLC |
| | | | Docetaxel | NSCLC, breast cancer, prostate cancer, stomach cancer, head and neck cancer |
| | | | Cabazitaxel | Prostate cancer |
| | | | Nab-paclitaxel | Breast cancer, pancreas cancer |
| | | Epothilones | Ixabepilone | Breast cancer |
| | | | Patupilone | Clinical trials for brain metastases in breast and ovarian cancers, melanoma, and other solid tumors |
| | | | Sagopilone | Clinical trials in GBM, prostate, and lung cancers |
| | | | KOS-1584 (epothilone D analog) | Phase II trials in NSCLC |
| Others | Estramustine – binds to microtubule-associated protein | | | Prostate cancer; clinical trials with taxanes, vincas, and ixabepilone for prostate cancer |

**Note:** Adapted from Dumontet C, Jordan MA. Microtubule-binding agents: a dynamic field of cancer therapeutics. Reprinted by permission from Macmillan Publishers Ltd: *Nature Reviews Drug Discovery* © 2010.[30]

**Table 1-2. Aberrant regulation of HDACs in cancer** (West and Johnstone 2014)

| HDAC | Normal and oncogenic protein associations | Expression in cancer | Genetic evidence | Reference |
|---|---|---|---|---|
| **Class I (homologous to RDP3 yeast protein, nuclear location, ubiquitous tissue expression)** | | | | |
| HDAC1 | HDAC2, CoREST, NuRD, Sin3, AML1-ETO, PML, PLZF, BCL6, p53, AR, ER, Rb/E2F1 | Elevated in gastric[A], breast[B], colorectal, HL, lung[A], liver[A] | KD induced growth arrest, decreased viability, and increased apoptosis in colon, breast, and osteosarcoma cancer cells and increased survival of mice with overt PML-RARα–mediated APL; HDAC1 KO/HDAC2 KD induced growth arrest in fibroblasts; KO induced genomic instability and arrest and reduced survival of transformed cells in vivo | 7–9, 11, 12, 95–106 |
| HDAC2 | HDAC1, CoREST, NuRD, Sin3, AML1-ETO, PML, PLZF, Bcl6 | Elevated in gastric[A], prostate[A], colorectal[A], HL, CTCL | KD induced growth arrest, decreased viability, and increased apoptosis in colon and breast cancer cells and induced apoptosis and decreased lung cancer in vivo; HDAC1 KO/HDAC2 KD induced growth arrest in fibroblasts; KO induced genomic instability and arrest and reduced survival of transformed cells in vivo; KD induced apoptosis and decreased lung cancer in vivo | 6, 7, 12, 96–101, 103, 106–109 |
| HDAC3 | HDAC4, HDAC5, HDAC7, NCoR/SMRT, AML1-ETO, PML, PLZF, PML-RARα, PLZF-RARα, Bcl6, STAT1, STAT3, GATA1, GATA2, NF-κB | Elevated in gastric[A], breast[AB], ALL, colorectal, HL; decreased in liver | KD in colon cancer cells decreased survival, increased apoptosis, and relieved transcriptional repression mediated by PML-RARα in APL cells | 7, 8, 12, 25, 78, 96, 97, 99, 100, 105, 110–113 |
| HDAC8 | | Elevated in neuroblastoma | KD reduced proliferation of lung, colon, and cervical cancer cells | 50, 71 |
| **Class IIa (homologous to Hda1 yeast protein, shuttle between nucleus and cytoplasm, tissue-restricted expression)** | | | | |
| HDAC4 | HDAC3-NCoR, GATA1 | | KD in chondrosarcoma cells increased VEGF expression and reduced growth and induced apoptosis of colon and glioblastoma tumors in vivo | 76–78, 105, 114 |
| HDAC5 | HDAC3-NCoR, GATA1, GATA2 | Elevated in medulloblastoma; decreased in lung | KD decreased medullablastoma cell growth and viability | 9, 78, 105, 115 |
| HDAC7 | HDAC3-NCoR, ERα | Elevated in ALL; decreased in lung | KD induced growth arrest in colon and breast cancer cells | 10, 78, 110, 116 |
| HDAC9 | | Elevated in ALL, medullablastoma | KD of HDAC9/10 inhibited homologous recombination and increased sensitivity to DNA damage and decreased medullablastoma cell growth and viability | 110, 115, 117 |
| **Class IIb (homologous to yeast protein Hda1, mostly cytoplasmic location, tissue-restricted expression)** | | | | |
| HDAC6 | α-Tubulin, HSP90, HDAC11 | Elevated in breast[B], CTCL; decreased in lung | KD decreased VEGF expression and decreased cell viability due to accumulation of misfolded proteins | 10, 16, 83, 105, 118, 119 |
| HDAC10 | | | KD of HDAC9/10 inhibited homologous recombination and increased sensitivity to DNA damage and decreased VEGF expression | 117, 119 |
| **Class IV (unknown yeast protein homology, cytoplasmic location, tissue-restricted expression)** | | | | |
| Class 11 | HDAC6 | Elevated in breast, renal, liver | KD induced apoptosis in colon, prostate, breast, and ovarian cancer lines | 94, 120, 121 |

[A]Independent prognosis indicator. [B]Associated with enhanced prognosis. KD, knockdown; HL, Hodgkin lymphoma; ALL, acute lymphoblastic leukemia.

**Table 1-3. HDACis in current clinical trials** (West and Johnstone 2014)

| HDACi | Highest phase trial | Cancer type | Best clinical outcome | Reference |
|---|---|---|---|---|
| Panobinostat (LBH-589) | III | CTCL | Ongoing; promising in phase II against CTCL (74% tumor reduction), HL (74% tumor reduction and 27% OR), and WM (MR or better in 47% of patients, 50% SD) | 122–124 |
| Belinostat (PXD101) | II | Thymoma | Significantly enhanced survival | 125 |
| Entinostat (MS275) | II | Melanoma | Some clinical activity, promising PK and PD values | 126–128 |
| Mocetinostat (MGCD01030) | II | B cell malignancies | Disease control (35% rate) in HL | 129 |
| Givinostat (ITF2357) | II | $JAK2^{V617F}$-expressing myeloproliferative neoplasms | Pruritus relief (~100%), splenomegaly reduction (75% of PV/ET and 38% of MF patients) | 130 |
| Practinostat (SB939) | II | Prostate cancer | Limited clinical efficacy to date but promising PK values | 131, 132 |
| Chidamide (CS055/HBI-8000) | II | Solid tumors and lymphomas | Ongoing; PR was observed in 5/31 patients during phase I | 61 |
| Quisinostat (JNJ-26481585) | II | CTCL | Ongoing; 31.6% reduction in mSWAT score of tumor burden, 1/19 CR, 4/19 PR | 63 |
| Abexinostat (PCI- 24781) | II | FL | Tumor reduction in 86%, ORR of 64% | 64 |
| CHR-3996 | I | Various (mostly solid tumors) | Favorable PK and PD values | 60 |
| AR-42 | I | Hematological malignancies | Ongoing, minor clinical responses in myeloma and T cell lymphoma | 62 |

CR, complete response; ET, essential thrombocythemia; FL, follicular lymphoma; MF, myelofibrosis; MR, minimal response; OR, overall response; ORR, overall response rate; PD, pharmacodynamic; PK, pharmacokinetic; PR, partial response; PV, polycythaemia vera; SD, stable disease; WM, Waldenström macroglobulinemia.

**Table. 1-4. Preclinical activities of vorinostat combination therapies** (Richon, Garcia-Vargas et al. 2009).
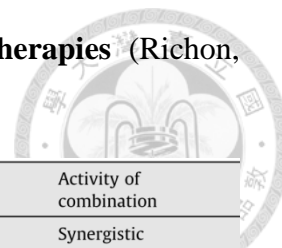
| Combination | Transformed cell lines | Activity of combination |
|---|---|---|
| Vorinostat + 5-aza-2′deoxycytidine | CTCL (HH) | Synergistic |
| Vorinostat + 17-AAG | Leukemia (U937, K562, LAMA84) | Synergistic |
| Vorinostat + ATRA | APL (NB4) | Additive |
| Vorinostat + bortezomib | Bcr-Abl+ leukemia (K562, LAMA84); myeloma; non-small lung carcinoma; mantle cell lymphoma, hepatoma, pancreatic | Synergistic |
| Vorinostat + cisplatin | Breast (MCF-7); squamous cell (HSC-3) | Enhanced cell death |
| Vorinostat + docetaxel | Breast (BT-474, SKBR-3) | Synergistic |
| Vorinostat + trastuzumab | Breast (BT-474, SKBR-3) | Synergistic |
| Vorinostat + epirubicin | Breast (MCF-7) | Synergistic |
| Vorinostat + etoposide | Breast (MCF-7) | Enhanced cell death |
| Vorinostat + flavopiridol | Leukemia (U937), Breast (MDA-MB-231, MCF7) | Synergistic |
| Vorinostat + 5-FU + irinotecan | Hepatocellular carinoma (HepG2, Hep1B) | Enhanced cell death |
| Vorinostat + radiation | Prostate (LNCaP) Squamous carcinoma; melanoma, NSCLC | Synergistic; enhanced sensitivity |
| Vorinostat + TRAIL | Leukemia; lung, prostate breast carcinoma; melanoma | Synergistic |
| Vorinostat + LY294002 | Leukemia (U937, HL-60, K562, Jurkat) | Synergistic |
| Vorinostat + PD184352 | Leukemia (K562, LAMA84) | Synergistic |
| Vorinostat + perifosine | Leukemia (U937, HL-60, Jurkat) | Synergistic |
| Vorinostat + Bay 11-7082 | Leukemia (U937, HL-60, Raji, Jurkat) | Synergistic |
| Vorinostat + gemcitabine | NSCLC (A549, H460), pancreatic (PANC1) | Enhanced sensitivity |
| Vorinostat + bicalutamide | Prostate (LNCaP) | Synergistic |
| Vorinostat + zoledronic acid | Prostate (LNCaP, PC3) | Synergistic |
| Vorinostat + cis-retinoic acid | Medulloblastoma (D283) | Synergistic |
| Vorinostat + MK-0457 (VX-680) | CML (K562, primary), AML (HL-60, OCI-AML3, primary) | Synergistic |
| Vorinostat + imatinib | CML (K562, LAMA84) | Additive synergistic |
| Vorinostat + desatinib | CML (K562, LAMA84, primary), BaF3 | Synergistic |
| Vorinostat + sorafenib | CML (K562, LAMA84), pancreatic (MiaPaCa2, PANC1), hepatic (HEPG2, HuH7, HEP3B) renal (A498, CAKI-1, UOK121LN) | Synergistic |
| Vorinostat + sulindac | NSCLC (H460, A549) | Enhanced sensitivity |
| 17-AAG – 17-allylamino-17-demethoxygeldanamycin |  |  |
| ATRA – All Trans Retinoic Acid |  |  |
| 5-FU – 5-fluorouracil |  |  |
| TRAIL – Tumor necrosis factor-related apoptosis-inducing ligand |  |  |

**Table 1-5. Summary of clinical trials using rapamycin or its analogs** (Easton and

Houghton 2006)

| Condition | Rapalogs | Monotherapy | Additional concurrent therapies |
|---|---|---|---|
| Endometrial cancer | CCI-779 | Yes | |
| | RAD001 | Yes | |
| | AP23573 | Yes | |
| Sarcoma | AP23573 | No | Doxorubicin |
| Recurrent or refractory B-cell lymphoma, non-Hodgkin's lymphoma, CML, CLL, ALL and AML | CCI-779 | Yes | Imatinib mesylate aracytin |
| | RAD001 | Yes | |
| | Rapamycin | Yes | |
| Hormonally treated prostate cancer patients | CCI-779 | No | Surgery |
| Mantle cell lymphoma | CCI-779 | Yes | Rituximab |
| | RAD001 | Yes | |
| Refractory or advanced non-small cell lung cancer | CCI-779 | Yes | |
| | Rapamycin | No | Gefitinib |
| Relapsed or refractory multiple myeloma | CCI-779 | Yes | |
| Metastatic or unresectable low grade neuroendocrine carcinoma | RAD001 | No | Octreotide depot |
| Advanced clear-cell renal carcinoma | RAD001 | No | Bevacizumab |
| RCC | CCI-779 | Yes | Interferon-α |
| Metastatic and refractory breast cancer | RAD001 | Yes | Docetaxel Trastuzumab Erlotinib Letrozole |
| | CCI-779 | Yes | |
| Pediatric patients with recurrent or refractory tumors | CCI-779 | Yes | |
| | RAD001 | Yes | |
| Glioblastoma multiforme | Rapamycin | Yes | |

Abbreviations: ALL, acute lymphocytic leukaemia; AML, acute myeloid leukaemia; CLL, chronic lymphocytic leukaemia; CML, chronic myeloid leukaemia; RCC, renal cell carcinoma.

**Table 1-6. PI3K/Akt/mTOR inhibitors in clinical trials for hematologic malignancies.** (Tasian, Teachey et al. 2014)
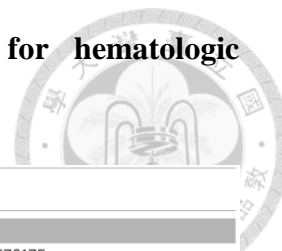
| | Target(s) | Phase of testing | Clinical trial number |
|---|---|---|---|
| **MTOR INHIBITORS** | | | |
| Sirolimus (rapamycin) | mTOR | FDA-approved | *NCT01162551 *NCT01658007 *NCT01670175 |
| Temsirolimus (CCI-779) | mTOR | FDA-approved | *NCT01403415 (COG ADVL1114) *NCT01614197 (TACL 2008-004) |
| Everolimus (RAD001) | mTOR | FDA-approved | *NCT01523977 |
| Ridaforolimus (AP23573) | mTOR | FDA-approved | completed |
| **PI3K INHIBITORS** | | | |
| BKM120 | Pan-PI3K (class I) | Phase 1/2 | NCT01396499 NCT01660451 NCT01693614 NCT01719250 NCT02049541 |
| BAY80-6946 | Pan-PI3K (class I) | Phase 1/2 | NCT01660451 |
| BYL719 | PI3K p110α | Phase 1/2 | NCT01905813 |
| GSK2636771 | PI3K p110β | Phase 1/2 | NCT01458067 |
| SAR260301 | PI3K p110β | Phase 1 | NCT01596270 |
| Idelalisib (GS-1101, CAL-101) | PI3K p110δ | FDA-approved | Multiple single-agent and combination trials |
| INCB040093 | PI3K p110δ | Phase 1 | NCT01905813 |
| AMG 319 | PI3K p110δ | Phase 1 | NCT01300026 |
| TGR 1202 | PI3K p110δ | Phase 1 | NCT01767766 |
| IPI-145 | PI3K p110γ/δ | Phase 1/2/3 | NCT02004522 NCT01882803 NCT01871675 NCT01476657 |
| **PI3K/MTOR INHIBITORS** | | | |
| BEZ235 | PI3K/mTOR | Phase 1/2 | NCT01756118 |
| SAR245409 | PI3K/mTOR | Phase 1/2 | NCT01410513 NCT01403636 |
| GDC-0980 | PI3K/mTOR | Phase 1/2 | NCT00854152 |
| VS-5584 | PI3K/mTOR | Phase 1 | NCT01991938 |
| **AKT INHIBITORS** | | | |
| MK-2206 | Akt | Phase 1/2 | NCT01369849 |
| GSK2110183 | Akt | Phase 1/2 | NCT00881946 NCT01532700 |
| **MTORC1/MTORC2 INHIBITORS** | | | |
| OSI-027 | TORC1/TORC2 | Phase 1 | NCT00698243 |
| DS-3078a | TORC1/TORC2 | Phase 1 | NCT01588678 |
| CC-223 | TORC1/TORC2 | Phase 1 | NCT01177397 NCT02031419 |
| **OTHER INHIBITORS** | | | |
| CC-115 | dual DNA-PK/mTOR | Phase 1 | NCT01353625 |
| CUDC-907 | PI3K & HDAC | Phase 1 | NCT01742988 |

Akt, A serine/threonine protein kinase B; COG, Children's Oncology Group; DNA-PK, DNA-dependent protein kinase; HDAC, histone deacetylase; mTOR, mammalian target of rapamycin; PI3K, phosphatidylinositol 3-kinase; TACL, Therapeutic Advances in Childhood Leukemia consortium NCT, ClinicalTrials.gov identifier
Open pediatric trials.

**Estimated New Cases**

| | | | Males | Females | | | |
|---|---|---|---|---|---|---|---|
| Prostate | 220,800 | 26% | | Breast | 231,840 | 29% |
| Lung & bronchus | 115,610 | 14% | | Lung & bronchus | 105,590 | 13% |
| Colon & rectum | 69,090 | 8% | | Colon & rectum | 63,610 | 8% |
| Urinary bladder | 56,320 | 7% | | Uterine corpus | 54,870 | 7% |
| Melanoma of the skin | 42,670 | 5% | | Thyroid | 47,230 | 6% |
| Non-Hodgkin lymphoma | 39,850 | 5% | | Non-Hodgkin lymphoma | 32,000 | 4% |
| Kidney & renal pelvis | 38,270 | 5% | | Melanoma of the skin | 31,200 | 4% |
| Oral cavity & pharynx | 32,670 | 4% | | Pancreas | 24,120 | 3% |
| Leukemia | 30,900 | 4% | | Leukemia | 23,370 | 3% |
| Liver & intrahepatic bile duct | 25,510 | 3% | | Kidney & renal pelvis | 23,290 | 3% |
| **All Sites** | **848,200** | **100%** | | **All Sites** | **810,170** | **100%** |

**Estimated Deaths**

| | | | Males | Females | | | |
|---|---|---|---|---|---|---|---|
| Lung & bronchus | 86,380 | 28% | | Lung & bronchus | 71,660 | 26% |
| Prostate | 27,540 | 9% | | Breast | 40,290 | 15% |
| Colon & rectum | 26,100 | 8% | | Colon & rectum | 23,600 | 9% |
| Pancreas | 20,710 | 7% | | Pancreas | 19,850 | 7% |
| Liver & intrahepatic bile duct | 17,030 | 5% | | Ovary | 14,180 | 5% |
| Leukemia | 14,210 | 5% | | Leukemia | 10,240 | 4% |
| Esophagus | 12,600 | 4% | | Uterine corpus | 10,170 | 4% |
| Urinary bladder | 11,510 | 4% | | Non-Hodgkin lymphoma | 8,310 | 3% |
| Non-Hodgkin lymphoma | 11,480 | 4% | | Liver & intrahepatic bile duct | 7,520 | 3% |
| Kidney & renal pelvis | 9,070 | 3% | | Brain & other nervous system | 6,380 | 2% |
| **All Sites** | **312,150** | **100%** | | **All Sites** | **277,280** | **100%** |

**Figure 1-1. Ten Leading Cancer Types for the Estimated New Cancer Cases and Deaths by Sex, United States, 2015**.

Estimates are rounded to the nearest 10 and cases exclude basal cell and squamous cell skin cancers and in situ carcinoma except urinary bladder (Siegel, Miller et al. 2015).
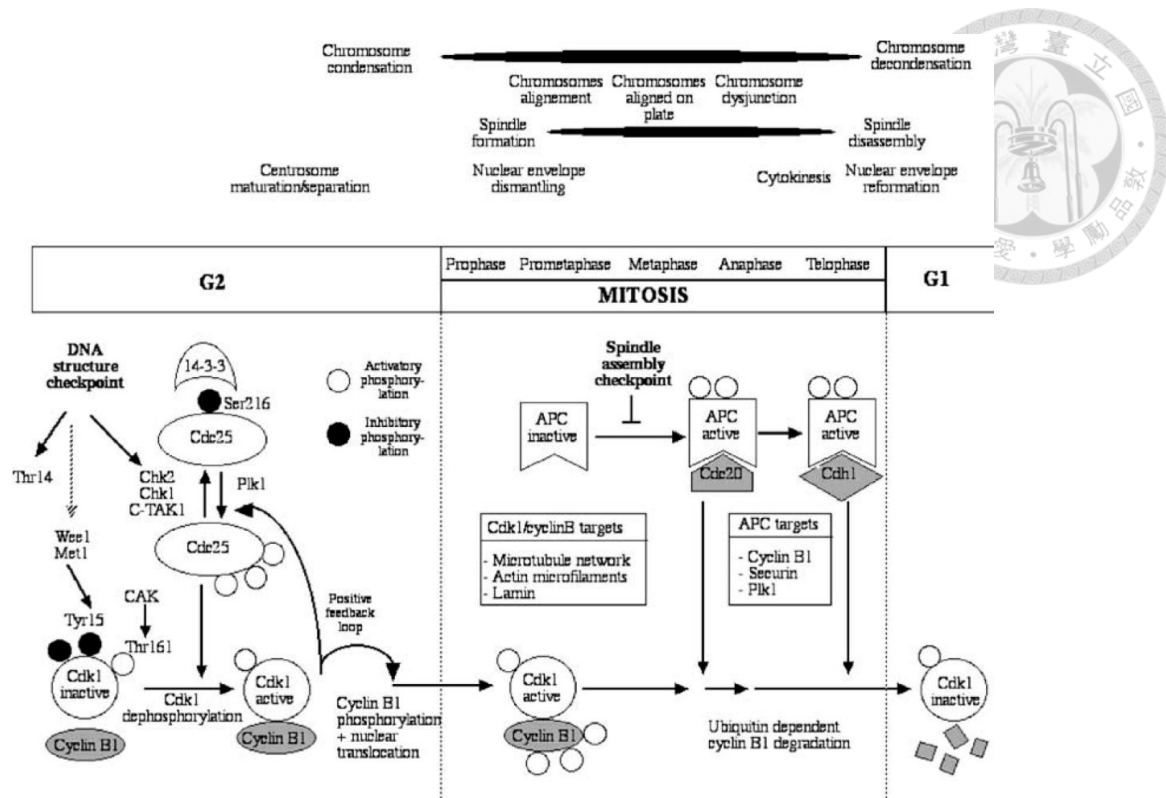
**Figure 1-2. Place of the Cdk1/cyclin B complex in mitosis.**

To allow cells to progress from the G2 to the M phase, the Cdk1/cyclin B complex is active, meaning that Cdk1 has undergone an activating phosphorylation (on Thr161) by CAK, that the inhibitory phosphorylation (on Thr14 and Tyr15) has been removed by active Cdc25C phosphatase, that Cdk1 associates with cyclin B and that the complex translocates to the nucleus. In the nucleus, the active Cdk1/cyclin B complex then phosphorylates mitotic substrate proteins. During the anaphase, the APC becomes activated and destroys Cdk1, a step that is a conditio sine qua non for entry into the anaphase. The DNA structure checkpoint activates checkpoint kinases (such as Chk1 and Chk2), which phosphorylate Cdc25C on Ser216, thereby causing its inactivation (and failure to activate Cdk1). The activation of the spindle checkpoint delays maturation of the APC (and thus prevents cyclin B degradation) (Castedo, Perfettini et al. 2004).

33
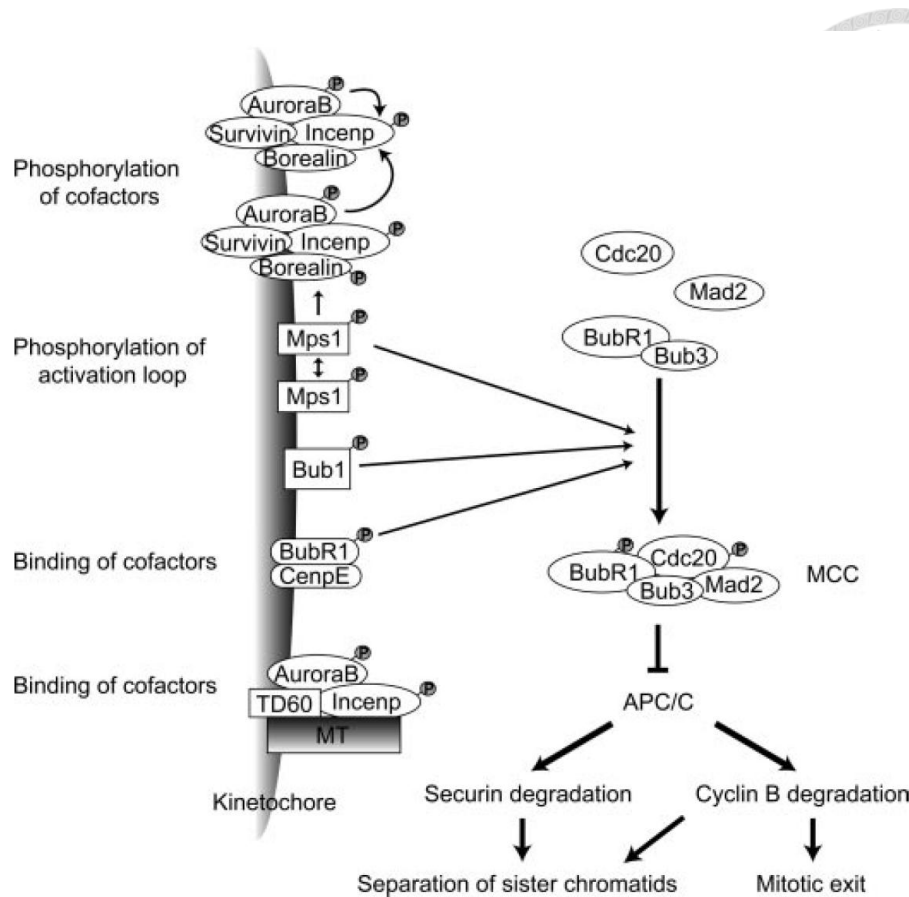
**Figure 1-3. Activation mechanisms of the spindle checkpoint kinases at the kinetochores.**

The spindle checkpoint kinases are recruited to kinetochores in a hierarchical fashion. Kinetochore binding activates these kinases through multiple mechanisms, including phosphorylation of cofactors and activation loops and binding of cofactors. The active kinases then phosphorylate downstream checkpoint components and promote the formation of the mitotic checkpoint complex (*MCC*), which inhibits APC/C. APC/C inhibition stabilizes its substrates, securin and cyclin B, which block anaphase onset and mitotic exit. *MT*, microtubules (Kang and Yu 2009).

34
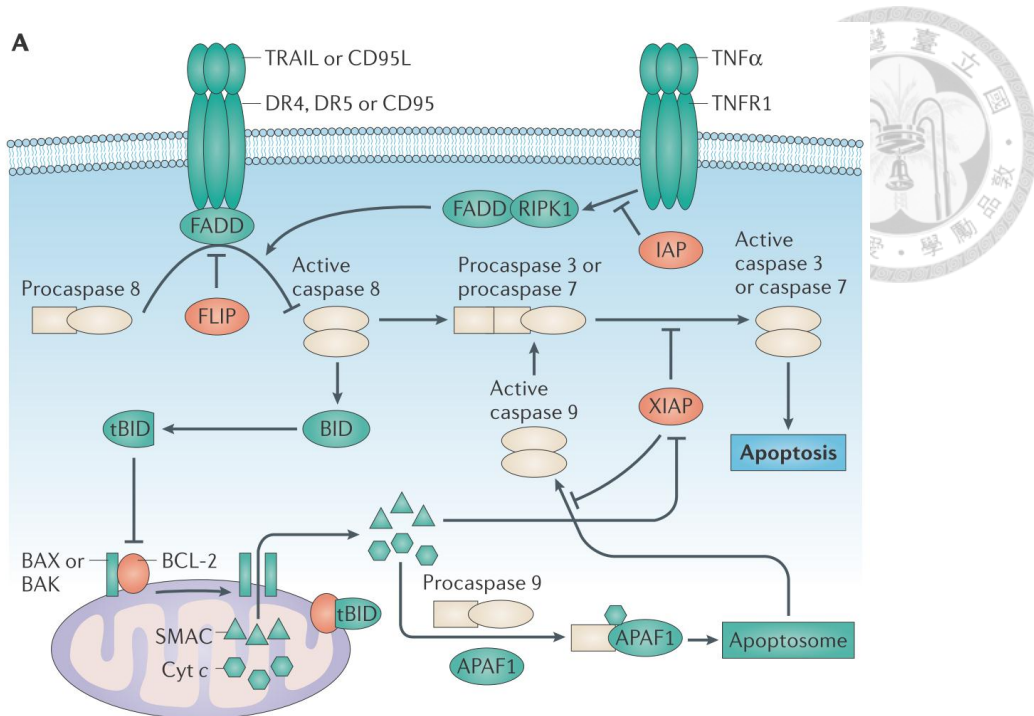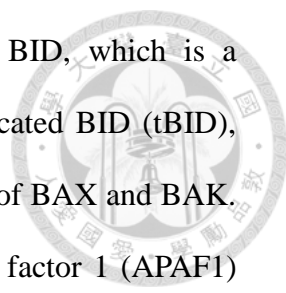
**Figure 1-4. Apoptosis signalling.**

A. Overview of apoptosis signalling. The death receptors CD95 (also known as FAS), death receptor 4 (DR4), DR5 and tumour necrosis factor receptor 1 (TNFR1) can all induce apoptosis when bound by their ligands. For example, when TNF-related apoptosis-inducing ligand (TRAIL) binds to DR4 or DR5, the receptors recruit FAS-associated protein with death domain (FADD). The resulting complex, termed the death-inducing signalling complex (DISC), recruits procaspase 8 monomers, which are then activated by homodimerization-induced cleavage to form caspase 8. Dimerization of procaspase 8 at the DISC is inhibited by FLIP. Mitochondria-mediated apoptosis is controlled by the BCL-2 family of pro- and anti-apoptotic proteins. When pro-apoptotic BAX and BAK oligomerize, they form pores in the outer mitochondrial membrane that allow the release into the cytoplasm of cytochrome c (Cyt c), second mitochondria-derived activator of caspases (SMAC) and other pro-apoptotic factors. BAX and BAK oligomerization is controlled by

35

anti-apoptotic BCL-2 proteins, including BCL-2 and BCL-XL. BID, which is a BH3-only protein, can also be cleaved by caspase 8 to form truncated BID (tBID), which translocates to the mitochondria to promote oligomerization of BAX and BAK. Cytochrome c forms a complex with apoptotic protease-activating factor 1 (APAF1) and procaspase 9 that is termed the apoptosome, in which procaspase 9 dimerizes and becomes activated. Activation of initiator caspases 8 and 9 results in the activation of downstream executioner caspases 3 and 7, which selectively cleave a range of proteins that bring about the morphological characteristics of apoptosis. Activation of caspases 3, 7 and 9 is inhibited by inhibitor of apoptosis proteins (IAPs), particularly XIAP. XIAP itself is antagonized by SMAC released from the mitochondria. IAP1 and IAP2 promote the ubiquitination of receptor-interacting serine/threonine protein kinase 1 (RIPK1) at TNFR1 'complex 1', and this leads to downstream activation of nuclear factor-κB (NF-κB) and MAPK pathways. In the absence of IAP1 and IAP2, RIPK1 is deubiquitylated and forms a second complex, 'complex 2', containing FADD that can recruit and activate procaspase 8 (Holohan, Van Schaeybroeck et al. 2013).
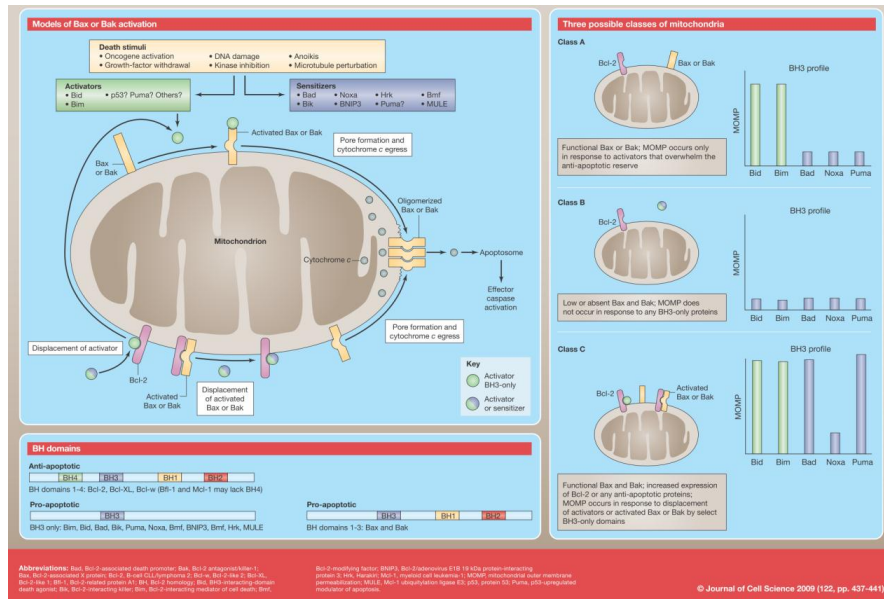
**Figure 1-5. Control of Mitochondrial Apoptosis by the Bcl-2 Family** (Brunelle and

Letai 2009)
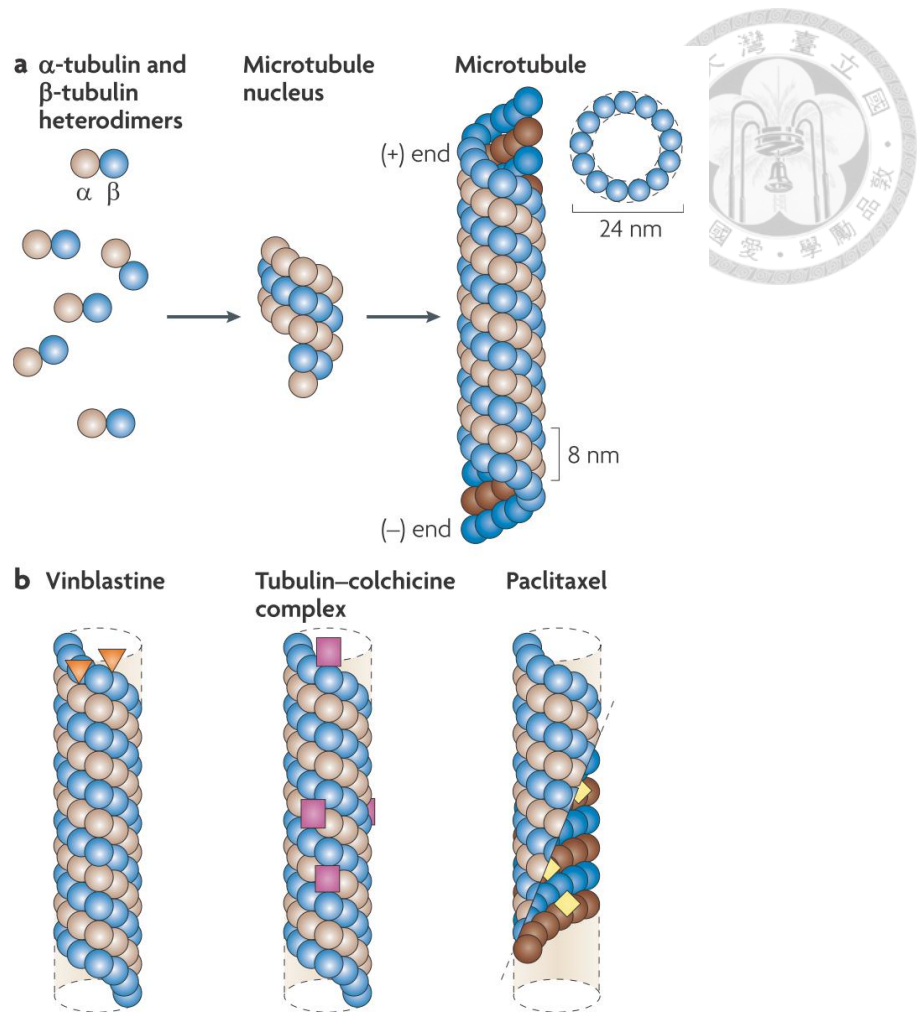
**Figure 1-6. Microtubule formation and the binding sites of microtubule inhibitors.**

a. Soluble tubulin dimers, containing one α-tubulin peptide and one β-tubulin peptide, polymerize to form a microtubule nucleus. Additional dimers are added head-to-tail and the resulting microtubules are highly dynamic structures containing a (+) end, characterized by an exposed β-tubulin peptide and a (–) end, characterized by an exposed α-tubulin peptide. b. Binding sites of microtubule inhibitors are shown (orange triangles, purple squares and yellow diamonds). Although vinca alkaloids, such as vinblastine, bind to microtubule ends, colchicine binds to soluble dimers, which can be incorporated in the microtubules. Taxanes, such as paclitaxel, bind along the interior surface of the microtubules (Dumontet and Jordan 2010).
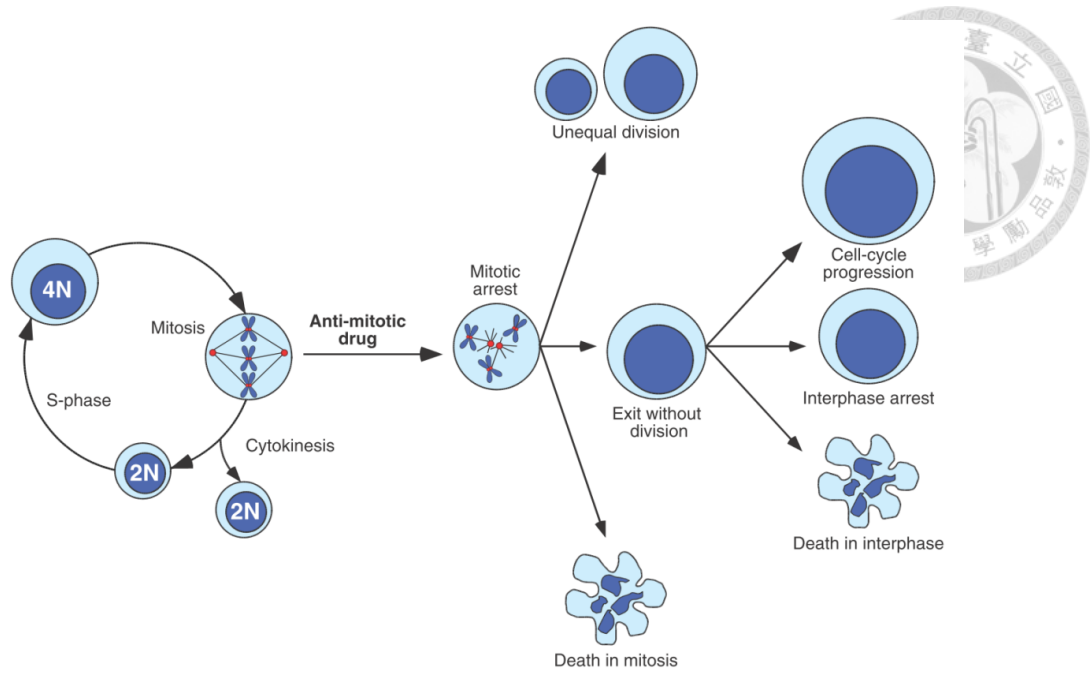
**Figur 1-7. Cell fate in response to anti-mitotic drug treatment.**

When cells are exposed to an anti-mitotic agent such as taxol, they arrest in mitosis due to chronic activation of the spindle-assembly checkpoint. They then undergo one of several fates. Cells might die directly in mitosis, or divide unequally to produce aneuploid daughter cells. Alternatively, cells might exit mitosis without undergoing division. In this case, cells might then die in interphase, arrest in interphase indefinitely or enter additional cell cycles in the absence of division (Gascoigne and Taylor 2009).
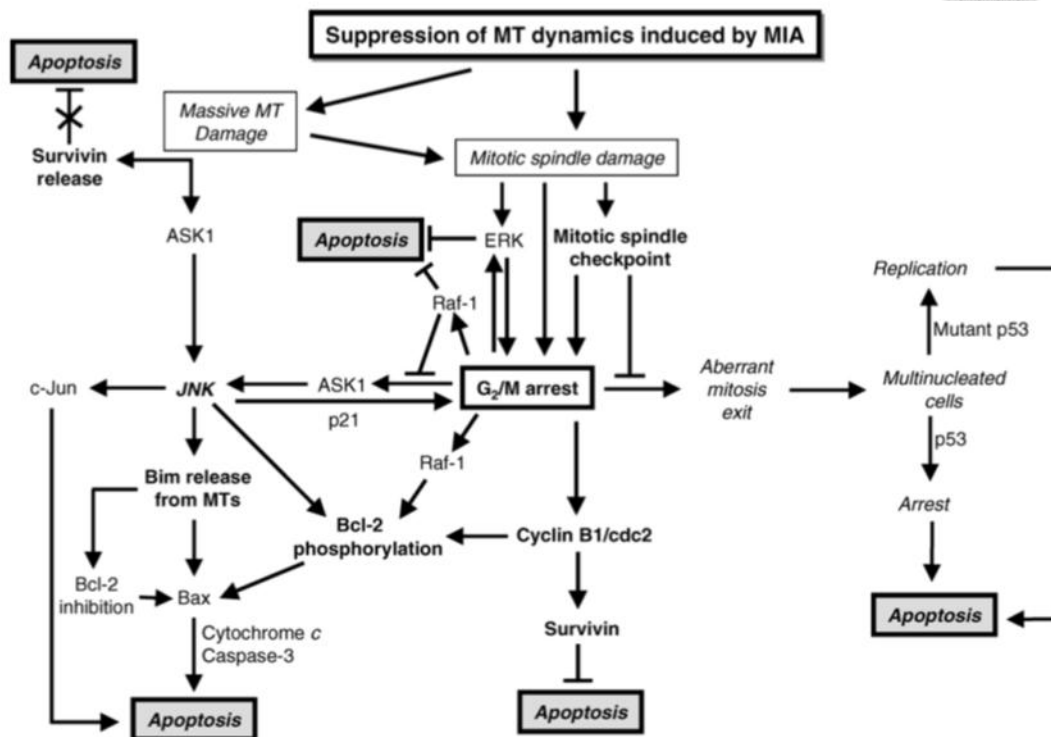
**Figure 1-8. A schematic diagram of putative events involved in MIA-induced apoptosis.**

The interaction of MIAs with microtubules results in suppression of microtubule dynamics that leads to damage in the mitotic spindle (low concentrations of MIAs) or to a massive microtubule damage (high concentrations of MIAs) depending on drug concentration and time of exposure. These actions induce a cell cycle arrest at the M phase or a general failure in microtubule-related functions depending on the level of microtubule damage. These effects together with the abnormal exit of mitosis, which leads to multinucleated cells and eventually to cell death, are the major mechanisms involved in MIA-induced apoptosis. The persistent activation of a number of signaling routes (labeled in bold) could play a major role in the ultimate apoptotic response. MIA: microtubule-interfering agent; MT: microtubule. (Mollinedo and Gajate 2003)
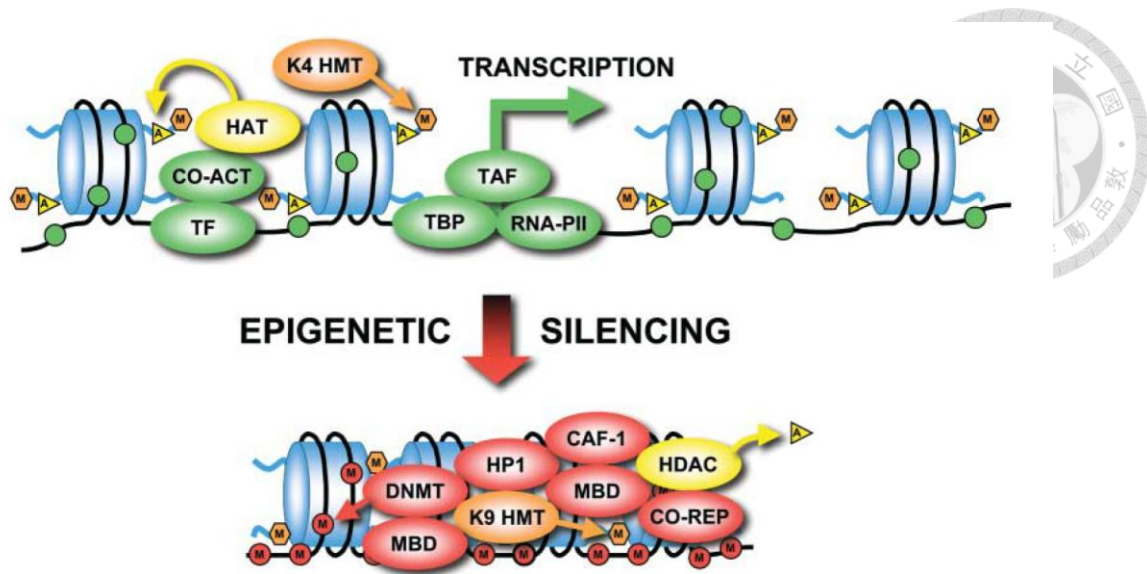
**Figure 1-9. Epigenetic Silencing.** Schematic of some of the molecular events that occur at CpG-rich promoters undergoing epigenetic silencing in cancer cells. The open chromatin structure of a transcriptionally active gene with loosely spaced nucleosomes (blue cylinders) is shown at the top and the transcriptionally silenced state with more tightly packed nucleosomes is shown at the bottom. DNA is indicated by a thin black line wrapped around nucleosomes. Proteins are indicated by shaded ovals, histone H3 acetylation is indicated by yellow triangles, hstone H3 methylation is indicated by orange hexagons and CpG dinucleotides are indicated by circles strung along the DNA, with green circles denoting an unmethylated state and red circles indicating a methylated state. Proteins involved in transcriptional activation are indicated in green (TF, tanscription factor; CO-ACT, co-activator; TBP, tata-binding factor; TAF, TBP-associated factor; RNA-PII, RNA polymerase II). Histone acetyl transferases (HAT) and histone deacetylases (HDAC) are indicated in yellow. Histone H3 lysine-4 (K4 HMT) and lysine-9 (K9-HMT) are indicated in orange. Proteins involved in transcriptional silencing are indicated in red (DNMT, DNA methyltransferase; MBD, methyl-binding domain protein; CO-REP, co-repressor; HP1, heterochromatin protein 1; CAF-1, chromatin assembly factor-1) (Laird 2005).
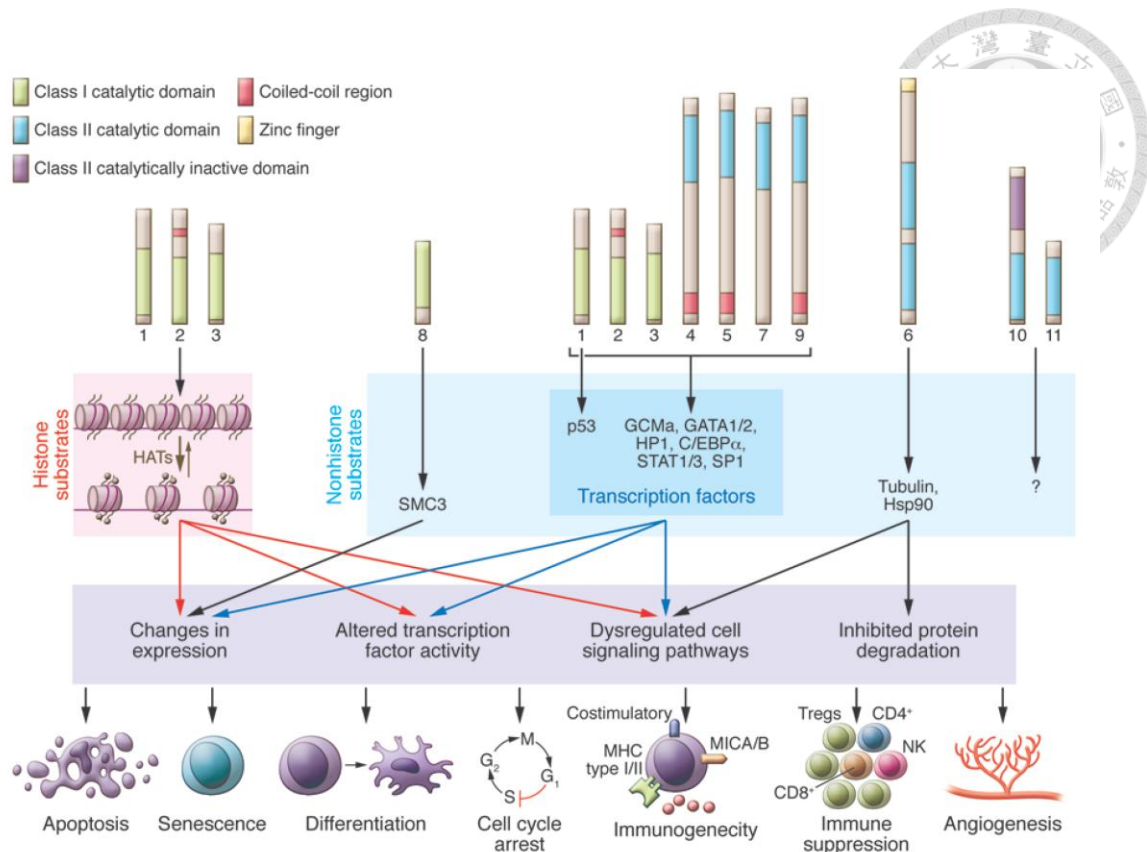
**Figure 1-10. The molecular targets of HDACs, downstream cellular pathways, and anticancer outcomes of HDAC inhibition.**

HDAC substrates include histones and nonhistone proteins. Histones are the primary substrates for HDAC1, -2, and -3, while other cellular proteins are targeted by one or more class I and class II HDACs. Some known HDAC targets, downstream molecular changes that occur following HDAC inhibition, and associated biological pathways that mediate antitumor responses are shown. The HDACs, substrates, and molecular responses are color matched to illustrate functional relationships. The best-characterized biological consequences of HDACi treatment of tumor cells are shown on the lowest tier of the diagram. SMC3, structural maintenance of chromosomes 3; GCMa, glial cells missing homolog 1; HAT, histone acetyltransferase; HP1, heterochromatin protein 1.(West and Johnstone 2014)

| | HDAC1 | HDAC2 | CoREST | NuRD | Sin3 | HDAC3 | NCoR | HDAC8 | HDAC6 | HDAC10 |
|---|---|---|---|---|---|---|---|---|---|---|
| Apcidin | ++ | ++ | ++ | ++ | ++ | ++ | ++ | – | – | – |
| Belinostat | ++ | ++ | ++ | ++ | ++ | ++ | ++ | – | ++ | – |
| Entinostat | ++ | ++ | ++ | ++ | – | ++ | ++ | + | – | – |
| Mocetinostat | ++ | ++ | ++ | ++ | – | ++ | ++ | – | – | – |
| Panobinostat | ++ | ++ | ++ | ++ | ++ | ++ | ++ | – | – | + |
| Abexinostat | ++ | ++ | ++ | ++ | ++ | ++ | ++ | – | ++ | ++ |
| PCI-334051 | – | – | – | – | – | – | – | ++ | – | – |
| Romidepsin | ++ | ++ | ++ | ++ | ++ | ++ | ++ | – | – | – |
| Vorinostat | ++ | ++ | ++ | ++ | ++ | ++ | ++ | – | ++ | + |
| Trichostatin A | ++ | ++ | ++ | ++ | ++ | + | ++ | – | + | – |
| Valproic acid | ++ | ++ | ++ | ++ | – | + | + | – | – | – |
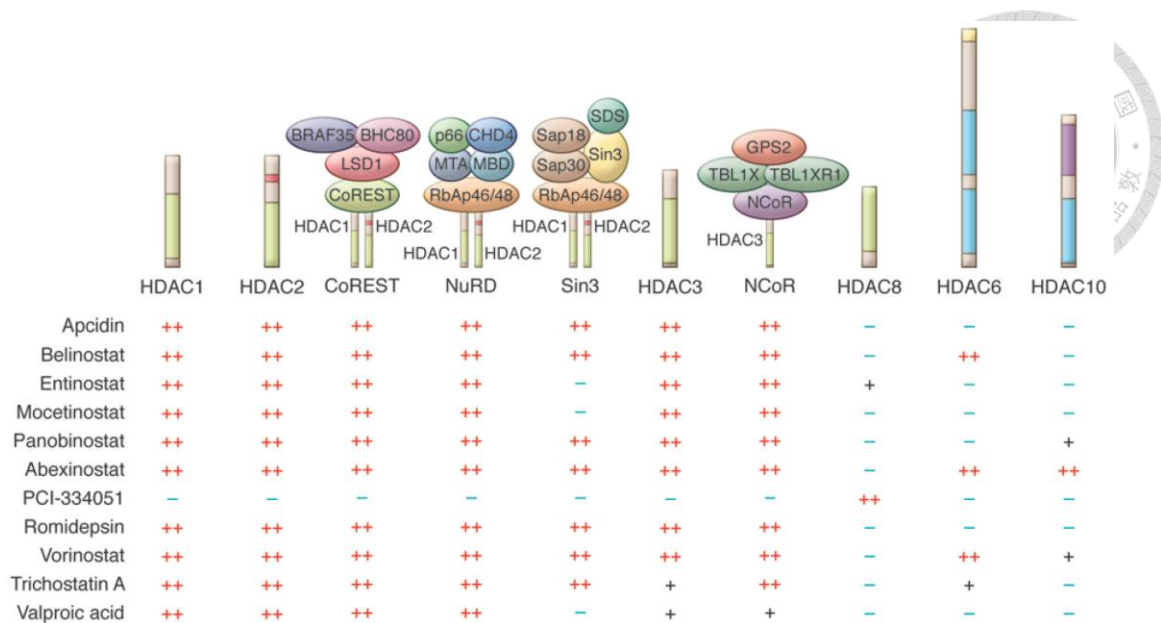
**Figure 1-11. The specicity of HDACis for HDACs and associated protein complexes.** The specicity of HDACis for HDAC isoforms has been recently reclassied using sophisticated chemoproteomics and chemical phylogenetic approaches, revealing that HDACis have surprising affinity for both HDACs and individual HDAC-dependent multiprotein complexes. This new specicity is shown for class I HDAC1, -2, -3, and -8 as well as class IIb HDAC6 and -10; specicity is calculated from average KD app values generated by Bantscheff et al. and Bradner et al.. Illustration based on data from Deubzer et al., Bolden et al., Bantscheff et al., and Bradner et al.. BHC80, BRAF35-HDAC complex protein; CHD4, chromodomain helicase DNA binding protein 4; CoREST, REST corepressor 1; LSD1, lysine-specic demethylase 1; MTA, metastasis-associated protein; MBD, methyl-CpG binding domain protein; NuRD, nucleosome remodeling and deacetylase; RbAp46, retinoblastoma-binding protein p46; Sap30, Sin3A-associated protein, 30 kDa; SDS, serine dehydratase; TBL1X, transducin β-like 1X-linked; TBL1XR1, transducin β-like 1 X-linked receptor 1; GPS2, G protein pathway suppressor 2. (West and Johnstone 2014)
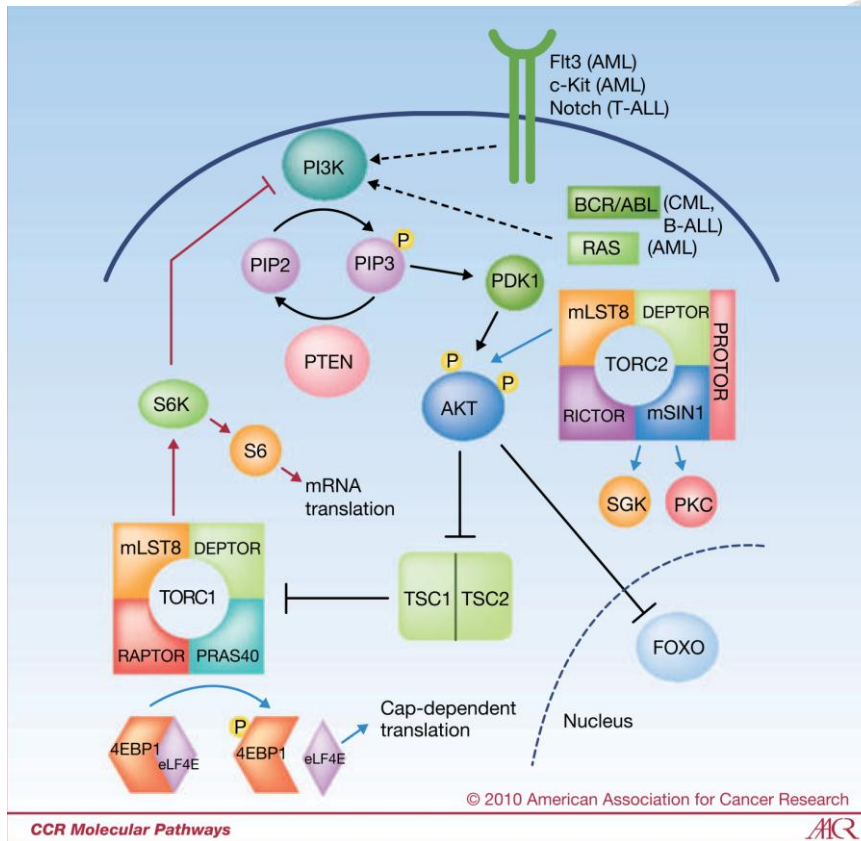
**Fig. 1-12. Diagram of key features of the PI3K/AKT/TOR signaling network.**

The lipid kinase PI3K is activated downstream of oncogenic receptors or intracellular proteins (dashed arrows) in various hematological diseases, with examples shown. PI3K generates the second messenger PIP3. The TOR serine-threonine kinase is present in two distinct multiprotein complexes, termed TORC1 and TORC2. Key substrates are shown, and their activities are either increased (pointed arrows) or decreased (block arrows) by TOR-mediated phosphorylation. Rapalogs inhibit the processes shown in red. as mTORi block these events, as well as those shown in blue, though it should be noted that rapalogs have partial effects on 4EBP1 phosphorylation in a context-dependent manner. Some molecular details and functional outcomes have been omitted for simplicity (Vu and Fruman 2010).
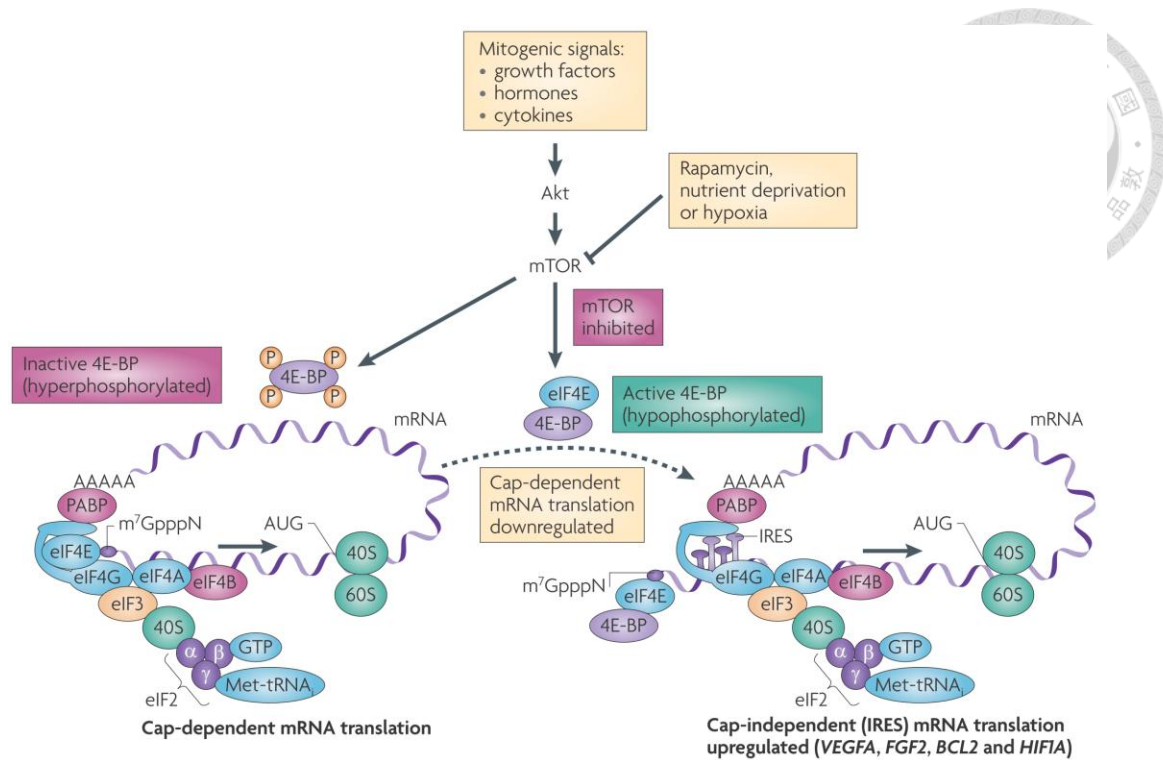
**Figure 1-13. A cap-dependent to cap-independent translation switch mediated by the Akt–mTOR-4EBP pathway.**

Mitogenic signals such as growth factors, hormones and cytokines activate the protein kinase Akt, which in turn phosphorylates and activates mTOR, the kinase component of mTOR complex 1 (mTORC1). Activated mTOR phosphorylates and inactivates the eukaryotic initiation factor 4E (eIF4E) inhibitory binding proteins (4E-BPs), freeing eIF4E to bind eIF4G and promoting cap-dependent translation. Downregulation of mTOR activity by physiological stresses such as hypoxia, nutrient deprivation and the drug rapamycin, leads to hypophosphorylated (activated) 4E-BP proteins that compete with eIF4G for binding to eIF4E, preventing cap-dependent translation. The eIF4E–4E-BP complex might remain bound to the m7GpppN cap (as shown), possibly aiding the inhibition of cap-dependent mRNA translation owing to blockade of the mRNA 5´ end. Increased levels of hypophosphorylated 4E-BPs, in conjunction with elevated levels of eIF4G, can then function as a switch, as observed in certain locally advanced

cancers, impairing the initiation of translation on purely cap-dependent mRNAs but enhancing translation of dual mechanism mRNAs that also contain an internal ribosome entry site (IRES) to which eIF4G may bind directly. These mRNAs include vascular endothelial growth factor A (VEGFA), fibroblast growth factor 2 (FGF2), BCL2 and hypoxia-inducible factor 1α (HIF1A). This switch is activated by hypoxia and other stresses to preserve tumour cell viability and promote tumour angiogenesis. PABP, polyA tail binding protein (Silvera, Formenti et al. 2010).

# Chapter 2 Materials and Methods

## 2-1 Materials

Vincristine, suberoylanilide hydroxamic acid (SAHA) and paclitaxel were purchased from Sigma Chemical Co. (St. Louis, MO, USA); tubastatin A, Acy1215 (HDAC6 inhibitor) and MPT0B392 were synthesized from Dr. Jing-Ping Liou (Taipei Medical University, Taiwan); YXM110 was designed by Dr. Kuo-Hsiung Lee and Dr. Xiao-Ming Yang (Natural Products Research Laboratories, Eshelman School of Pharmacy, University of North Carolina at Chapel Hill, NC). All the above drugs were reconstituted in dimethysulfoxide (DMSO) and then preserved at -20℃.

Rhodamine 123, 3-(4, 5-dimethylthiazol-2-yl)-2,5-diphenyltetrazolium (MTT), propidium iodide (PI), anti-β-tubulin, FITC-conjugated anti-mouse IgG and all of the other chemical reagents used in this study were purchased from Sigma Chemical (St. Louis, MO, USA) and of analytical grade. Primary antibodies against Cdc2 (pY15)、 Aurora B、caspase-8、caspase-9、HDAC1、HDAC2、HDAC3、HDAC4、Bid、 p-mTOR、t-mTOR、p-AKT、p-P70S6K、P70S6K、p-4EBP、t-4EBP were all purchased from Cell Signaling Technologies (Beverly, MA); Cyclin B1、Cdc25C、Cdc2、PARP、 Mcl-1、Bcl-2、Bcl-xl、pBcl-2 and secondary antibodies were purchased from Santa Cruz (Santa Cruz, CA, USA); MPM2 (pSer/Thr) and H3 (pS10) were purchased from Upstate Biotechnology (Lake Placid, NY, USA); PLK (pT210)、caspase 6 and caspase 7 were purchased from BD Bioscience (San Jos, CS, USA); caspase 3 was purchased from Imgenex (San Diego, CA, USA); acetyl-histone 3 was purchased from Millipore (Billerica, MA, USA); internal control, GAPDH and actin, were purchased from Novus

Biologicals (Littleton, CO, USA). Vectasheld® mounting medium with DAPI was purchased from Burlingame, CA, USA.

# 2-2 Methods

**Cell Culture and hypoxia**

HL60 (acute promyelocytic leukemia), MOLT-4 (acute lymphoblastic leukemia), CCRF-CEM (acute lymphoblastic leukemia), BEAS (normal human bronchial epithelium) and HUVEC (human umbilical vein endothelial cell) were purchased from BCRC (Bioresource Collection and Research Centre, Taiwan); NCI/ADR-RES cell line was obtained from the DTP Human Tumor Cell Line Screen; MV4-11(acute myeloid leukemia cell) and MOLM-13 (acute myeloid leukemia cell) were kindly gifted from National Health Research Institutes. Human colorectal cancer cell line HCT116, HT-29 and Colo205 were purchased from American Type Culture Collection (ATCC; Manassas, VA, USA); SW480, SW620, Caco-2 and CCD-18co were kindly gift from Min-Chuan Huang (Graduate institute of Anatomy and Cell Biology, College of Medicine, National Taiwan University) and Kuen-Haur Lee (Program for Cancer Biology and Drug Discovery, College of Medical Science and Technology, Taipei Medical University).

HL60, MOLT-4, CCRF-CEM, BEAS, MV4-11, MOLM-13, HCT116, HT-29 and Colo205 were maintained in RPMI-1640 medium (Invitrogen, NY, USA); SW480, SW620 and Caco-2 were maintained in DMEM medium (Gibco, Invitrogen, Carlsbad, CA, USA); CCD-18co was in MEM medium (Gibco, Invitrogen, Carlsbad, CA, USA). All of above were supplemented with 10% (v/v) fetal bovine serum (FBS, Gibco BRL Life Technologies, Grand Island, NY, USA). HUVEC were grown in endothelial cell medium (ECM) (ScienCell Research Laboratory, Carlsbad, CA) supplemented with 20% FBS. Penicillin 100 U/ml, streptomycin 100 μg/ml, and amphotericin B 2.5

μg/ml were added to the mediums. All cell lines were incubated in 5% $CO_2$/95% air at 37℃. Hypoxia incubations were performed in hypoxia chamber, which was flushed with 1% $O_2$, 5% $CO_2$, and 94% $N_2$ at 37 ℃ (BioSpherix Proox 110), and incubated for the indicated time.
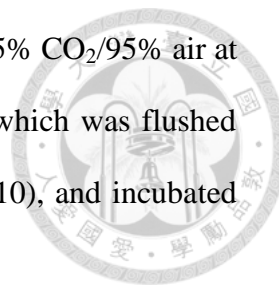
**Cell viability assay**

Suspension cell

Cell viability was verified by MTT assay. Firstly, cells were seeded in a 24-well plate at a density of $4\times10^5$ cells/well in 1 ml culture medium then treated with various concentrations of drugs or reagents for indicated time. After treatment with drugs, 100 μl MTT solution (0.5 mg/ml in PBS, phosphate-buffered saline) per well was added to 24-well plate in the dark and the plate was incubated at 37℃. The mitochondrial dehydrogenase of viable cells reduced 3-(4,5-dimethylthiazol-2-yl) -2,5-diphenyltetrazolium bromide, MTT (yellow) to insoluble formazan dyes (purple). One hour later, the crystal formazan dyes were dissolved in the extraction buffer (0.1 M sodium acetate buffer, 100 μl/well). The absorbance was spectrophotometrically analyzed at 550 nm by ELISA reader (Packard, Meriden, CT, USA).

Adhesion cell

Cells were seeded in 96-well plates in growth medium overnight. Cells were treated with vehicle (0.1% DMSO) or different concentrations of compound for 24 h, then incubated with MTT reagent at 37℃ for 1 h. After incubation, the insoluble formazan produced in living cells. The formazan crystals were dissolved with DMSO and the absorbance was measured at 550 nm. Results were calculated as: cell viability (%) =

average O.D. of wells/ average O.D. of control wells.
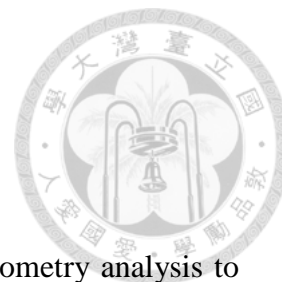
**Flow cytometry analysis**

Evaluation of the cell cycle histogram was performed by flow cytometry analysis to detect the changes of DNA content. $4\times 10^5$ cells were seeded in 6-well plates in 2 ml fresh medium and treated with graded concentrations of drugs for the indicated time. Then, cells were collected, washed with PBS and fixed with 70% (v/v) ice cold ethanol at -20℃ for 30 min. The fixed cells were centrifuged to remove the ethanol, rinsed with (PBS), resuspensed in 0.1 ml DNA extraction buffer (0.2M $Na_2HPO_4$-0.1M citritic buffer, pH 7.8) for 20 min and subsequently stained with 500 ul PI solution (80 μg/ml propidium iodide, 100 μg/ml RNase A, and 1% Triton X-100 in PBS) for 20 min at room temperature in the dark. Data were analyzed by FACScan Flow Cytometer and CellQuest software (Bectman Dickinson).

***In vitro* tubulin polymerization assay**

To determine the microtubule polymerization of the indicated drugs in cell-free condition, CytoDYNAMIX screen 03 kit (Cytoskeleton Inc.) was performed. General Tubulin Buffer、GTP stock (100 mM)、Tubulin protein (10 mg/ml) were all prepared well following the protocol. The 96-well plate was placed in the Spectrophotometer to pre-warm at 37 ℃ for 30 min before detection. Then preparing the iced tubulin polymerization (TP) buffer, all mentioned processes were needed on the ice. Next, the drugs (2 μl) were added into the each eppendorf included with 85 μl TP buffer. The drugs must include DMSO (the control group)、paclitaxel (10 μM) and vincristine (10 μM). Paclitaxel and vincristine were used as positive control. Paclitaxel would induce the microtubule polymerization, in contrast, vincristine depolymerize microtubule.

51

Finally, 30 µl tubulin proteins was added into the eppendorf and transferred to the well-warmed 96 well plate. The absorbance was measured by spectrophotometer and recorded every one minute for 30 min at 340 nm and 37 ℃.
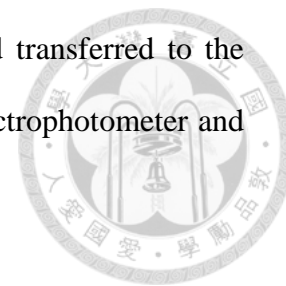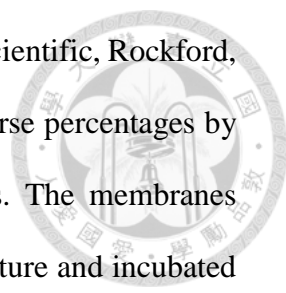
**Immunofluorence analysis**

Microtubule distribution and morphology were detected by immunofluorescence. Cover slides were placed in the 24-well plate and coated with poly-D-lysine for 1 day at least to enhance the suspension cells attached to the cover slides. Cells were seeded into the 24-well plate ($8 \times 10^5$ cells/well) and treated with vincristine, SAHA, or both drugs for 24 h. The following experiments were performed at room temperature. The cells were fixed with 8 % paraformaldehyde in PBS for 15 min. After washing with PBS for several times, the cells were permeabilized with 0.1 % Triton X-100 in PBS for 10 min. Then, the cells were rinsed with PBS for 10 min three times. For blocking, 3 % BSA in PBS was used. After 1 h, the cells were washed with PBS and incubated with a primary β-tubulin antibody (1:200) for 2 h and FITC-conjugated anti-mouse IgG antibody (1:200) for 2 h. The mounting medium, which contains DAPI stain, was dropped onto the slides, and cover slides were recovered to the slides. Images were detected and captured with the ZEISS LSM 510 META confocal microscope.

**Western blot analysis.**

After the treatment, cells ($10^6$ cells/ml) were harvested. Whole cell pellets were washed twice with PBS, lysed in lysis buffer (50 mM Tris, pH 7.4; 150 mM NaCl; 1 % Triton X-100; 1 mM EDTA; 1 mM EGTA) supplemented with protease inhibitors (1 mM PMSF, 10 µg/ml aprotinin, 10 µg/ml leupeptin, 1 mM sodium orthovanadate, and 1 mM NaF) for 30 min, and then centrifuged for 30 min at 13,000 rpm at 4 ℃. Total protein

content was quantified by BCA Protein Assay Kit (Thermo Fisher Scientific, Rockford, IL, USA). Equivalent amounts of proteins were separated into diverse percentages by SDS-PAGE and subsequently transferred onto PVDF membranes. The membranes were blocked with 5 % nonfat milk in PBS for 1 h at room temperature and incubated with primary antibody in PBST buffer (0.1 % Tween 20 in PBS) at 4 °C overnight. After washing the membranes with PBST, blots were developed with the corresponding HRP-conjugated secondary antibody diluted in 0.5 % nonfat milk in PBS for 1 h at room temperature. The membrane was washed frequently with PBST, and finally immunoreactive protein bands were displayed using an enhanced chemiluminescence detection kit (Amersham, Buckinghamshire, UK).

**Mitochondrial membrane potential loss**

Rhodamine 123 was used to evaluate mitochondrial membrane potential. Rhodamine 123 is a kind of cationic fluorescent dye, which localizes in the mitochondria. Loss of mitochondrial membrane potential is associated with a lack of rhodamine 123 retention and a decrease of fluorescence intensity. Cells were treated with vincristine, SAHA, or combination for the indicated time. Rhodamine 123 (final concentration 10 μM) was added and incubated for 30 min at 37 °C in the dark. Then, cells were harvested and rinsed with PBS. The fluorescence intensity was measured by FACScan Flow Cytometer and CellQuest software (Becton Dickinson)

**P-gp activity assay**

Cells were treated with or without the indicated agents for 30 min and then co-treated with 10 μM rhodiamine 123 for 30 min at 37℃. Cells were trpsinized, washed with PBS and analyzed by flow cytometry (FACSCalibur, BD Biosciences).

**Tumor xenograft model**

Tumor xenograft model was used to estimate the effect of drugs *in vivo*. MOLT-4 cells were implanted ($10^7$ cells/ml) into serve combined immunnodeficient (SCID) mice. When average tumor size reached to 100 mm$^3$, mice were treated with indicated dosage of vincristine or SAHA alone or combination or B392 alone. Mice were scarified until the average tumor size was larger than 2,500 mm$^3$. Tumors size was measured by caliper measurement (mm) and ellipsoid sphere formula (LW2/2, L: length; W: width). Then, tumors were resected and frozen for the western blot analysis to evaluate the effect of vincristine/SAHA combination *in vivo*. All animal experiments followed ethical standards, and protocols have been reviewed and approved by Animal Use and Management Committee of National Taiwan University.

**Immunohistochemical Staining**

Tumor tissues were resected, immersed in formaldehyde, embedded in paraffin and sectioned. The sectioned slides were stained with the primary antibody cleavage caspase 3 or hematoxylin and eosin staining. HRP-polymer conjugated secondary antibody (SuperPicture Polymer Detection kit) was used and then sectioned slides were stained with DAB Chromogen for 5 min. Mayer's Hematoxylin solution was used for counterstaining. Other sectioned slides in the same tissues were stained with hematoxylin and eosin (H&E), the color of nuclei was blue and of cytoplasma was pink.

For 4E-BP1

Non-cancerous and colorectal cancer tissues were sectioned from patients and

formalin-fixed and paraffin-embedded. These sections were deparaffinized with xylen, rehydrated in different concentration of alcohol and immersed in 3% $H_2O_2$ for removing endogenous peroxidase. Sections were heated in a microwave in citrate buffer (pH 6.0) for antigen retrieval. Washing with PBS, the sections were blocked with 3% BSA/PBS for 30 min and incubated with anti-4E-BP1 antibody (Cell Signaling) at 4°C overnight. The streptavidin peroxidase method was performed (Dako, LSAB kit) to develop the signal.

**Study Subjects**

Primary colorectal cancer patients were admitted to Taipei Medical University Hospital, China Medical University Hospital and Chung Shan Medical University Hospital. All of them wrote informed consent approved by the Institutional Review Board (IRB number: 201402018 and 201312018). The enrolled patients did not receive any chemotherapy or radiation therapy prior to surgery. The TNM stages of all colorectal cancer patients were determined according to the American Joint Committee on Cancer/International Union Against Cancer TNM staging system.

**Quantitative RT-PCR**

Total RNA was extracted with TRIzol reagent by the manufacturer's protocol (Invitrogen, USA). 5 µg mRNA was incubated with random primer at 65°C for 5 min, then mixed with M-MLV RT at 37°C for 1 h to obtain cDNA. The SYBR Green PCR reaction (SYBR® Green PCR Master Mix; Roche, Switzerland) was used to evaluate the amplification of *HIF-1α*, *HIF-1b, VEGFA* and *VEGFC* genes. Primer sequences used for amplification are as follows: HIF-1α, 5'-ATC CAT GTG ACC ATG AGG AAA TG-3' and 3'-TCG GCT AGT TAG GGT ACA CTT C-5';

HIF-1β, 5'-TTTATCCCTAGAGATGGGTACAGG-3' and 5'-CCACAGGCTGGACAGAAACC-3; VEGFA, 5'-AAC CAT GAG TTT ATC GCC ACC-3' and 5'-AGC GTT ACA TTG CCT GCA TTT-3'; VEGF-C, 5'-GCCAACCTCAACTCAAGGAC-3' and 5'-CCCACATCTGTAGACGGACA-3'. Fluorescent signal was detected and recorded by StepOne Real-Time PCR System (Applied Biosystems, USA), and each amplification reaction was checked for the absence of nonspecific PCR products by melting curve. Relative fold changes in gene expression are calculated as $2^{-\Delta\Delta Ct}$.

**Transient transfection**

For luciferase assay, cells were seeded in 24-well plates (15,000 cells/well) overnight, and then transfected with 5-HRE-Luciferase reporter plasmid with Lipofectamine 2000 Transfection Reagent (Invitrogen) according to the manufacturer's protocol. HCT116 cells were treated with vehicle (0.1% DMSO) or YXM110 (0.1 or 0.3 μM) under normoxia or hypoxia conditions for 24 h. The promoter activity was determined by using Luciferase Assay System (#E1500) from Promega. For cap-dependent and cap-independent translation assay, cells overexpressing wild-type 4E-BP1 were transfected with pFR-LUCs plasmid, which is a kind gift from Tarn, Woan-Yuh (Institutive of Biomedical Sciences, Academia Sinica, Taiwan), expressing bicistronic mRNA reporter containing a cap-dependent Firefly luciferase and cap-independent Renilla luciferase. The dual luciferase activity was determined by using Dual-Luciferase® Reporter Assay (Promega).

**VEGF ELISA**

HCT116 cells were seeded in 24-well (15,000 cells/well) overnight, and then treated

with vehicle or YXM110 under normoxia or hypoxia conditions for 24 h. Culture medium were collected to measure the amount of VEGF by Human VEGF Quantikine ELISA Kit (R&D, Minneapolis, USA) according to the manufacturer's instructions.
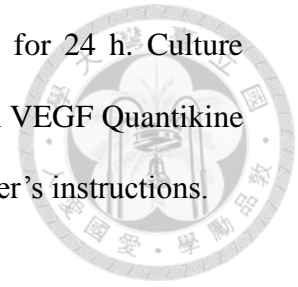
**Statistical analysis**

All experimental data were repeated at least three times and expressed as means (±SD). Logistic regression analysis was used to assess the association of 4E-BP1 and age, gender, tumor progression. The survival and recurrence time of animal experiments were estimated by Kaplan-Meier method. Statistical analysis of data was performed with one-way ANOVA followed by the Student's *t* test, and *p* <0.05 were considered significant (\*$P$ <0.05, \*\*$P$ <0.01, \*\*\*$P$ <0.001).

# Chapter 3

# 探討 vincristine 和 vorinostat 合併使用在人類血癌細胞中之加成性抗癌機轉

# The synergic anticancer effect of vincristine and vorinostat in leukemia *in vitro* and *in vivo*

# 中文摘要

　　合併療法是一種重要的抗癌治療策略，目的是為了可以減少抗藥性的產生。Vincristine 屬於微管抑制劑，在臨床上一直被用來治療急性白血病。為了能夠降低 vincristine 所產生的毒性以及抗藥性，本實驗主要目的是探討 vincristine 和廣效性的 HDAC 抑制劑，vorinostat (SAHA) 合併使用在急性 T 細胞型淋巴性白血病細胞株具有協同作用及其可能的作用機轉。從 MTT 試驗中，vincristine 和 SAHA 可有效地抑制血癌細胞存活率，$IC_{50}$ 分別為 3.3 nM 和 840 nM，當兩個藥物合併使用後 vincristine 之 $IC_{50}$ 降至 0.88 nM。從細胞週期結果發現兩個藥物合併使用能夠濃度依賴性並加成性地讓癌細胞聚集到 $G_2/M$ 期，且隨著時間的增加，癌細胞聚集到 $subG_1$ 期的數目也隨之增加並且活化 caspases。此外，vincristine 和 選擇性 HDAC6 抑制劑 (乙醯化 α-tubulin) 合併使用的結果和 vincristine/SAHA 的效果一致，因此推測 SAHA 可能是透過抑制 HDAC6 進而改變微管的動態平衡。綜合以上結果發現，於人類 T 細胞白血病細胞中 vincristine 和 SAHA 的合併使用，雙管齊下改變細胞的微管動態平衡，導致細胞停滯在 M 期，最後誘發細胞進入凋亡途徑。所以希冀 vincristine 和 SAHA 的合併機轉能做為未來臨床試驗的研究基礎依據。

# **Abstract**
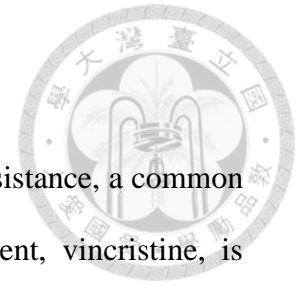
Combination therapy is a key strategy for minimizing drug resistance, a common problem in cancer therapy. The microtubule depolymerizing agent, vincristine, is widely used in the treatment of acute leukemia. In order to decrease toxicity and chemoresistance of vincristine, this study will investigate the effects of combination vincristine and vorinostat (suberoylanilide hydroxamic acid, SAHA), a pan-histone deacetylase inhibitor, on human acute T cell lymphoblastic leukemia cells. Cell viability showed that the combination of vincristine and SAHA exhibited greater cytotoxicity with an $IC_{50}$ value of 0.88 nM, compared to each drug alone, 3.3 and 840 nM. This combination synergically induced $G_2/M$ arrest, followed by an increase in cell number at the sub-$G_1$ phase and caspase activation. Moreover, the results of vincristine combined with a HDAC6 inhibitor, which acetylated $\alpha$-tubulin, were consistent with the effects of vincristine/SAHA co-treatment, thus suggesting that SAHA may alter microtubule dynamics through HDAC6 inhibition. These findings indicate that the combination of vincristine and SAHA on T cell leukemic cells resulted in a change of microtubule dynamics contributing to M phase arrest followed by induction of the apoptotic pathway. These data suggest that the combination effect of vincristine/SAHA could have an important preclinical basis for future clinical trial testing.

# 3-1 Results
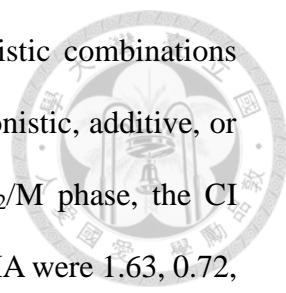
**Cytotoxic effects of vincristine and SAHA, alone and in combination, in human leukemic MOLT-4 cells**

A MTT assay was performed to investigate the cytotoxicity of microtubule destabilizing agent vincristine and HDACi vorinostat (SAHA) on human ALL MOLT-4 cells. We first tested the cytotoxic effect of SAHA and vincristine alone and in combination. As shown in Figure 3-1A, there was no significant cytotoxicity at concentrations up to 500 nM of SAHA. However, SAHA had an $IC_{50}$ of 840 nM for 48 h, when concentration reached the highest level (1,000 nM). In addition, vincristine exhibited cytotoxicity against human leukemic MOLT-4 cells with an $IC_{50}$ of 3.3 nM at 48 h (Fig. 3-1B). To determine whether an interaction between SAHA and vincristine took place, the cytotoxic potency of a combination assay was measured. Cells treated with 500 nM SAHA and various concentrations of vincristine (0.3 to 3 nM) significantly inhibited cell survival compared to each treatment alone (Fig. 3-1C).

**Effects of vincristine in combination with SAHA on human T-cell leukemic cell survival**
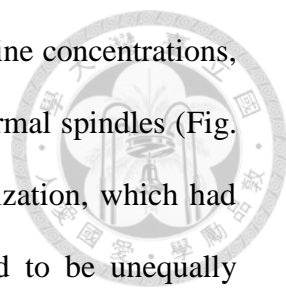
To further explore the synergistic cytotoxic effects, we determined the effects on cell cycle distribution. As compared with SAHA, treatment with vincristine induced an increase in the $G_2/M$ phase of the cell cycle. In particular, the combination of vincristine plus SAHA caused an almost complete arrest of cells in the $G_2/M$ phase following short-term treatment (24 h), and a subsequent induction in the sub-$G_1$ phase following long-term treatment (48 h) (Fig. 3-2A). Figure 2B shows the statistical results. Next, the

combination index (CI) method was used to evaluate the synergistic combinations (Chou 2006). A CI value of >1.0, 1.0, and <1.0 indicates an antagonistic, additive, or synergistic interaction, respectively, between the drugs. In the $G_2$/M phase, the CI values of vincristine (0.3, 1, and 3 nM) combined with 500 nM SAHA were 1.63, 0.72, and 0.32, respectively, and the CI values in the sub-G1 phase were 0.97, 0.77, and 0.28, respectively (Fig. 3-2C). And this synergistic combination effect also was noted in the other T-cell leukemic cell line, CCRF-CEM (Fig. 3-2D), rather than in acute myeloid leukemic cells (Supplementary Fig. 3-2). Moreover, vincristine (1 or 3 nM) combined with various concentrations of SAHA also shows synergistic effect (Supplementary Fig. 3-1). These data indicates that vincristine and SAHA interact in a synergistic manner to induce cell arrest in the $G_2$/M phase and subsequently in the sub-$G_1$ phase.

**Effects of SAHA in combination with vincristine on mitotic arrest in human leukemic MOLT-4 cells**
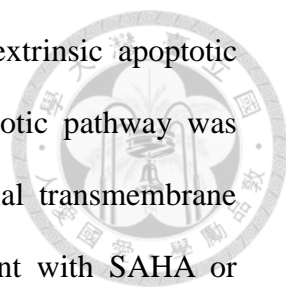
To further elucidate the synergistic effects mechanism on the $G_2$/M phase of cell cycle progression, we investigated SAHA in combination with vincristine on tubulin polarization change and mitosis-related proteins. As shown in Fig. 3-3A, there were no obvious tubulin polarization changes following SAHA treatment under cell-free conditions. However, in combination with vincristine, a significant induction of microtubule depolymerization was observed (Fig. 3-3A). Supplementary Fig. 3-3 shows more comprehensive result, including various concentrations of vincrisitine and SAHA alone *in vitro* tubulin polymerization assay. To understand the effects of microtubule dynamics on mitosis following drug treatment, the microtubule arrangement in human leukemic MOLT-4 cells was examined by β-tubulin staining. As shown in Fig. 3-3B-b, there was no significant change in microtubule distribution and

cell morphology after SAHA treatment. In addition, at low vincristine concentrations, cells had accumulated at the metaphase stage of mitosis with abnormal spindles (Fig. 3-3B-c). In this study, spindles with bipolar and multipolar organization, which had abnormal long astral microtubules and chromosomes were found to be unequally distributed. Nevertheless, at a high vincristine concentration, microtubule depolymerization was observed (Fig. 3-3B-d). In the present study, the vincristine and SAHA combination exerted more explicit effects than vincristine alone with regards to abnormal spindles and chromosomes (Fig. 3-3B & Supplementary Fig 3-4). These results suggest that SAHA potentiated the effects of vincristine due to inhibition of microtubule dynamics.

M phase-regulating proteins were also analyzed. The combination of various concentrations of vincristine (0.3, 1, and 3 nM) with SAHA (500 nM) for 24 h increased the phosphorylation of two mitotic markers (MPM2 and H3S10) in a concentration-dependent manner. These results proved that the combination of vincristine and SAHA induced M phase arrest. Moreover, vincristine in combination with SAHA also induced mitotic arrest by stimulating cyclin B1, aurora B, phospho-Cdc2 (Thr161), and phospho-PLK1 expression, and suppressing Cdc25c and phospho-Cdc2 (Tyr15) levels. The magnitude of these changes was more obvious than those observed with vincristine treatment alone (Fig. 3-3C). These findings demonstrate that SAHA enhanced vincristine-induced M phase arrest and that the combination therapy induced microtubule dynamics instability and mitotic activation.

**Effects of SAHA in combination with vincristine on the apoptotic pathway and HDAC activity in human leukemic MOLT-4 cells**

Mitochondria play a crucial role both in the intrinsic and extrinsic apoptotic pathways. To test whether the vincristine/SAHA-mediated apoptotic pathway was associated with mitochondrial function, a change in mitochondrial transmembrane potential ($\Delta\psi m$) was assessed. As shown in Fig. 3-4A, treatment with SAHA or vincristine alone was insufficient to affect the mitochondrial membrane potential; however, this phenomenon was enhanced by co-treatment with SAHA in a time-dependent manner. The Bcl-2 protein family plays a regulatory role in controlling the mitochondrial apoptotic pathway. The data showed that the combination treatment more effectively downregulated the expression of the pro-survival members of the Bcl-2 family, such as Bcl-2, Bcl-xl, and Mcl-1, than did either treatment alone (Fig. 3-4B).

Caspase activation plays an important role in the classic apoptotic pathways. In this study, it was also found that caspases 3, 6, 7, 8, 9, and PARP were activated by the combination treatment for 48 h (Fig. 3-4C). Moreover, to confirm whether HDACs, both in the single or combination treatment, were involved in the apoptosis pathway, the expression of HDACs and H3 acetylation were evaluated. Vincristine (3 nM) in combination with SAHA effectively inhibited HDAC3 and HDAC6 expression and enhanced H3 acetylation, which represents an inhibition in HDAC activity, in a time-dependent manner (Fig. 3-4D).

**HDAC6 inhibition was involved in vincristine/SAHA-induced apoptosis**

Previous findings have shown HDAC6-induced tubulin acetylation to affect the dynamics and function of microtubules (Hubbert, Guardiola et al. 2002, Matsuyama, Shimazu et al. 2002, Zhang, Li et al. 2003, Boyault, Sadoul et al. 2007). As shown in
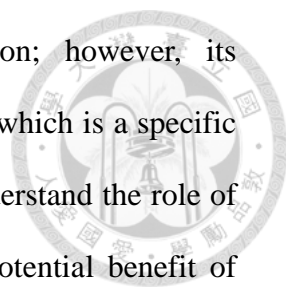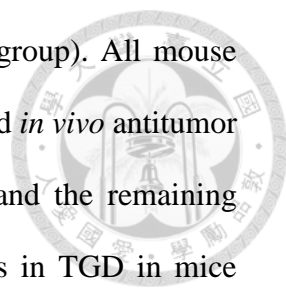
Fig. 3-5A, SAHA, a pan-HDACi, induced tubulin acetylation; however, its combination with vincristine had no synergic effect. Tubastatin A, which is a specific HDAC6 inhibitor (Bulinski, Richards et al. 1988), was used to understand the role of HDAC6 in the vincristine/SAHA-treated cells. To evaluate the potential benefit of vincristine in combination with tubastatin A, the cytotoxicity of co-treatment was determined and the combination effects were analyzed. However, compared to tubastatin A alone, vincristine significantly enhanced the cytotoxicity of tubastatin A (Fig. 3-5B). Moreover, vincristine (1 and 3 nM) combined with various concentrations of tubastatin A induced cell accumulation at the $G_2/M$ phase followed by the sub-$G_1$ phase (Fig. 3-5C). The CI values were <1 in combination of vincristine and tubastatin at the $G_2/M$ phase and sub-$G_1$ phase (Fig. 3-5D). Co-treatment of vincristine and tubastatin revealed MPM2 and PARP activation consistent with the induction of apoptosis by western blot analysis (Fig. 3-5E). And vincristine and HDAC6 inhibitor combined synergism effect was further corroborated by the observation of vincristine and ACY1215 co-treatment in CCRF-CEM cells (Fig. 3-5F). These findings suggest that SAHA treatment may alter microtubule dynamics in cells through HDAC6 inhibition, even though the effect was insufficient to arrest cells in the $G_2/M$ phase. However, in combination with vincristine, which also had an effect on microtubules, SAHA caused extreme microtubule stress thus causing cell death.

**The antitumor activity of vincristine and SAHA combination therapy *in vivo***

To evaluate whether the synergistic effect of vincristine plus SAHA could be clinically relevant, the antitumor activity of this co-treatment in severe combined immunodeficiency mice bearing established MOLT-4 tumor xenografts was investigated. Once a tumor was palpable (approximately 100 mm$^3$), mice were

randomized into vehicle control and treatment groups (n = 6 per group). All mouse tumors were allowed to reach an endpoint volume of 2,000 mm$^3$, and *in vivo* antitumor efficacy was expressed as tumor growth delay (TGD; Fig. 3-6A) and the remaining percentage of survival (Fig. 3-6B). There were no improvements in TGD in mice treated with vincristine (0.1 mg/kg once weekly) or SAHA (50 mg/kg once daily) alone. However, log-rank analysis showed that the co-treatment exhibited significant antitumor activity in the MOLT-4 xenograft model ($P = 0.0389$). In addition, Kaplan–Meier curves displayed antitumor activity for the co-treatment group (vincristine, 0.025 mg/kg once weekly; SAHA, 200 mg/kg once daily) (Fig. 3-6B). Notably, the mice tolerated all of the treatments without overt signs of toxicity; no significant body weight difference or other adverse side effect was observed (Fig. 3-6D & Supplementary Fig. 3-5). To correlate the *in vivo* antitumor effects with the mechanisms identified *in vitro*, intratumoral biomarkers were assessed by western blot analysis. Consistent with *in vitro* results, the combined treatment markedly induced caspase 3 activation and PARP cleavage in tumors, indicating elevated apoptosis (Fig. 3-6E). Taken together, these findings suggest that combination of vincristine and SAHA, both *in vitro* and *in vivo*, dramatically enhanced vincristine-induced cell death.

# 3-2 Discussion
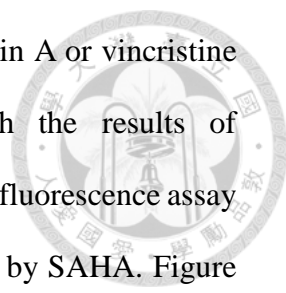
Recent preclinical studies have reported that due to their broad anticancer potency and low toxicity, HDACis are often used in combination therapy to enhance conventional chemotherapeutic and molecular-targeted drugs. SAHA was the first HDACi approved by the FDA for T cell lymphoma. Moreover, vinca alkaloids, have been extensively used in the clinical treatment of ALL. In spite of their usefulness, drug resistance and neuron toxicity remains a serious clinical problem. Therefore, the purpose of this study was to investigate the anticancer activity of vincristine and SAHA in a T cell ALL cell lines. Cytotoxic experiments have shown that the combination of vincristine and SAHA significantly induces cell death. Analyses of cell cycle and regulatory protein expressions have indicated that co-treatment with the two drugs has a synergistic effect on M phase arrest and consistent with an increase of cell numbers in the sub-$G_1$ phase. Furthermore, combination treatment promotes cell apoptosis through intrinsic and extrinsic pathways. *In vivo* xenograft animal models demonstrated that, compared to treatment with either drug alone, vincristine in combination with SAHA prolongs survival time in mice, as suggested by the *in vitro* results.

During these studies, the level of the effects of vincristine and SAHA on MOLT-4 cells was determined. Combinations with various concentrations of both drugs were investigated to determine the lowest effective concentration of vincristine or SAHA that would provide the maximum cytotoxic effects. It was established that the cytotoxicity of 3 nM vincristine combined with 500 nM SAHA is much more potent in inhibiting cell survival (Fig. 3-1) and altering cell cycle distribution (Fig. 3-2) compared to either treatment alone. The CI value small than 1 at the $G_2$/M or sub-$G_1$

phases, suggests that the combination of vincristine and SAHA had synergistic action on T cell leukemic cells at certain concentrations (Fig. 3-2).
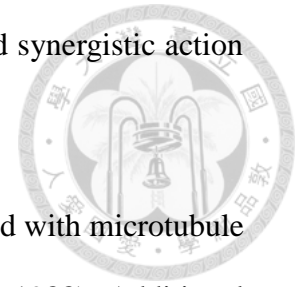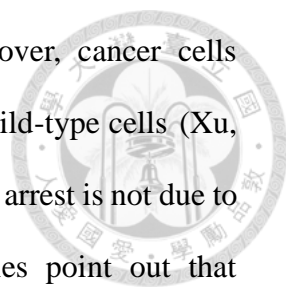
Prior studies have shown that α-tubulin acetylation is associated with microtubule dynamics and is regulated by HDAC6 (Bulinski, Richards et al. 1988). Additional research has also found that HDACis induce microtubule acetylation and polymerization through HDAC6 inhibition (Hubbert, Guardiola et al. 2002, Matsuyama, Shimazu et al. 2002, Zhang, Li et al. 2003, Boyault, Sadoul et al. 2007). Whether the polymerization or the depolarization of microtubules following the vincristine and SAHA combination treatment was responsible for $G_2/M$ cell cycle arrest needs to be determined for a complete understanding of this mechanism. In vitro tubulin polymerization assays showed that a high concentration of vincristine (10 μM) definitely caused microtubule depolymerization, but a high concentration of SAHA (50 μM) had no influence on microtubule polymerization (Fig. 3-3A). However, SAHA indeed causes the acetylation of tubulin (Figs. 3-4D and 3-5A). These results suggest that SAHA may induce tubulin acetylation, subsequently affecting microtubule polymerization by inhibiting HDAC6 activity. Nevertheless, SAHA-induced polymerization was not proven (Fig. 3-3A) since HDAC6 was not available in the in vitro tubulin polymerization kits, which contained only tubulin and GTP. Therefore, no SAHA-induced polymerization effects were observed in this assay. In addition, the literature indicates that tubulin acetylated by certain HDACis, such as trichostatin A, is associated with microtubule dynamics without affecting the polymerization of microtubules. Therefore, to further demonstrate the role of HDAC6, tubastatin A, a specific HDAC6 inhibitor, was used (Bulinski, Richards et al. 1988). Tubastatin A and vincristine co-treatment was found to synergically induce cell death and $G_2/M$ phase

cell arrest, proceeding to the sub-$G_1$ phase, compared with tubastatin A or vincristine alone (Fig. 3-5). These phenomena were in agreement with the results of vincristine/SAHA combination treatment. Consequently, an immunofluorescence assay was performed to demonstrate whether microtubules were affected by SAHA. Figure 3-3B shows that at low vincristine concentrations, abnormal spindles (star-like monopolar and multiple polars) and chromosome disorganization were observed, as has been previously reported by Jordan et al. (Jordan, Thrower et al. 1992). However, the microtubule distribution remained unchanged following cell treatment with 500 nM SAHA. However, following SAHA/vincristine combination treatment, more cells were observed to have deteriorated spindles although without microtubule depolymerization or polymerization. Prior studies have shown that only higher concentrations (>10 nM) of microtubule agents, such as vinca alkaloids and taxol, affect microtubule mass, but microtubule dynamics are suppressed by low microtubule agent concentrations (<10 nM) (Dumontet and Jordan 2010). Taken together, vincristine/SAHA-induced synergistic $G_2$/M arrest may result from HDAC6 inhibition-induced microtubule dynamic alternation because of SAHA as well as vincristine. In brief, vincristine and SAHA exerted a synergic action on microtubule dynamics, albeit though different mechanisms.

A large amount of research shows that HDACis arrest cells in the $G_1$ phase mainly through p21 induction. Only a few studies mention the role of these compounds in $G_2$/M, and the mechanism remains uncertain. For example, Blagosklonny et al. found that the HDACi trichostatin A causes tubulin acetylation that contributes to M phase arrest (Blagosklonny, Robey et al. 2002). HDACis have also shown the capability to cause immature sister chromatid separation and slippage from the mitotic spindle

assembly checkpoint (SAC) (Heinicke and Fulda 2014). Moreover, cancer cells without wild-type p21 or p53 more easily become polyploid than wild-type cells (Xu, Perez et al. 2005). These results indicate that HDACi-induced $G_2/M$ arrest is not due to an influence on transcriptional activity. In contrast, other studies point out that trichostatin A causes $G_2/M$ cell cycle arrest and SAC slippage through an increase in p21 transcriptional activity (Noh and Lee 2003). The mechanisms proposed above to explain vincristine/SAHA-induced $G_2/M$ phase arrest should not be excluded. We found that p21 mRNA and protein level were elevated after treatment with vincristine or SAHA alone and was not enhanced by combined treatment (data not shown). It has been reported that all HDACis induced p21 but differentially caused tubulin acetylation, mitotic arrest, and cytotoxicity. Mitotic arrest rather than induction of p21 determined HDACi cytotoxicity (Blagosklonny, Robey et al. 2002). Moreover, p21 is required for $G_1$ arrest, not for cell death, and is associated with resistance to HDACi-induced apoptosis (Sandor, Senderowicz et al. 2000). Upregulated p21 was also found in vincristine-treated cells even though vincristine caused cell arrest in the $G_2/M$ phase, leading to apoptosis (Sandor, Senderowicz et al. 2000). Therefore, we considered that in our study, increased p21 expression of vincristine-SAHA combined treatment was the cellular protection mechanism for repairing damaged DNA, and this phenomenon was not sufficient to cause apoptosis. Furthermore, vincristine and SAHA did not alter p53 protein and mRNA levels (data not shown). Consequently, the involvement of p53 and p21 in drug-induced $G_2/M$ arrest was eliminated.

The expression of related proteins in the M phase was evaluated to understand the exact phase at which the cells arrest ($G_2$ or M). Cdc25c is a tyrosine phosphatase that removes the inhibitory phosphorylation of Cdc2 at Tyr15, which has already been

phosphorylated on Thr161 and contributes to Cdc2 activation. The Cdc2/cyclin B complex then forms to move cells into the M phase (Castedo, Perfettini et al. 2004). Figure 3-3C shows that Cdc25c and p-Tyr15 Cdc2 protein levels declined and p-Thr161 Cdc2 increased following combination treatment. In addition, expression of the M phase markers pMPM2 and H3S10 was also induced (Nowak and Corces 2004). These results demonstrate that combination treatment induces cell arrest in the M phase and not in $G_2$.

From the above data, we speculate that the vincristine/SAHA combination may alter microtubule dynamics, resulting in incorrect microtubule attachment to the centromere of chromosomes or loss of spindle tension across kinetochore pairs, subsequently causing SAC activation in the metaphase. An increased aurora B and PLK kinase protein expression and aurora B kinase activity, detected by H3S10 expression downstream of aurora B, are shown in Fig. 3-3C. SAC activation inhibits anaphase-promoting complex/cytochrome activity and decreases cyclin B degradation to inter-anaphase to accomplish cell division. Cells proceed to apoptosis owing to an inability to repair the dysfunction(Gascoigne and Taylor 2009). Therefore, we suggest that co-treatment-induced cell death was due to an inability to repair microtubule function even if the SAC was activated (Figs. 3-3C and 3-4C). In contrast, Dowling et al. have found that the synergistic effect of the HDACi trichostatin A and microtubule agents occurs through SAC inactivation (Dowling, Voong et al. 2005). In addition, studies have shown that HDACis induce aurora B kinase degradation and subsequently inactivate the SAC via HDAC3 inhibition (Eot-Houllier, Fulcrand et al. 2008). Although HDAC3 is inhibited by 24-h vincristine and SAHA co-treatment (Fig. 3-4D), the protein level of aurora B kinase was increased (Fig. 3-3C). We believe that

the arrest at the $G_2$/M phase does not occur through the inhibition of HDAC3.

Caspase activation plays a vital role in the apoptosis pathways. Figure 3-4C shows that the activation of caspases 3 and 6 to 9 and PARP was synergistically induced by vincristine combined with SAHA. This result indicates that combination treatment activates both the intrinsic and the extrinsic apoptosis pathways. Therefore, the expression of mitochondrial proteins and mitochondrial membrane potential were investigated. Bid is a key protein linking the extrinsic and intrinsic apoptosis pathways. As Figure 3-4B shows, the protein level of pro-form Bid decreased in response to co-treatment with vincristine and SAHA. Decreases in pro-survival mitochondrial proteins Bcl-2, Bcl-xl, and Mcl-1 also occurred. A decrease in mitochondrial membrane potential was significantly induced by the combination in a time-dependent manner.

Taking all of the above findings into consideration, when vincristine and SAHA treatments were combined, MOLT-4 cell survival was significantly inhibited, mainly through the induction of M stage arrest and intrinsic and extrinsic apoptosis pathways. Moreover, the selective HDAC6 inhibitor exhibited similar synergism when combined with vincristine. *In vivo* xenograft animal models produced the same results as those of *in vitro* models. Pan HDAC inhibitors influenced different types of HDACs, which caused side effects must be more than selective HDAC6 inhibitors. However, the most important and practical advantage to choose SAHA for this study is that SAHA has been approved for cancer treatment. Selective HDAC6 inhibitors such as tubastatin A and Acy-1215 are only in phase I or phase II clinical trial. The finding of this paper not only provides another choice for clinical treatment but also offers an idea for future application of HDAC6 inhibitors.
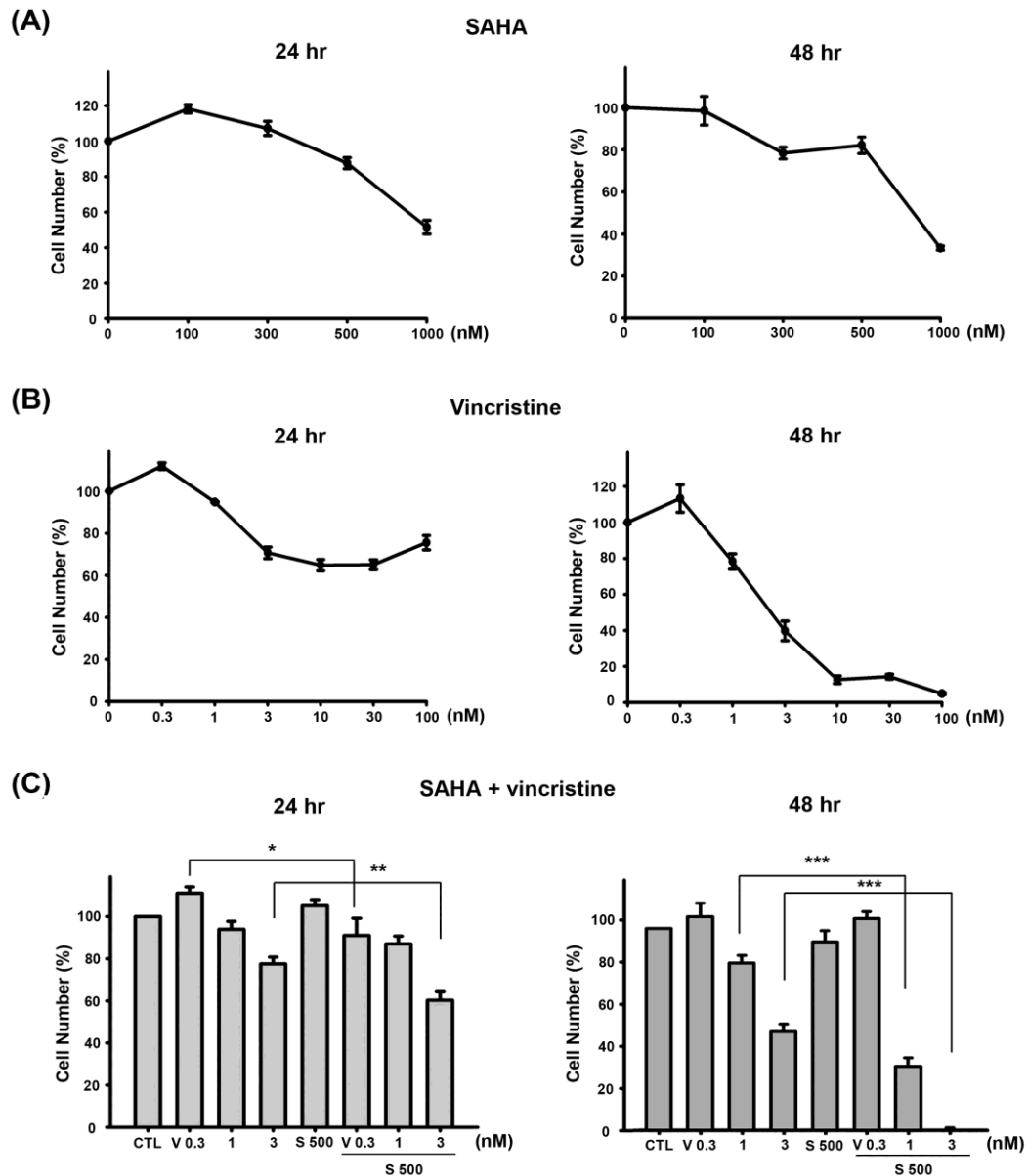
**Figure 3-1. Cell viability effects of SAHA、vincristine alone and in combination on MOLT-4 cell line.**

Cell viability was measured by MTT assay. (A) (B) MOLT-4 cells were treated with various concentrations of SAHA and vincristine alone for 24 h and 48 h, respectively. (C) The combination of SAHA (S) and vincristine (V) was compared to the effect of vincristine alone. Data are expressed of at least three separate determinations. *$P<0.05$, ** $P< 0.02$, *** $P< 0.005$.

(A)

24 hr

48 hr

(B)

(C)

G2M phase

subG1 phase

(D)
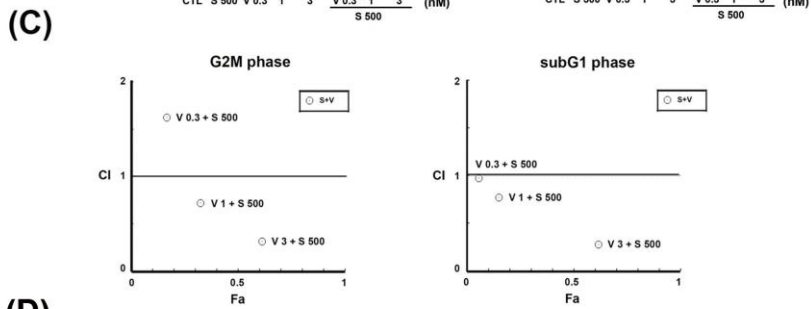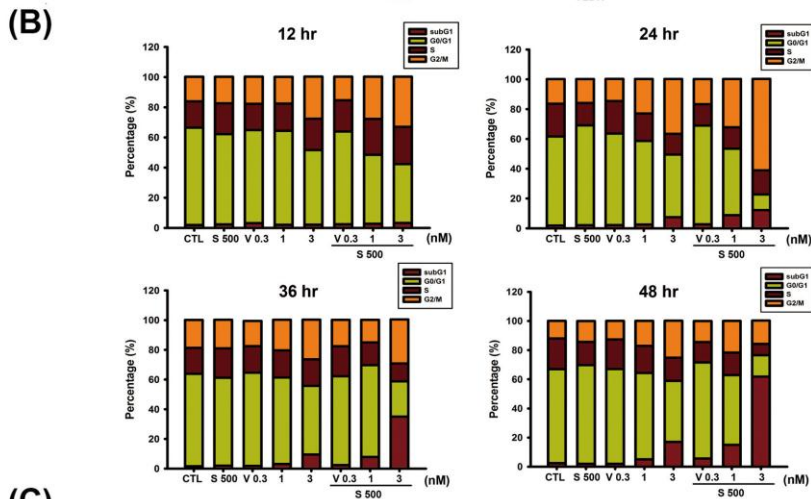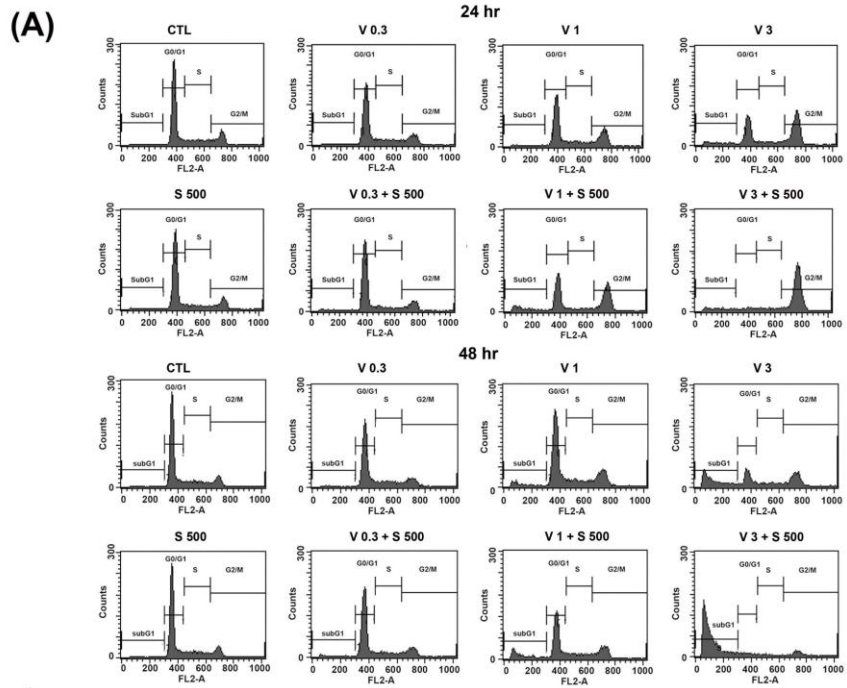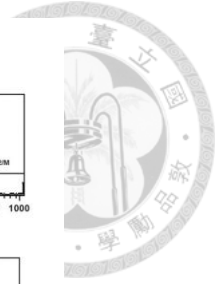
| | Dose SAHA | Dose Vincristine | Effect | CI |
|---|---|---|---|---|
| CCRF-CEM | 1 | 0.001 | 0.984 | 0.03774 |
| | 1 | 0.003 | 0.2767 | 0.42940 |
| | 1 | 0.01 | 0.4774 | 0.27615 |

74

**Figure 3-2. The combination of vincristine and SAHA had synergic effects on cell cycle kinetic changes.**

(A) MOLT-4 cells were treated with various concentrations of vincristine alone or in combination with SAHA (500 nM) for 24 and 48 h. (B) The quantitative data were shown in time course. Cell cycle was performed by cell cytometry after propidium iodide staining. (C) The combination effect of SAHA (500 nM) and vincristine (0.3, 1, 3 nM) on $G_2/M$ arrest (left figure) and apoptosis (right figure) were used by the combination index (CI). And the CI was analyzed with the program Compusyn (Ting-Chao Chou and Nick Martin). CI value $<1$ represents that two drugs have synergic effects. (D) CCRF-CEM cells were treated with the indicated concentrations of vincristine alone or in combination with SAHA (1000 nM) for 48 h. The effect of subG$_1$ phase was analyzed by flow cytometry. Data are expressed of at least three separate determinations. Abbreviation, S : SAHA, V：vincristine. Fa: fraction affected.
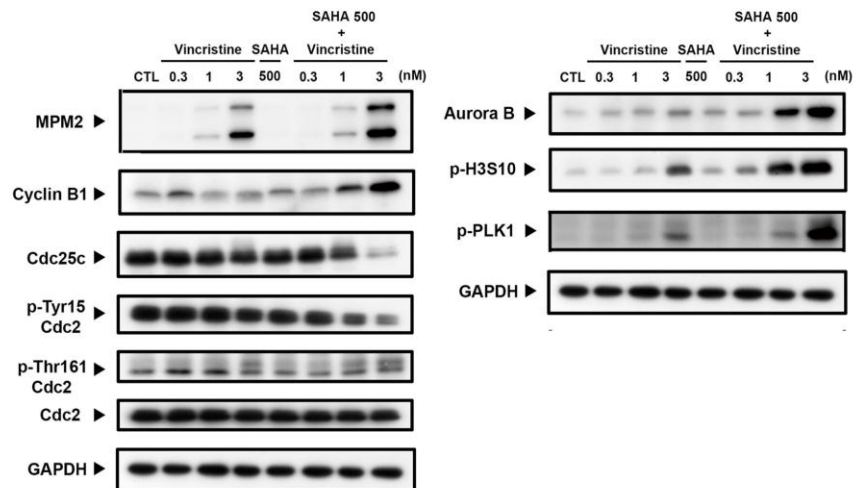
75

**(A)**
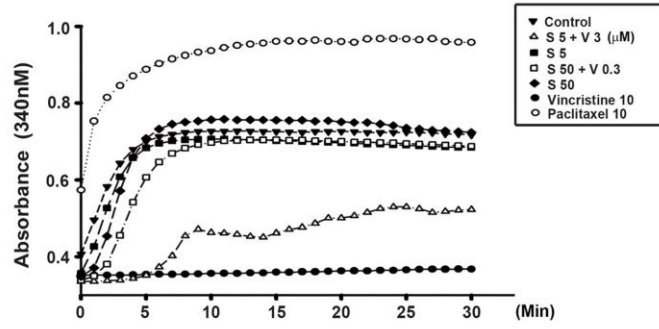


**(B)**
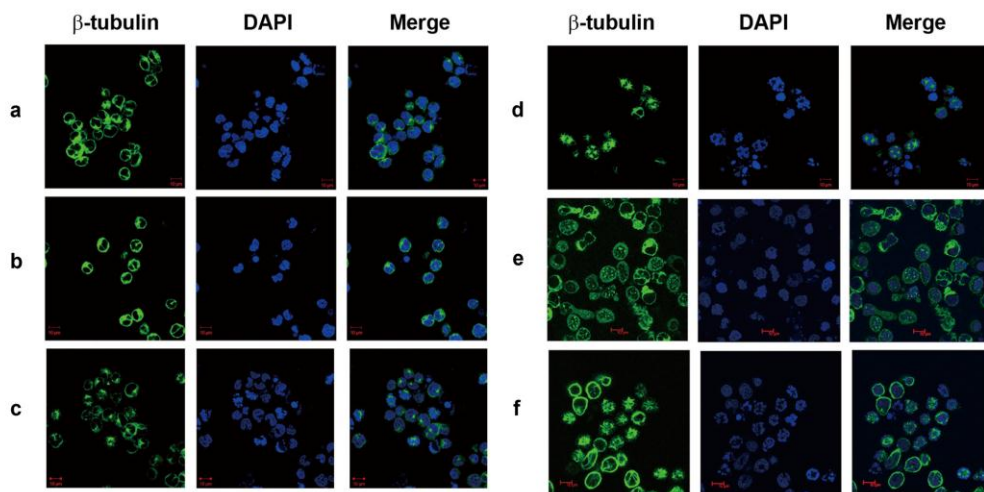


**(C)**

**Figure 3-3. SAHA sensitized MOLT-4 cells to vincristine-mediated mitotic arrest.**
(A) Tubulin assembly was determined by *in vitro* tubulin polymerization kit and then detected by spectrophotometry. Paclitaxel (10 μM) and vincristine (10 μM) were used as positive controls. Paclitaxel is a polymerizing agent and vincristine belongs to a depolymerizing agent. "S 5" represents SAHA 5 μM. And "S 50 + V 3" represents SAHA 50 μM combining with vincristine 3 μM. This experiment was examined in a cell-free condition. (B) MOLT-4 cells were treated with SAHA and vincristine alone or co-treatment for 24 h then stained with β-tubulin and DAPI. The immunofluorescence images were captured by ZEISS, LSM 510 META confocal microscope. All images were under 400x microscopic magnification. a: control, b: 500 nM SAHA, c: 3 nM vincrisitine, d: SAHA co-treated with vincristine. e: 30 nM vincrisintine, f: 30 nM Paclitaxel. (C) Cells were treated with vincristine (0.3, 1, 3 nM) alone or co-treated with SAHA (500 nM) for 24 h. Then total cell lysates were obtained to evaluate the $G_2/M$ phase regulatory protein expression and the tubulin acetylation. Data are expressed of at least three separate determinations. Abbreviation, S : SAHA, V：vincristine.
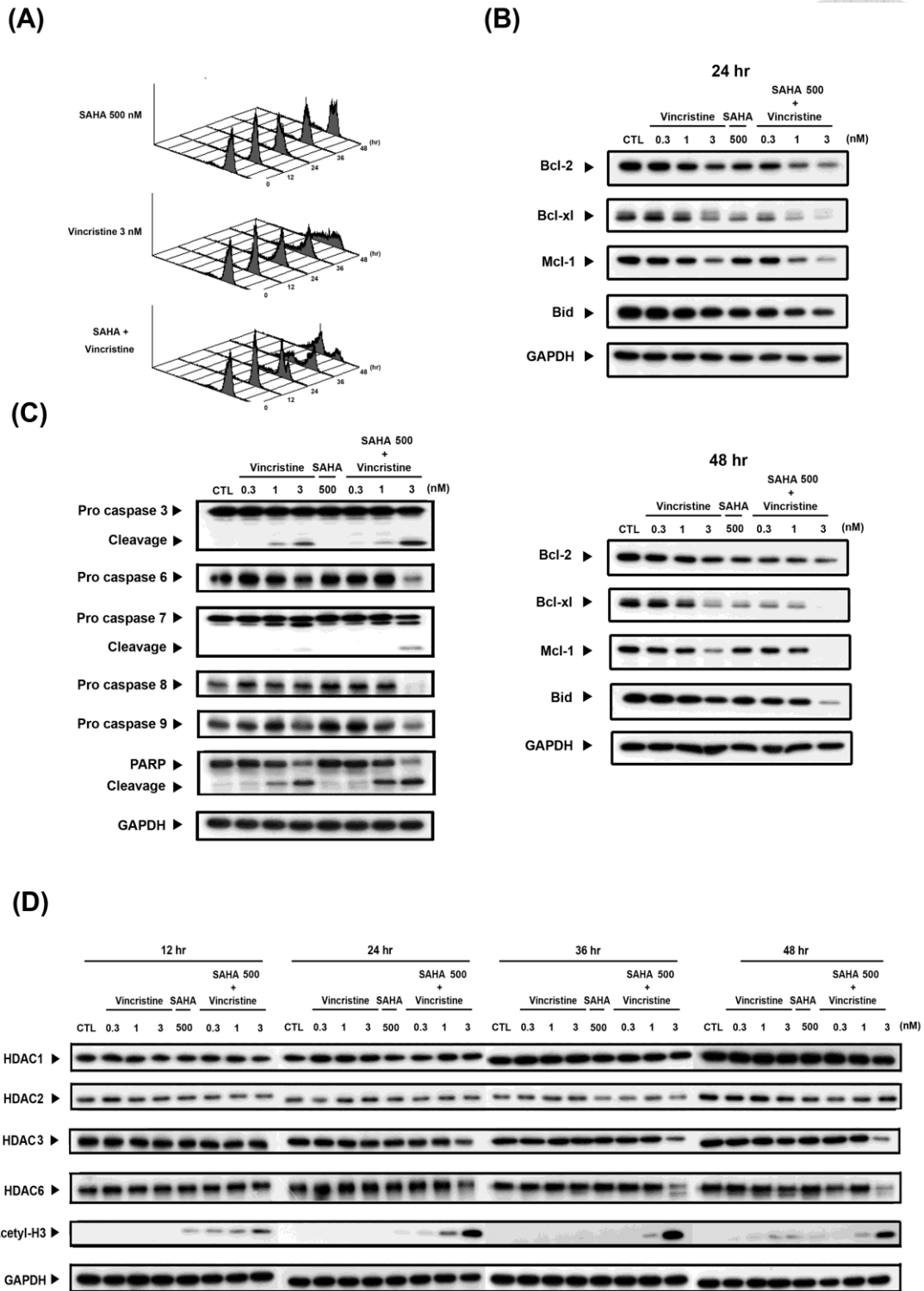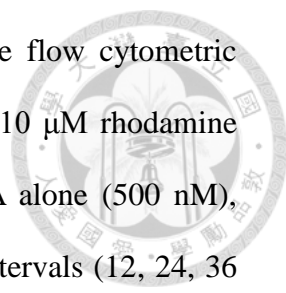
**Figure 3-4. Co-treatment with vincristine and SAHA induced mitochondrial membrane potential loss, casapses activation and HDAC activity.**

(A) The mitochondrial membrane potential was measured by the flow cytometric analysis of rhodamine 123. The MOLT-4 cells were stained with 10 μM rhodamine 123 and incubated at 37°C for 30 min in the presence of SAHA alone (500 nM), vincristine alone (3 nM) or coexistence of both at different time intervals (12, 24, 36 and 48 h). The horizontal axis shows the relative fluorescence intensity and the vertical axis presents the cell number. (B) MOLT-4 cells were treated with different concentration of vincristine (0.3, 1, 3 nM) alone, a single concentration of SAHA (500 nM) alone and co-treated with both drugs for 24 and 48 h. Then the cell lysates were collected for western blot analysis to detect the Bcl-2 family protein levels. (C) Cells were incubated with vincristine and SAHA for 48h and detected of caspase 3, 6, 7, 8, and 9 activations and PARP cleavage. Similarly, (D) the total cell lysates were analyzed to measure HDAC 1, 2, 3 and 6 expression and HDAC activity (H3 acetylayion). Data are expressed of at least three separate determinations. Abbreviation, S : SAHA；V：vincristine.

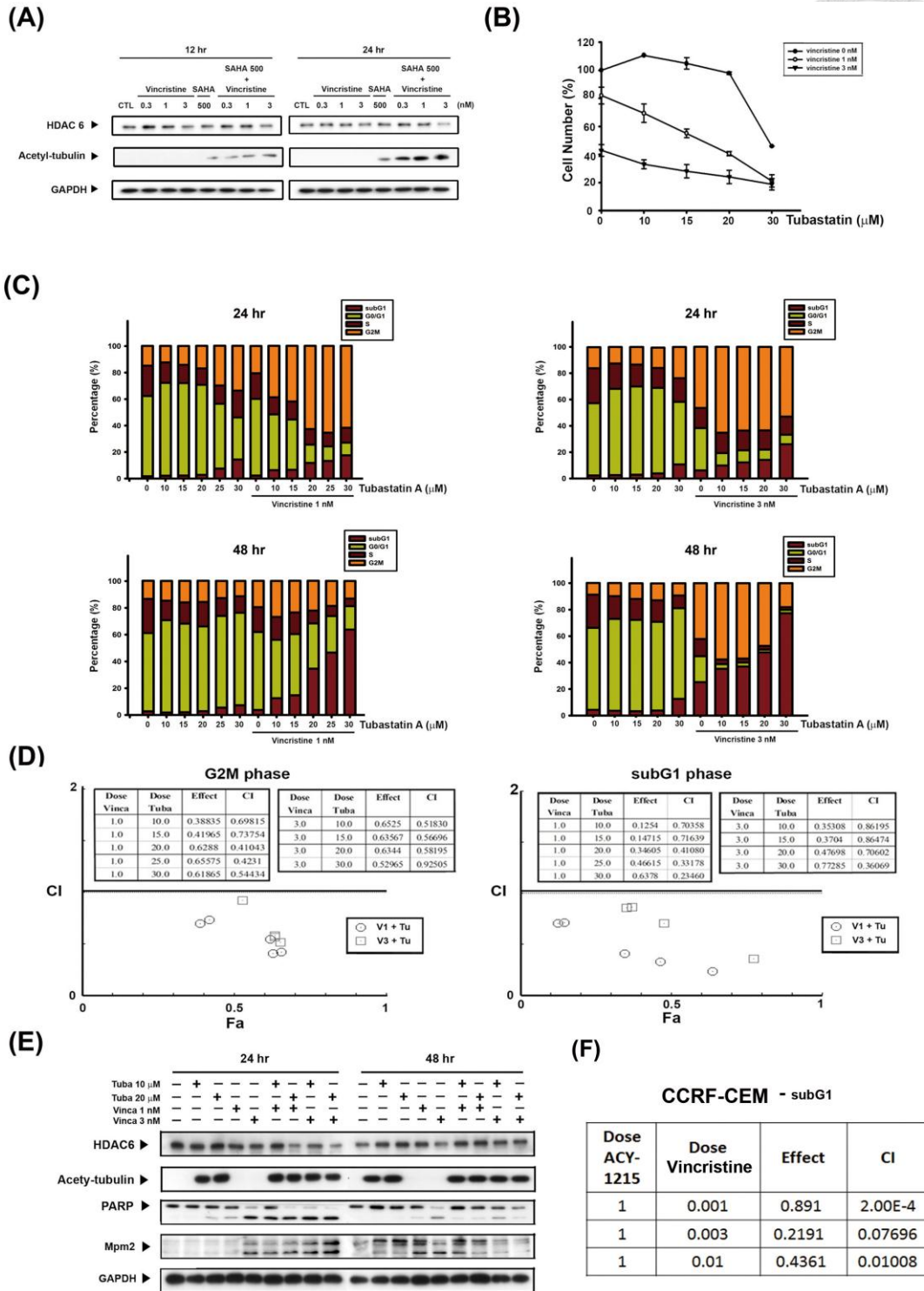**(A)** ... 12 hr / 24 hr / Vincristine / SAHA / SAHA 500 + Vincristine / CTL 0.3 1 3 500 0.3 1 3 (nM) / HDAC 6 ► / Acetyl-tubulin ► / GAPDH ►

**(B)** Cell Number (%) vs Tubastatin (μM); vincristine 0 nM, vincristine 1 nM, vincristine 3 nM

**(C)** 24 hr / 48 hr; Percentage (%) vs Tubastatin A (μM); Vincristine 1 nM; Vincristine 3 nM; subG1, G0/G1, S, G2M

**(D)** G2M phase

| Dose Vinca | Dose Tuba | Effect | CI | Dose Vinca | Dose Tuba | Effect | CI |
|---|---|---|---|---|---|---|---|
| 1.0 | 10.0 | 0.38835 | 0.69815 | 3.0 | 10.0 | 0.6525 | 0.51830 |
| 1.0 | 15.0 | 0.41965 | 0.73754 | 3.0 | 15.0 | 0.63567 | 0.56696 |
| 1.0 | 20.0 | 0.6288 | 0.41043 | 3.0 | 20.0 | 0.6344 | 0.58195 |
| 1.0 | 25.0 | 0.65575 | 0.4231 | 3.0 | 30.0 | 0.52965 | 0.92505 |
| 1.0 | 30.0 | 0.61865 | 0.54434 | | | | |

subG1 phase

| Dose Vinca | Dose Tuba | Effect | CI | Dose Vinca | Dose Tuba | Effect | CI |
|---|---|---|---|---|---|---|---|
| 1.0 | 10.0 | 0.1254 | 0.70358 | 3.0 | 10.0 | 0.35308 | 0.86195 |
| 1.0 | 15.0 | 0.14715 | 0.71639 | 3.0 | 15.0 | 0.3704 | 0.86474 |
| 1.0 | 20.0 | 0.34605 | 0.41080 | 3.0 | 20.0 | 0.47698 | 0.70602 |
| 1.0 | 25.0 | 0.46615 | 0.33178 | 3.0 | 30.0 | 0.77285 | 0.36069 |
| 1.0 | 30.0 | 0.6378 | 0.23460 | | | | |

CI vs Fa; V1 + Tu, V3 + Tu

**(E)** 24 hr / 48 hr; Tuba 10 μM / Tuba 20 μM / Vinca 1 nM / Vinca 3 nM; HDAC6 ► / Acety-tubulin ► / PARP ► / Mpm2 ► / GAPDH ►

**(F)**

**CCRF-CEM - subG1**

| Dose ACY-1215 | Dose Vincristine | Effect | CI |
|---|---|---|---|
| 1 | 0.001 | 0.891 | 2.00E-4 |
| 1 | 0.003 | 0.2191 | 0.07696 |
| 1 | 0.01 | 0.4361 | 0.01008 |

**Figure 3- 5. HDAC 6 was involved in vincristine/SAHA-induced cell death.**

(A) MOLT-4 cells were treated with the indicated drugs for 12 and 24 h. The cell lysates were used to determine the HADC 6 protein level and activity. (B) Cells were

treated with tubastatin A alone, which is a specific HDAC 6 inhibitor, or combined with 1 nM and 3 nM vincristine for 48 h. The cell viability was evaluated with MTT assay. (C) Cells incubated with tubastatin A alone or in combination with the indicated concentration of vincristine for 24 and 48 h. The cell cycle distribution was measured by flow cytometry. The figures were shown as quantitative data in time course. (D) The CI value of combining tubastatin A with vincristine on $G_2$/M and subG$_1$ phase. (E) Cells were treated with 10 or 20 µM tubastatin A (Tuba) alone and combined with 1 or 3 nM vincristine. The cell lysates were used for Western bolt analysis. (F) CCRF-CEM cells were co-treated with vincristine and Acy1215, HDAC6 specific inhibitor, for 48 h. The CI value of combining treatment on subG$_1$ phase.

**(A)**

**(B)**

**(C)**

**(D)**

**(E)**
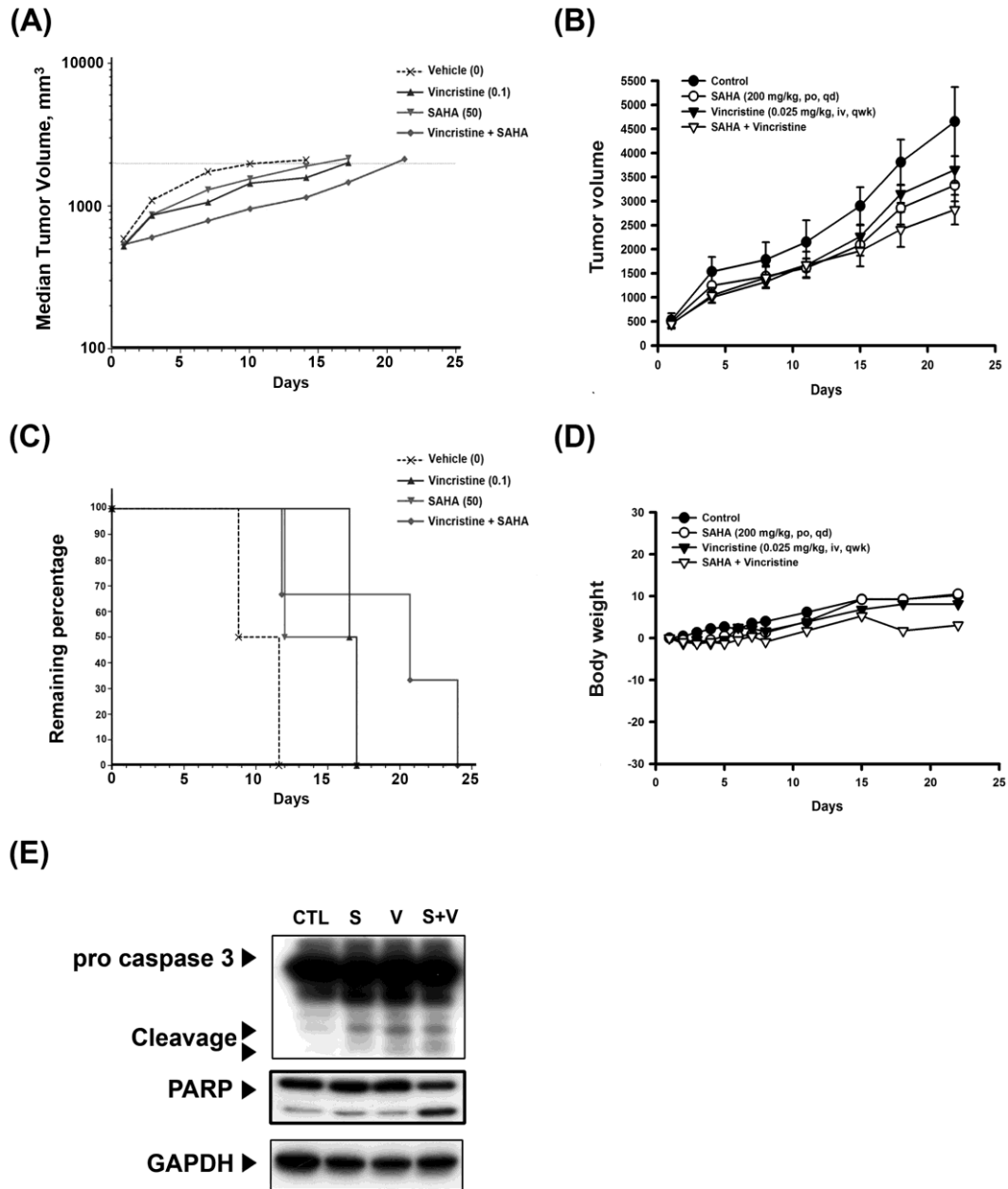
**Figure 3-6. The effect of vincristine and SAHA in MOLT-4 tumor xenograft.**

SCID mice were ectopically implanted with MOLT-4 cells, and when the tumor size reached 100 mm3, mice were injected with vincristine (i.p., qwk) or SAHA (p.o., qd) alone or a combination of both. (A) *In vivo* antitumor efficacy was expressed as tumor growth delay (TGD) (vincristine 0.1 mg/kg i.v. qwk; SAHA 50 mg/kg p.o. qd). (B)

Effects of combination on tumor volume. The growth curves are the means of the tumor sizes measured with each group (vincristine 0.025 mg/kg i.v. qwk; SAHA 200 mg/kg p.o. qd). (C) The remaining percentage of mice survival (vincristine 0.1 mg/kg i.v. qwk; SAHA 50 mg/kg p.o. qd). (D) Effects of combined treatment on mice body weight (vincristine 0.025 mg/kg i.v. qwk; SAHA 200 mg/kg p.o. qd). (E) Tumors were resected for the western blot analysis (vincristine 0.025 mg/kg i.v. qwk; SAHA 200 mg/kg p.o. qd)
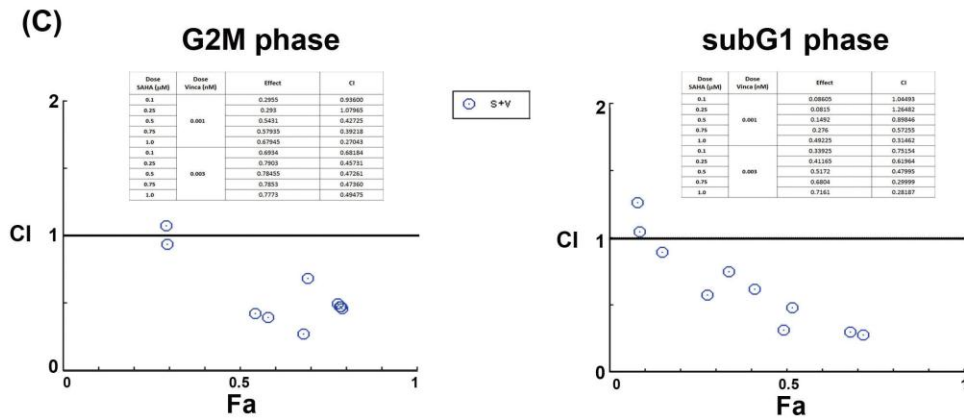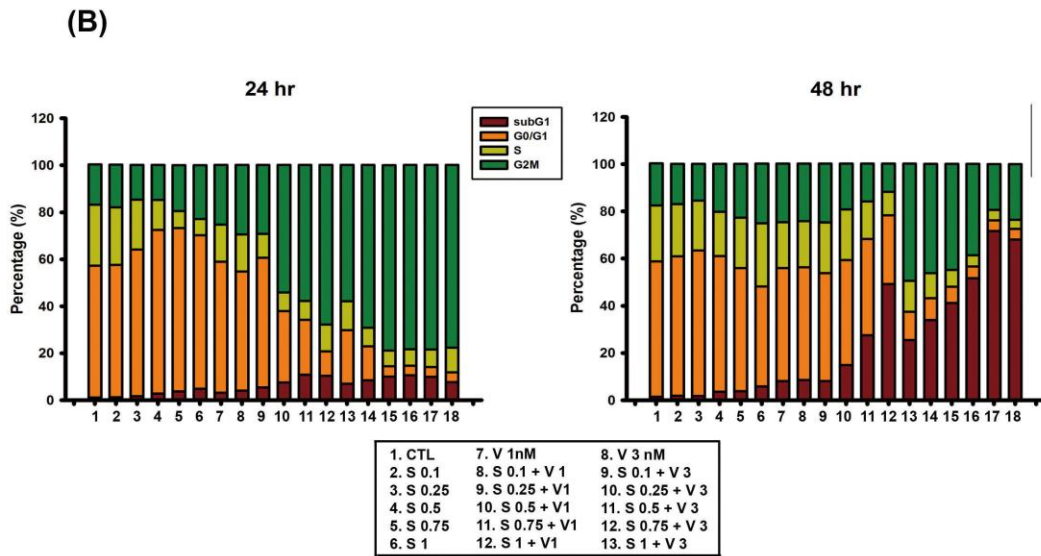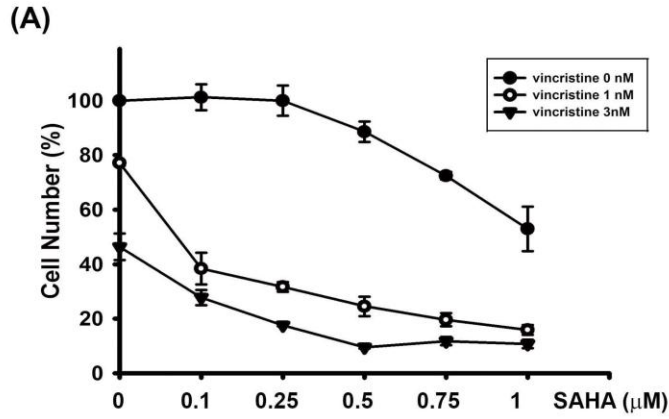
**Supplementary Figure 3-1. The effect of vincristine combined with various dose of SAHA.**

(A)  MOLT-4 cells were treated with various SAHA alone or combined with 1 nM and

3 nM vincristine for 48 hr. The cell viability was evaluated with MTT assay. (B) The distribution of cell cycle after MOLT-4 cells were treated with various concentrations of SAHA alone or in combination with vincristine 1 nM or 3 nM for 24 hr and 48 hr. The quantitative data were shown in time course. (C) The combination effect on $G_2/M$ arrest (left figure) and apoptosis (right figure) were used by the combination index (CI).

**(A)**

### sub G1 phase

**HL60**
(Acute promyelocytic leukemia)

| Dose SAHA | Dose Vinciristine | Effect | CI |
|---|---|---|---|
| 0.5 | 0.0003 | 0.095 | 0.56050 |
| 0.5 | 0.001 | 0.105 | 0.99279 |
| 0.5 | 0.003 | 0.1685 | 1.56525 |
| 0.5 | 0.01 | 0.2165 | 2.18889 |

**(B)**



1. CTL
2. V0.3
3. V1
4, V3
5, S0.5
6. V0.3+S
7. V1+S
8. V3+S
9. Tuba 20
10. Tuba 20+V1
11. Tuba 20+V3
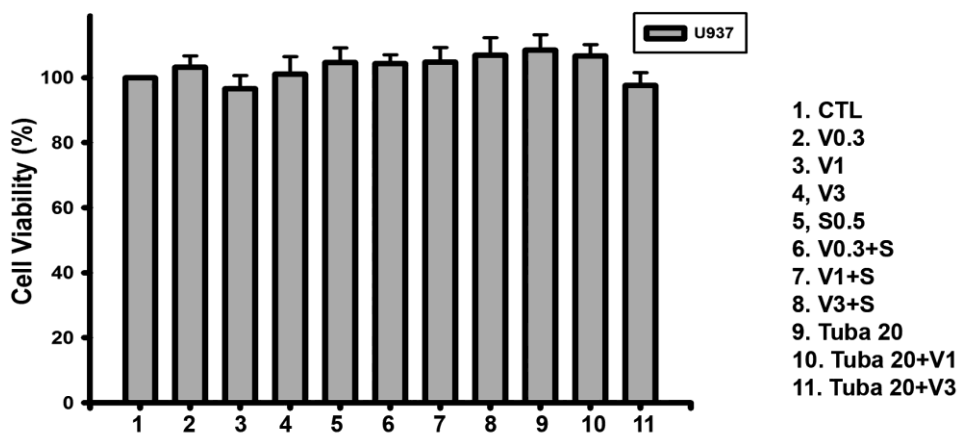
**Supplementary Figure 3-2. The effect of vincristine and SAHA co-treatment in acute myeloid leukemic cell lines.**

(A) HL60 (Acute promyleocytic leukemia) cells were co-treated with the indicated vincristine and SAHA then analyzing the CI values of sub-G1 phase. (B) The cell viability of U937 (Acute monocytic leukemia) after the indicated treatment. V, vincristine; S, SAHA; Tuba, Tubastatin A.
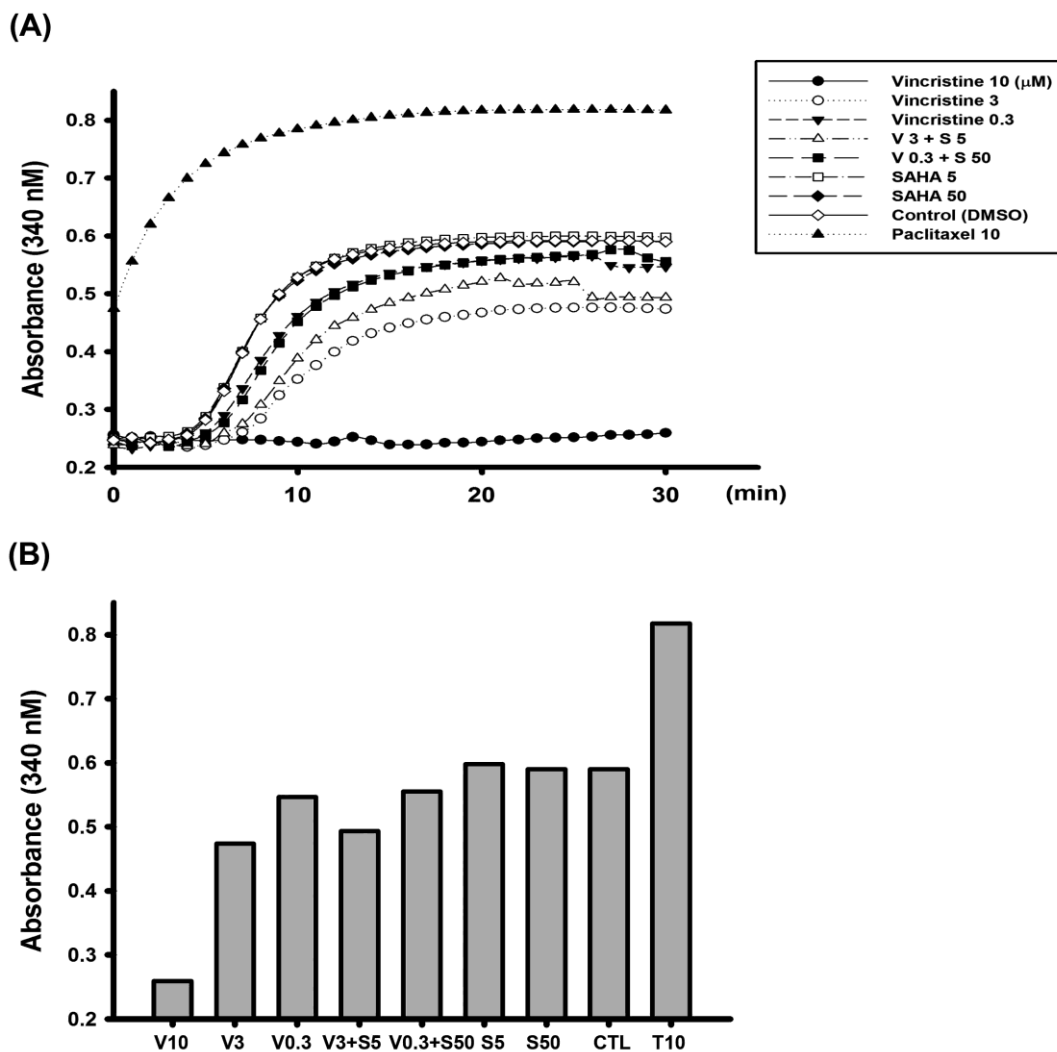
**Supplementary Figure 3-3. The results of vincristine alone (0.3 and 3 μM)** *in vitro*
**tubulin polymerization assay.**

(A) The figure shows more comprehensive result *in vitro* tubulin polymerization,
including paclitaxel (10 μM), vincristine (0.3, 3, 10 μM), SAHA (S, 5 and 10 μM)
alone and SAHA combined with vincristine (S 50 + V 0.3 and S 5 + V3) (B) The
absorbance of different drugs at the end point (30 min).
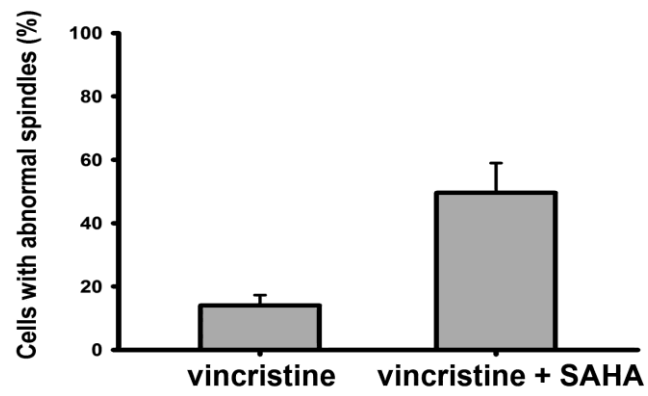
**Supplementary Figure 3-4. The quantity of abnormal spindles in vincristine alone and compared to combination with SAHA.**
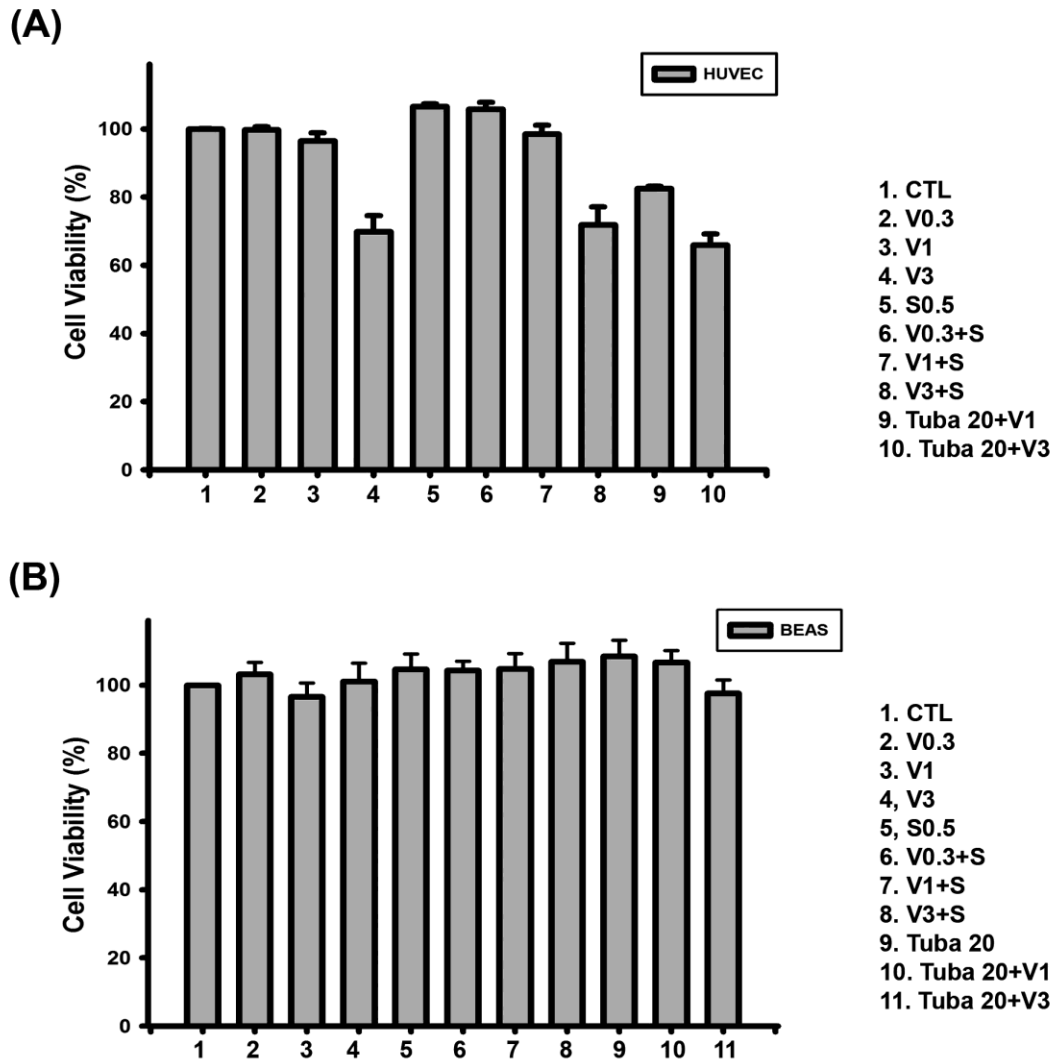
**Supplementary Figure 3-5. The cell toxicity of normal cells after combination.**

The cell viability (MTT assay) of (A) HUVEC (human umbilical vein endothelial cell)

and (B) BEAS-2B (human bronchial epithelial cell) after co-treating with the indicated

drugs for 48 h

# Chapter 4

新穎性口服的奎林類衍生物 MPT0B392
停滯細胞分裂及克服 sirolimus-resistant
在人類急性血癌細胞之機轉探討

# An oral quinoline derivative, MPT0B392, causes the mitotic arrest and overcomes sirolimus-resistant human acute leukemic cells

# 中文摘要

白血病是種基因異質性的血液腫瘤，目前是美國癌症死亡第六位，儘管過去在治療急性白血病上有很大的進展，但目前現有的化學療法還有很大的進步空間，而此篇研究主要是探討一個新合成的奎寧類衍生物 MPT0B392 (簡稱 B392) 在急性白血病的抗癌機轉。B392 能夠使細胞停留滯在細胞分裂期並最終導致細胞凋亡，我們進一步證明 B392 為一個新合成的去聚合型的微管抑制劑，而在體內動物模式實驗中，可口服的 B392 相較於只能靜脈注射的 vincristine 具有較佳的抗白血病作用。更深入發現，B392 會引發 mitotic spindle checkpoint 的活化，進而藉由活化 c-Jun N-terminal kinase (JNK) 讓粒線體失去膜電位，及 caspases 裂解。此外，在對 sirolimus 產生抗性的急性白血球細胞中，B392 能夠增強細胞對 sirolimus 的毒性，B392/sirolimus 合併給予可顯著地抑制 AKT/mammalian target of rapamycin (mTOR) 及其下游路徑並同時也影響了 myeloid cell leukemia (Mcl)-1 的表現。總結而言，B392 是一個有潛力的微管抑制劑，且能夠作為對 sirolimus 有抗藥性的急性白血病的輔助療法。

# Abstract

Leukemia is a genetically heterogeneous malignancies and the sixth leading cause of cancer death in the United States of America. Despite great advances in the treatment of acute leukemia, a renaissance of current chemotherapy needs to be improved. The present study elucidates the underlying mechanism of a new synthetic quinoline derivative, MPT0B392 (B392) against acute leukemia. B392 causes mitotic arrest and ultimately leads to apoptosis. It was further demonstrated to be a novel microtubule-depolymerizing agent. The effects of oral administration of B392 were compared with those after intravenous administration of vincristine in an *in vivo* xenograft model, and the former was found to have a potent anti-leukemia activity. Further investigation revealed that B392 triggered induction of the mitotic spindle checkpoint, followed by mitochondrial membrane potential loss and caspases cleavage by activation of c-Jun N-terminal kinase (JNK). In addition, B392 enhanced the cytotoxicity of sirolimus in sirolimus-resistant acute leukemic cells. Combination treatment with sirolimus and B392 dramatically decreased AKT/mammalian target of rapamycin (mTOR) cascades and pro-survival myeloid cell leukemia (Mcl)-1 level compared to sirolimus treatment alone. Taken together, B392 has potential as a mitotic drug and adjunct treatment for acute leukemia, especially in sirolimus-resistant cells.

# 4-1 Results

**Evaluating the anticancer effect of B392 in leukemic cell lines**

To determine the *in vitro* antitumor activity of MPT0B392 (B392) (Fig. 4-1A), we performed an MTT assay in leukemic cell lines. As shown in Figure 4-1B, B392 inhibited the cell viability of HL60, MOLT-4, and CCRF-CEM cells in a concentration-dependent manner, with $IC_{50}$ values of 0.02, 0.02, and 0.04 μM, respectively, at 48 h. Moreover, B392 caused less cytotoxicity in normal cells, including BEAS (human bronchial epithelial cells) and HUVECs (human umbilical vein endothelial cells) (Fig. 4-1C). To investigate the mechanism underlying the cytotoxicity exhibited by B392, we further evaluated cell cycle progression after treatment with B392. The data showed that B392 induced cells arrest in the $G_2/M$ phase, followed by accumulation in subG1 phase in a concentration and time-dependent manner (Fig. 4-1D & Supplementary Fig. 4-2A). In conclusion, B392 only had cytotoxic effect on leukemic cells rather than normal cells.

**Oral MPT0B392 induces apoptosis in xenograft model**

The MOLT-4 xenograft model study was performed to vet B392 as a potential anticancer drug for the treatment of leukemia. Mice were treated with B392, and vincristine orally and by intraperitoneal injection, respectively (n = 6). Figure 4-2A shows that B392 treatment resulted in significant tumor growth delay (83.3%) compared to that induced by vincrisitine (46.3%), and more tumor volume inhibition (P < 0.01), without loss of body weight (Fig. 4-2B). Moreover, immunochemistry staining shows that B392 treatment induced apoptosis in cancer cells, demonstrated by

detection of positive staining of cleaved-caspase 3 (Fig. 4-2C). Taken together, these data suggest that B392 exhibited anticancer activity with less cytotoxicity in normal cells both *in vitro* and *in vivo*.
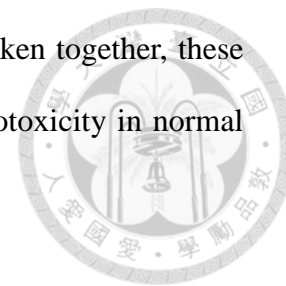
**The effect of MPT0B392 on microtubule dynamics**

Microtubules play an important role in cell mitosis, and administration of microtubule-binding agents usually result in mitotic arrest (Dumontet and Jordan 2010). Therefore, we used an *in vitro* tubulin-polymerization assay as well as tubulin staining (observed using confocal microscopy) to assess whether B392 had an effect on tubulin and would lead to cell accumulation in $G_2/M$ phase. As shown seen in Fig. 4-3A, B392 caused tubulin depolymerization *in vitro* and disrupted microtubule formation, as observed by diffusion of stained tubulin into the cytoplasm (Fig. 4-3B), which phenomena was also shown in vincristine treatment. Paclitaxel and vincristine were utilized as positive controls for tubulin polymerization and depolymerization, respectively.

To clarify the mechanism by which B392 induces $G_2/M$ cell cycle arrest in leukemic cells, we observed the expression of $G_2/M$ regulatory proteins. As cells enter mitosis, a variety of proteins are phosphorylated either directly or indirectly by M-phase-promoting factor (MPF) (Castedo, Perfettini et al. 2004). MPM2, an antibody that can specifically detect the phosphorylation of M phase regulatory proteins, is often used to differentiate the phase in which cells accumulate (e.g. $G_2$ or M phase). The results show that B392 treatment upregulated intracellular MPM2, and downregulated cyclin B1 and the inhibitory Try-15 residue of Cdk1 (cdc2), indicating that B392 induced cell arrest in M phase. Additionally, increased expression of Aurora A and B
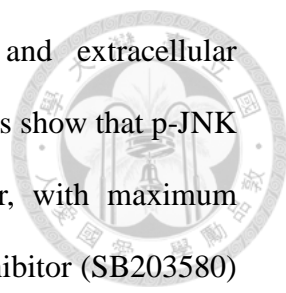
(mitotic spindle kinases), which play a role in the regulation of cell division (Keen and Taylor 2009) as well as phosphorylation of H3S10, demonstrated that B392 activated the mitotic checkpoint (Fig. 4-3C & Supplementary Fig. 4-2B). Our data suggests that B392 is a novel microtubule-destabilizing agent that induces checkpoint activation and mitotic arrest in leukemic cells.

**Evidence of MPT0B392-triggered apoptosis**

Mitochondria play a crucial role in cells undergoing the apoptotic process (Kim, Emi et al. 2006); hence, we further evaluated the expressions of mitochondrial proteins and mitochondrial function, which was assessed by measuring the permeability of their outer membranes. As shown seen in Fig. 4-4A, B392 caused the phosphorylation of Bcl-2, Bak increase and decrease in Mcl-1 (a key pro-survival Bcl-2 family protein which has important impact on mitochondrial function), which provided evidence that mitochondrial membrane potential time-dependently lost in HL60 cells (Fig. 4-4B). Induction of apoptosis by B392 was elucidated by the observation of a hypodiploid peak (subG$_1$) in leukemic cells (Fig 4-1D). The activation of caspase 3, 7, 8, 9 and poly (ADP-ribose) polymerase (PARP) cleavage in a time-dependent manner further confirmed B392-induced apoptosis (Fig. 4-4C). These data suggest that B392 has an effect on mitochondrial proteins, membrane potential as well as activation of the classic apoptosis pathway and ultimately cell death.

**JNK activation plays a key role in B392-induced apoptosis of leukemic cells**

It has been reported that differential regulation of mitogen-activated protein kinases (MAPKs) is induced by microtubule binding agents (Stone and Chambers 2000, Bacus, Gudkov et al. 2001). To further investigate the mechanism of B392-induced cell

apoptosis, we analyzed the phosphorylation of JNK, P38, and extracellular signal-regulated kinase (ERK) after treatment with B392. The results show that p-JNK and p-P38 were induced by B392 in a time-dependent manner, with maximum induction observed at 24 and 36 h (Fig. 4-5A). We used a p-P38 inhibitor (SB203580) and p-JNK inhibitor (SP600125) to identify the specific MAPK involved in B392-induced cell death. The data on cell cycle distribution revealed that only SP600125 was able to reverse B392-induced subG1 accumulation (Fig. 4-5B &C), as well as the expression of mitochondrial proteins (p-Bcl-2, and Mcl-1), caspase 3, and PARP (Fig. 4-5D) in HL60 cells. The above observation was not found after co-treatment with SB203580 and B392 (Data not shown).

**MPT0B392 enhanced the cytotoxicity of sirolimus in a sirolimus-resistant cell line**

It has been shown that a number of genetic mutations elevate PI3K/AKT/mTOR signaling, and contribute to cell proliferation, survival, and drug resistance in leukemia (Park, Chapuis et al. 2010, Vu and Fruman 2010). Thus, combining cytotoxic chemotherapy agents could enhance sensitivity to mTOR inhibitors and achieve better outcomes. We first evaluated the baseline sensitivity of sirolimus in different acute leukemic cells lines via the MTT assay. Fig. 4-6A shows that acute myeloid leukemic cells HL60, MOLM-13, and MV4-11 were more resistant to sirolimus, with $IC_{50}$ values of 12.5, 5.9, and 3.9 μM, respectively, compared to acute lymphoblastic leukemic cells MOLT-4 and CCRF-ECM, with $IC_{50}$ of 0.17 and 0.42 μM, respectively. In the sirolimus-resistant cell line HL60, a combination of sirolimus with B392 enhanced the cytotoxicity of sirolimus compared to sirolimus alone; however, this phenomenon was not observed in the sirolimus-sensitive cell line, MOLT-4 (Fig. 4-6B). The combination of B392 and sirolimus clearly induced PARP and caspase 3 cleavage, as well as
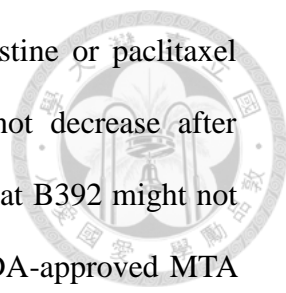
downregulated a key prosurvival protein, Mcl-1 (Fig. 4-6C, *left panel*). The effect of a sirolimus-B392 combination on AKT/mTOR signaling was also determined. B392 itself only had a slight effect on the AKT/mTOR pathway; however, the combination dramatically decreased the expression of p-AKT and p-mTOR, as well as mTOR's downstream targets, p-P70S6K and p-4EBP1 (Fig. 4-6C, *right panel*). Taken together, B392 can strengthen the effect of sirolimus on mTOR signaling and can enhance cytotoxicity in sirolimus-resistant acute myeloid leukemia (AML) cells.

# 4-2 Discussion
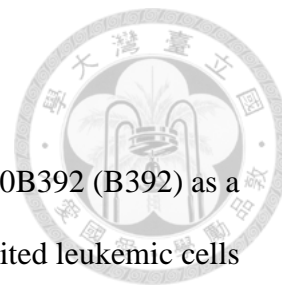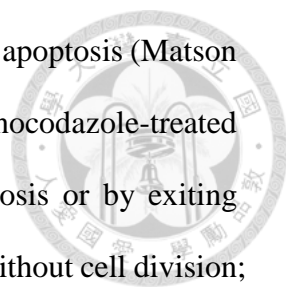
In this study, we reported a novel oral quinoline derivative, MPT0B392 (B392) as a potential drug candidate for anti-leukemia. B392 dramatically inhibited leukemic cells survival; however, it had less cytotoxicity on normal cells *in vitro* and *in vivo*. The further evidences demonstrated that B392 is a depolymerizing MTA, which caused SAC activation. JNK played an essential mediator in B392-induced cells apoptosis through mitochondria disruption which ultimately leading to caspases activation. Additionally, in sirolimus-resistant leukemic cells, B392 sensitized the cytotoxic effect of sirolimus.

Understanding the mechanisms of drug resistance to approved MTA, as well as their drawbacks in clinical therapy, is extremely important for the development of a promising and potent compound that targets microtubules. The main cause of MTA drug resistance in cancers, which has been mentioned previously, is alteration of tubulin and overexpression of members of the ATP-binding cassette (ABC) family, of which P-glycoprotein (P-gp) is the best known (Fojo and Menefee 2005). Several lines of evidence have revealed that vinca alkaloids and taxanes are pumped out by the membrane transporter P-gp, the product of multidrug resistance (*MDR)* gene and multidrug resistance-associated protein (MRP), thereby decreasing their intracellular concentrations and efficacy (Bruggemann, Currier et al. 1992, Breuninger, Paul et al. 1995, Huisman, Chhatta et al. 2005). Therefore, after we demonstrated that B392 is indeed a microtubule destabilizing agent, as manifested by the result of our *in vitro* tubulin binding assay (Fig. 4-3A), we also evaluated the susceptibility of B392 to P-gp in a P-gp-overexpressed NCI/ADR-RES cell line. The supplementary results show that
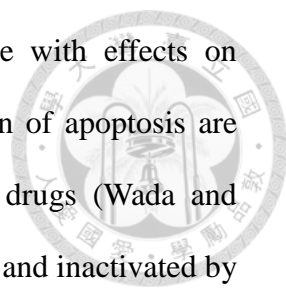
NCI/ADR-RES cells were more sensitive to B392 than to vincristine or paclitaxel (Supplementary Fig. 4-1A) and the efflux of rhodamine did not decrease after co-incubation with a B392 (Supplementary Fig. 4-1B), implying that B392 might not be excluded by membrane transporter p-gp. Furthermore, most FDA-approved MTA for cancer treatment require parenteral administration; however, B392 was particularly designed for oral administration. The xenograft animal model demonstrated that antitumor efficacy after oral administration of B392 was greater than that observed after parenteral administration of vincristine (Fig. 4-2). Thus, B392 can be considered a potential and promising MTA for the treatment of leukemia.

Cell cycle progression is precisely regulated by cyclin and cyclin kinase complexes (Bloom and Cross 2007). The activation of the cyclin B1/Cdk1 complex in the nucleus is responsible for entry into mitosis from the $G_2$ phase. The observed upregulation of cyclin B1, decrease of phosphorylated Cdc2 at Tyr-15, and the phosphorylation of MPM2 demonstrated that B392 induced mitosis arrest and not $G_2$ phase arrest (Fig. 4-1D & 4-3C). The cell-cycle checkpoint is a cell-cycle surveillance system that ensures the fidelity of division and determines whether cells need to undergo DNA repair, chromosome segregation, differentiation, or apoptosis. In mitosis, if a chromosome attaches incorrectly to microtubule, the metaphase checkpoint (also called spindle assembly checkpoint, SAC) would be activated to elicit signal cascades to inhibit the APC, which causes cyclin B1 degradation and results in cells exiting mitosis (Kang and Yu 2009). In the present study, we found that after treatment with B392, the expression of Aurora A and Aurora B increased, and their downstream target H3S10 was phosphorylated, implying that B392 disrupted microtubule formation and led to SAC (Fig. 4-3C).
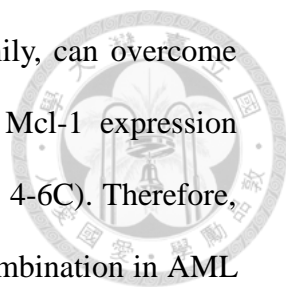
However, not every cancer cell with prolonged mitosis undergo apoptosis (Matson and Stukenberg 2011). It was reported that the majority (63%) of nocodazole-treated HeLa cells survive, either by continuing to progress through mitosis or by exiting mitosis to enter endocycle, a process which duplicates the genome without cell division; however, this phenomena does not occur after treatment with another MTA, paclitaxel. Paclitaxel also induces mitotic arrest in HeLa cells, but 73% cells exit the process and then die in the subsequent interphase (Gascoigne and Taylor 2008). This demonstrates that SAC, which is responsible for monitoring cellular progression from mitosis, does not play a direct role in the induction of apoptosis suggesting the presence of another pathway for apoptosis induction (Matson and Stukenberg 2011). Anti-apoptotic mitochondrial proteins, Bcl-2, Mcl-1, and Bcl-xL, have been shown to be critical factors involved in the MTA-induced apoptosis pathway (Ruvolo, Deng et al. 2001). Knockdown of Mcl-1 can sensitize cells to spindle poison treatment (Wertz, Kusam et al. 2011) and overexpression of phospho-defective mutant Bcl-2 can block mitotic death (Eichhorn, Sakurikar et al. 2013). Phosphorylation of Mcl-1/Bcl-2/Bcl-xl leads to the release of bound pro-apoptotic Bcl-2 proteins such as Bak and Bax and the disruption of mitochondrial membrane potential, which ultimately activates the classic apoptotic pathway (Shitashige, Toi et al. 2001). In the present study, we found that B392 induced SAC activation, Bcl-2 phosphorylation, Mcl-1 decrease and increase in Bak, which contributed to mitochondrial membrane potential loss, and caspase activation, indicating that B392 has actual cytotoxic abilities and does not merely increase cellular progression through mitosis or exit from mitosis like nocodazole.

Three MAPKs, ERK, JNK, and p38, have been found to be stress inducible in maintenance of cell functions. ERK was initially associated with cell proliferation and

survival, whereas JNK and p38 were considered stress-inducible with effects on apoptosis. However, the mechanisms underlying MAPK regulation of apoptosis are complex and controversial, and might depend on cell type and drugs (Wada and Penninger 0000, Stone and Chambers 2000). Bcl-2, phosphorylated and inactivated by the JNK pathway, is normally activated in $G_2/M$ phase (Yamamoto, Ichijo et al. 1999). Therefore, we investigated to determine the specific MAPK that contributes to B392-induced apoptosis. Fig 4-5 shows that JNK activation can reverse B392-induced phosphorylation of Bcl2, decrease in Mcl-1, cell cycle distribution, and PARP and caspase 3 cleavage. This implies that B392-induced JNK activation triggers the apoptotic pathway in leukemic cell lines.

Because mTOR signaling has proved to be crucial to cell proliferation and survival in hematological malignancies, mTOR inhibitors are being investigated in a myriad of preclinical and clinical trials (Teachey, Grupp et al. 2009). However, the results of clinical studies suggest that some cancers have intrinsic resistance against these agents, while some have acquired resistance (Witzig, Geyer et al. 2005, Kurmasheva, Huang et al. 2006). We hypothesized that the combination of B392 and sirolimus could potentially decrease drug resistance and increase the cytotoxicity of sirolimus. According to our results, AML cell lines (HL60, MOLM-13, and MV4-11) showed relative resistance to sirolimus when compared with ALL cell lines (MOLT-4 and CCRF-CEM) (Fig. 4-6A). The synergism of B392 and sirolimus co-treatment was only observed in AML cells (Fig. 4-6B). It was reported that almost all AML samples have been observed to contain activated mTOR1, which is independent of PI3K/AKT (Park, Chapuis et al. 2010). Inhibition of mTOR1 by sirolimus would overactivate PI3K/AKT, thus producing AML cell resistance to sirolimus. It was also noted that

downregulation of Mcl-1, a prosurvival member of the Bcl-2 family, can overcome resistance to sirolimus (Muller, Zang et al. 2013). p-AKT and Mcl-1 expression decreased dramatically after B392 and sirolimus co-treatment (Fig. 4-6C). Therefore, we hypothesized that the mechanism underlying this synergistic combination in AML cells might involve the inhibition of multiple pathways. Crazzolara. et al demonstrated that everolimus-vincristine co-treatment prolonged the survival of mice engrafted with ALL cells (Crazzolara, Cisterne et al. 2009). However, the combination of sirolimus and B392 had no effect on the ALL cell line, MOLT-4, in our *in vitro* study. We suggested that there might be more complicated mechanisms or factors influenced by the microenvironment that led to this diversity.

Acute myeloid leukemia or acute lymphoblastic leukemia is a kind of high and poor risk leukemia, containing many subtypes based on distinct and complicated cytogenetic or molecular abnormalities, in contrast to chronic leukemia. Although conventional microtubule targeting drugs are regarded as an outdated chemotherapy, it cannot be denied that they can still have an impact on current anticancer therapy, as long as their deficiencies are improved. In the present study, we developed a novel oral quinoline derivative B392, that has an ability to inhibit tubulin polymerization and induce leukemic cell apoptosis though JNK activation. It is also less susceptible to P-gp activity, and enhances the cytotoxicity of sirolimus in sirolimus-resistant cells. Thus, B392 is considered a potential drug for the treatment of acute leukemia.
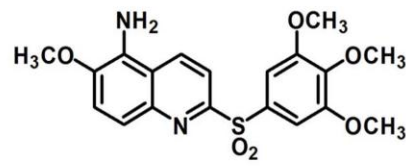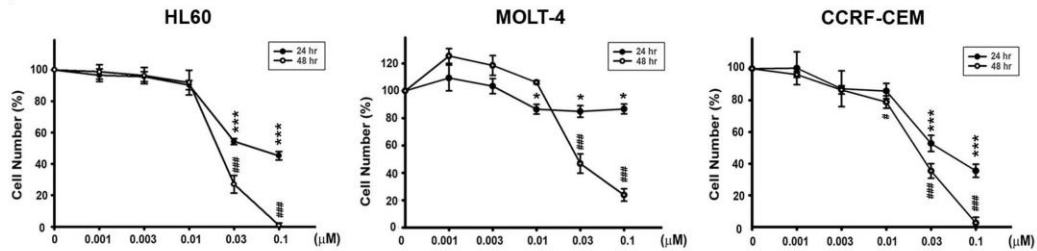
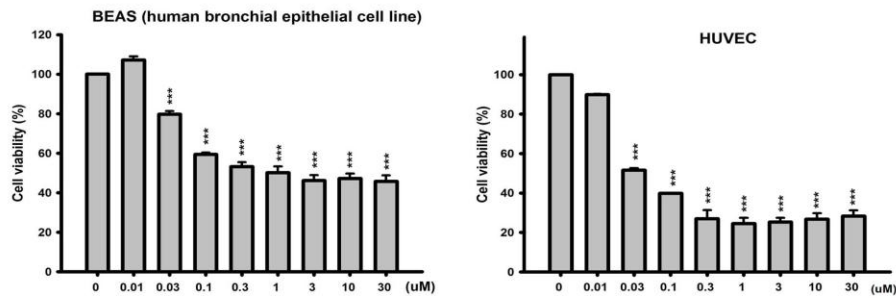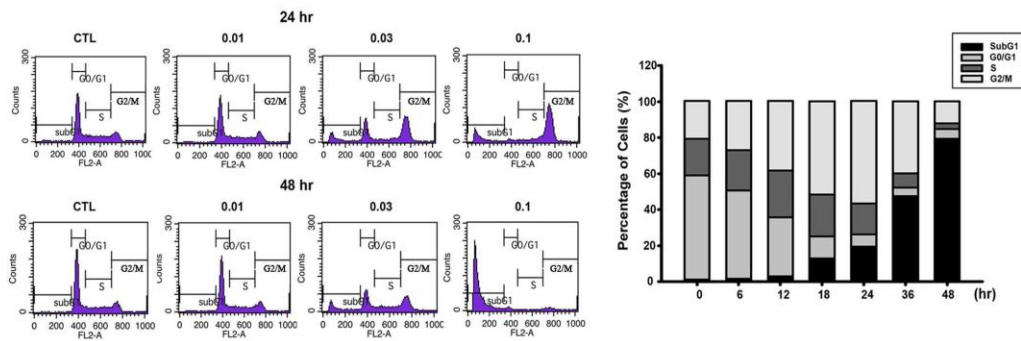**Figure 4-1. Chemical structure of B392 and its potential anticancer effect *in vitro*.**

(A) The chemical structure of MPT0B392. (B) Cell viabilities of B392 in HL60 (acute promyelocytic leukemia), MOLT-4 (acute lymphoblastic leukemia), CCRF-CEM (acute lymphoblastic leukemia) and (C) normal cells (BEAS, human bronchial epithelial and HUVEC, human umbilical vein endothelial cell) were determined by
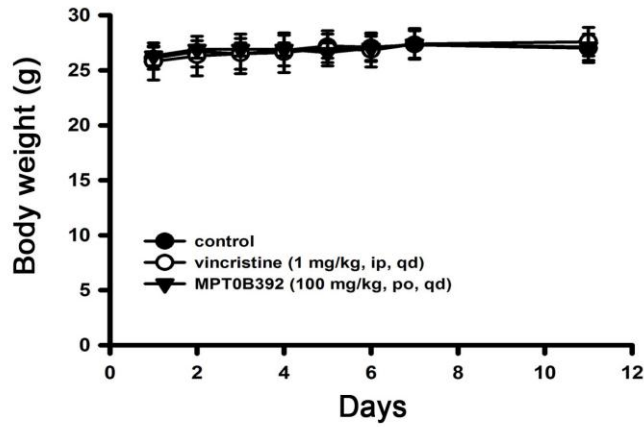
103

MTT assay. * $P < 0.05$, *** $P < 0.001$, [#] $P < 0.05$, [###] $P < 0.001$ compared with the control group. (D) Time (*right panel*) and concentration-dependent (*left panel*) of B392 on cell cycle progression. HL60 cells were treated with vesicle (0.1% DMSO) or 0.01, 0.03, 0.1 μM of B392 for 24 and 48 h. Cell cycle distribution was performed by flow cytometry.
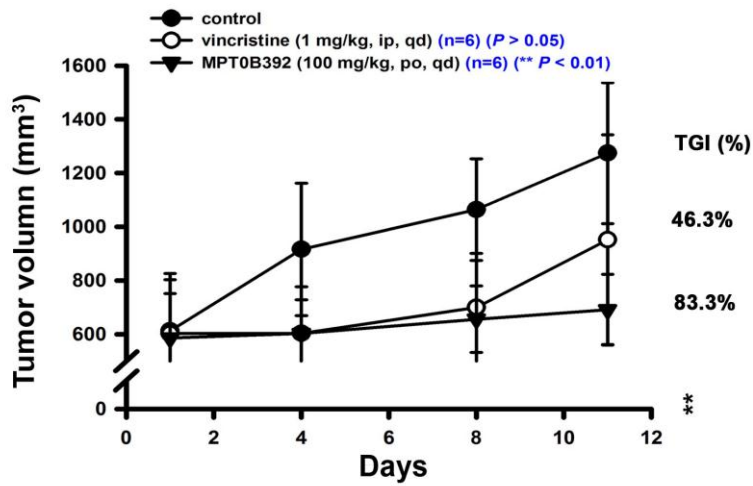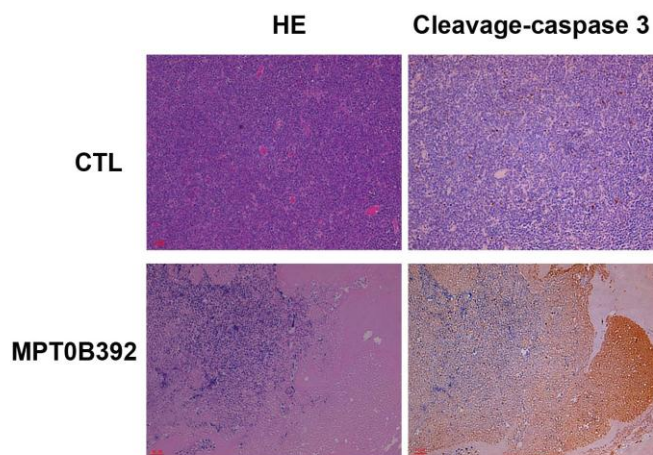
**Figure 4-2. The effect of B392 in MOLT-4 xenograft model.**

SCID mice were ectopically implanted with MOLT-4 cells. Vincristine 1mg/kg (i.p.)

or B392 100mg/kg (p.o.) were treated. (A) The curves show the effect of B392 on tumor volume and percentage of tumor growth delay (TGD) was calculated for treatment groups relative to control group. (B) The body weight of mice after indicated drugs treatment. (C) Immunohistochemical staining for the tumors' sections. *Upper panel* is the control, and *lower panel* is the B392 treatment group. *Left panel* was stained with hematoxylin and eosin; and *right panel* with cleavage caspase 3, which represents cells under apoptosis. Each tumor sample is under 200x magnification.
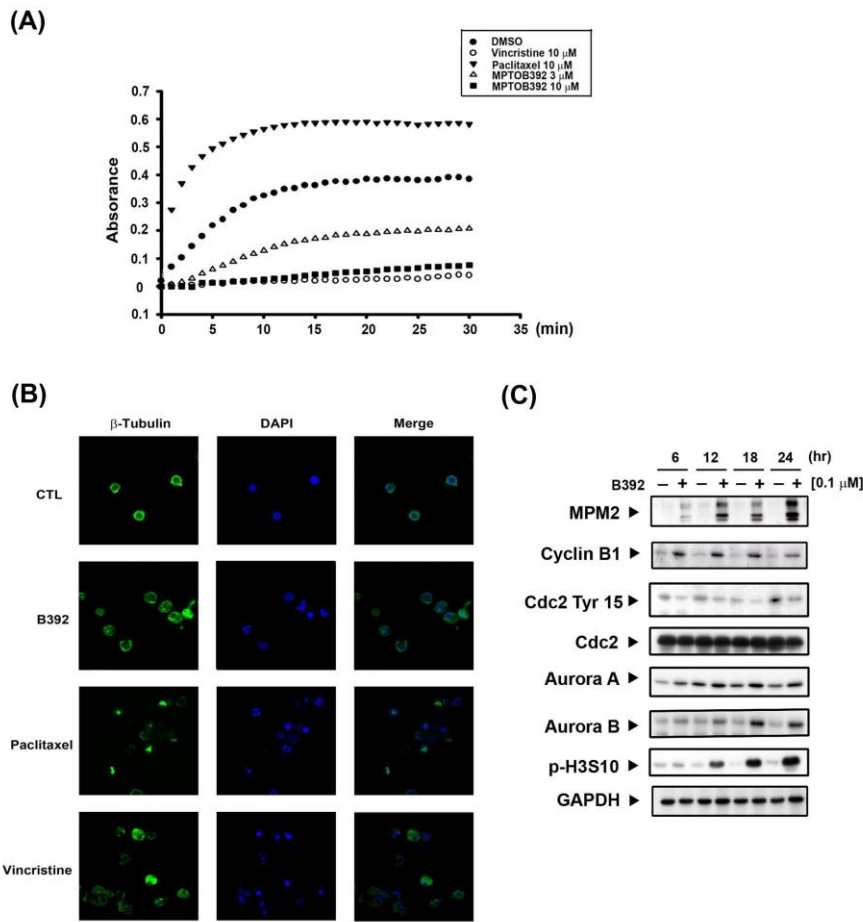
**Figure 4-3. B392 is a depolymerizing agent and caused mitotic arrest**

(A) *In vitro* tubulin polymerization assay was performed to evaluate the effect of B392 on microtubule dynamics. In cell-free condition, tubulin proteins were in reaction buffer in the presence or absence of B392 (3 or 10 μM), paclitaxel (10 μM) or vincristine (10 μM). Assembly of microtubules was determined by measuring absorbance at 340 nm. (B) HL60 cells were exposed to 0.1 μM B392, 10 μM vincristine and 10μM paclitaxel for 24 h. The changes of microtubule network were visualized by staining β-tubulin. Nuclear DNA was stained by DAPI. 10 μM vincristine and 10μM paclitaxel used as a positive control for tubulin depolymerization and tubulin polymerization. (C) HL60 cells were treated 0.1μM B392 time-dependently to detect the expressions of $G_2/M$ related proteins.
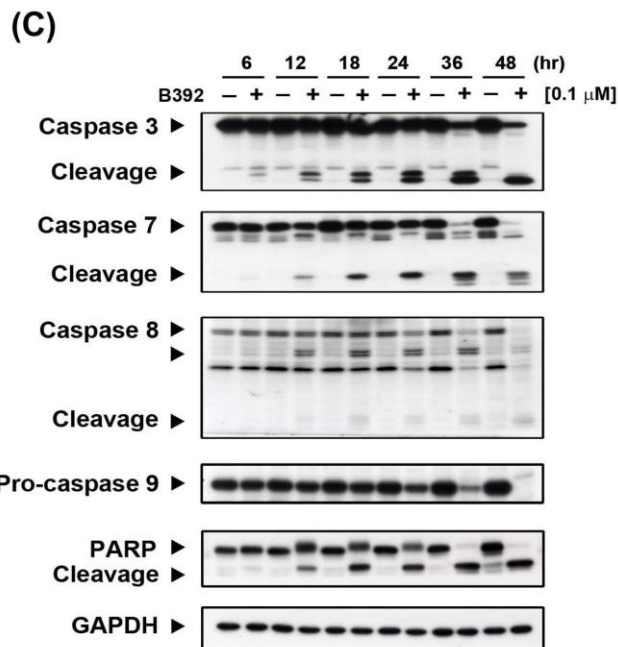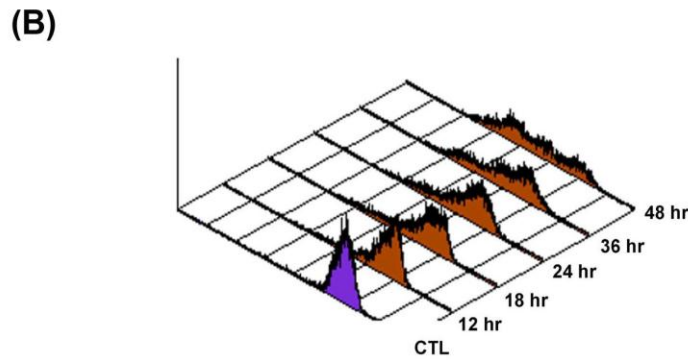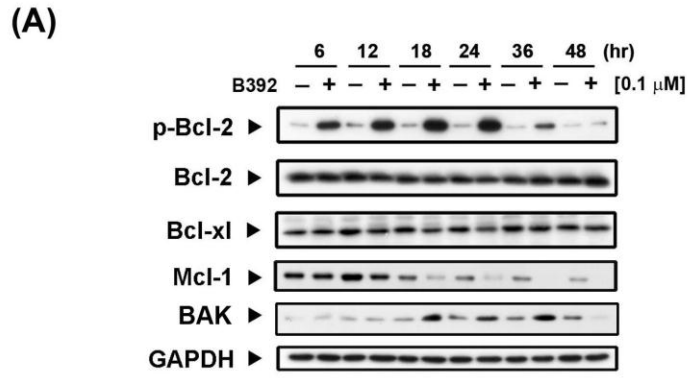
**(A)**



**(B)**



**(C)**



**Figure 4-4. The effect of B392 on apoptosis.**

(A)   HL60 cells were treated with 0.1 μM B392 for indicated time then were harvested for detection of p-Bcl-2, Bcl-xl, Bcl-2, Bak and Mcl-1 by western blot analysis. (B) The phenomena of mitochondria potential loss was measured by flow cytometry analysis with rhodamine 123. HL60 cells were treated with B392 (0.1μM) for indicated time and then incubated with rhodamine 123 (10 μM) at 37℃ for 30 min. The horizontal axis shows the relative fluorescence intensity, when the right curve shift to the left cure represents a loss of mitochondrial membrane potential. (C) HL60 cells were treated with vehicle (0.1% DMSO) or B392 (0.1 μM) for indicated times. The expressions of caspases and PARP cleavege were detected by western blot analysis. GAPDH used as an internal control.
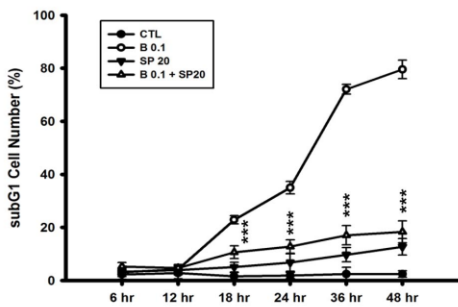
**(A)**
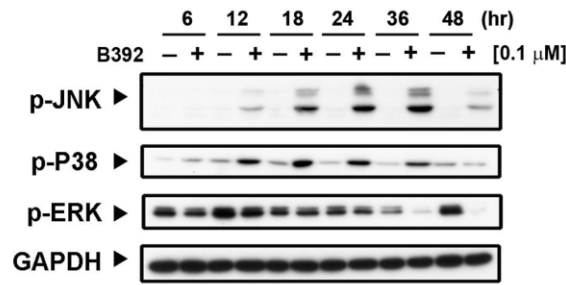


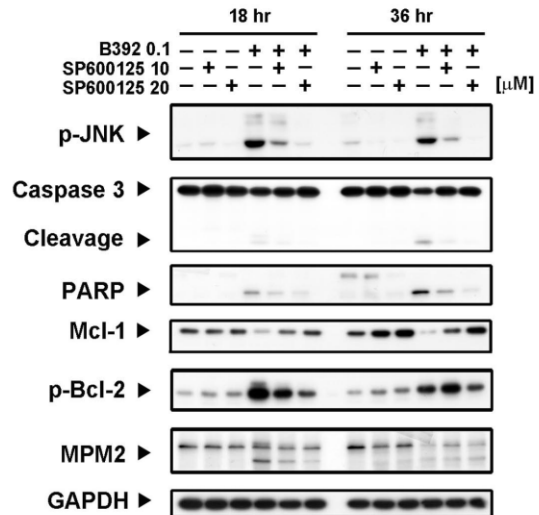**(B)**
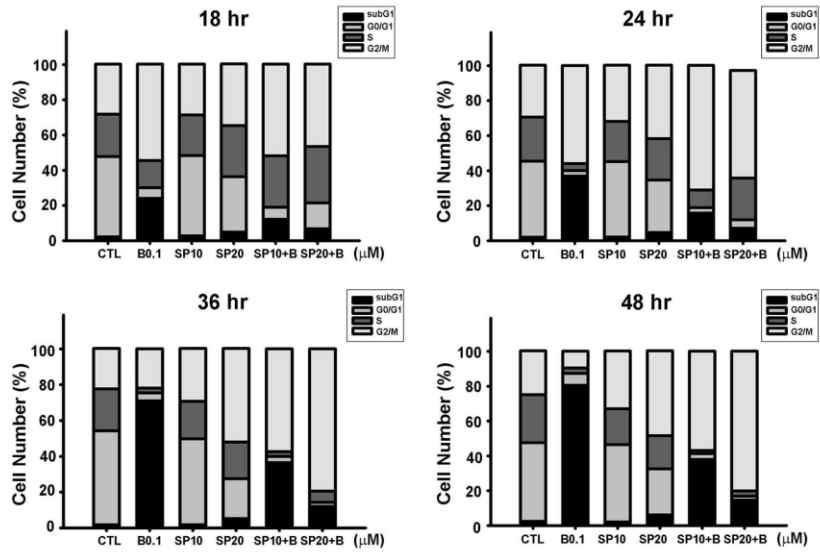


**(C)**



**(D)**



**Figure 4-5. JNK activation was involved in B392-caused cell apoptosis.**

(A)  HL60 cells were treated with vehicle (0.1 % DMSO) or B392 (0.1μM) for time

course. The cells were harvested for detection of p-JNK, p-P38, p-ERK and GAPDH by western blot analysis. (B) HL60 cells were exposed to B392 (0.1μM) in the absence or presence of SP600125 (10, 20 μM) for 18, 24, 36 and 48 h. Cell cycle distribution was analyzed by flow cytometry as well as determining (C) the percentage of subG$_1$ cell number. (*** $P < 0.001$) (D) The expression of p-JNK, caspase 3, PARP, Mcl-1, p-Bcl-2 and MPM2 was determined after treatment of HL60 with 0.1μM B392 in the absence or presence of SP600125 (10, 20 μM) pretreatment for 30 min. SP: SP600126, p-JNK inhibitor.

**(A)**



Cell viability dose-response curves for HL60, MOLM-13, MV4-11, MOLT-4, and CCRF-CEM cell lines treated with Sirolimus (μM) at 48 hr, 72 hr, and 96 hr.

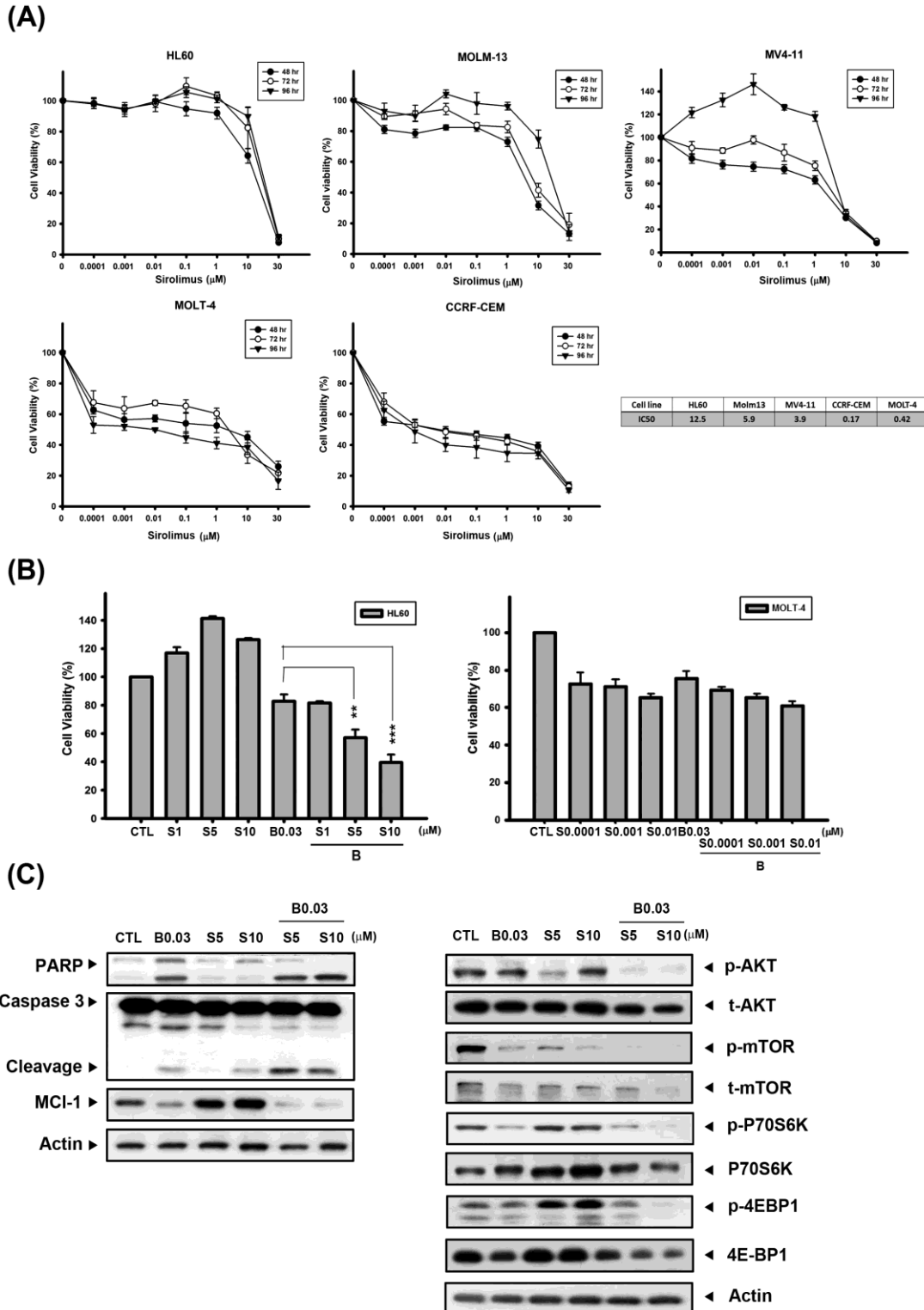| Cell line | HL60 | Molm13 | MV4-11 | CCRF-CEM | MOLT-4 |
|-----------|------|--------|--------|----------|--------|
| IC50 | 12.5 | 5.9 | 3.9 | 0.17 | 0.42 |

**(B)**



**(C)**



**Figure 4-6. B392 sensitized sirolimus anticancer activity in sirolimus-resistant cell line.**

(A) Acute myeloid leukemia cell lines (HL60, MV4-11, MOLM-13) and

112

lymphoblastic cell lines (MOLT-4, CCRF-CEM) were treated with the indicated concentration of sirolimus for 48, 72, 96 h. The cell viability was determined by MTT assay. The right table summarizes the $IC_{50}$ of sirolimus in 72 h. (B) The cell viability of B392 combined with sirolimus for 72h. (C) The expression of caspase 3, PARP, p-AKT, t-AKT, p-mTOR, t-mTOR, p-P70S6K, P70S6K, p-4EBP1, 4EBP, Mcl-1 and actin was determined after B392 combination with sirolimus for 72 h. S: sirolimus   ** $P < 0.01$, *** $P < 0.001$
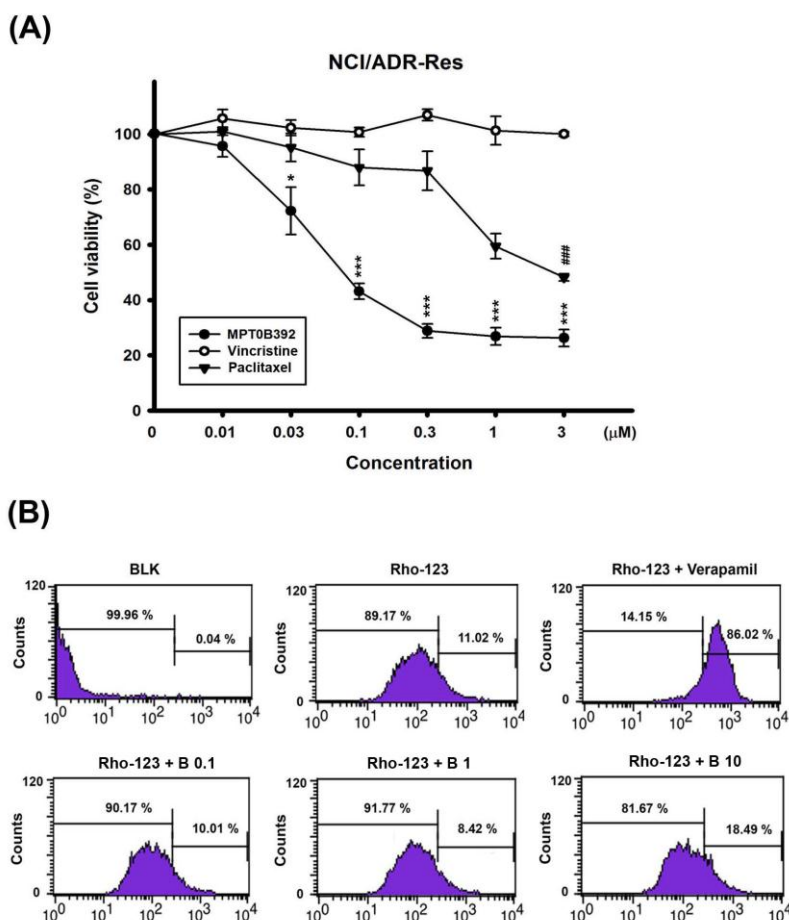
**Supplementary Figure 4-1. The cell viability of B392 on NCI/ADR-RES cell line and effect of B392 on p-gp activity.**

NCI/ADR-RES were treated with the indicated concentrations of B392, vincristine or paclitaxel for 48 h. The cell viability was determined by MTT assay. (* $P < 0.05$, ** $P < 0.01$, *** $P < 0.001$) (B) NCI/ADR-RES cells were treated NCI/ADR-RES cells were treated with or without indicated agents (Verapamil, 50 μM; B392, 0.1, 1, 10 μM) for 1 h. After treatment with indicated drugs for 30 min, 10 μM Rhodamine 123 (Rho-123) was added and incubation for 30 min at 37℃. The signal of Rhodamine 123 was detected by flow cytometry. BLK, blank; Rho-123, Rhodamine 123 (10 μM), p-gp inhibitor.
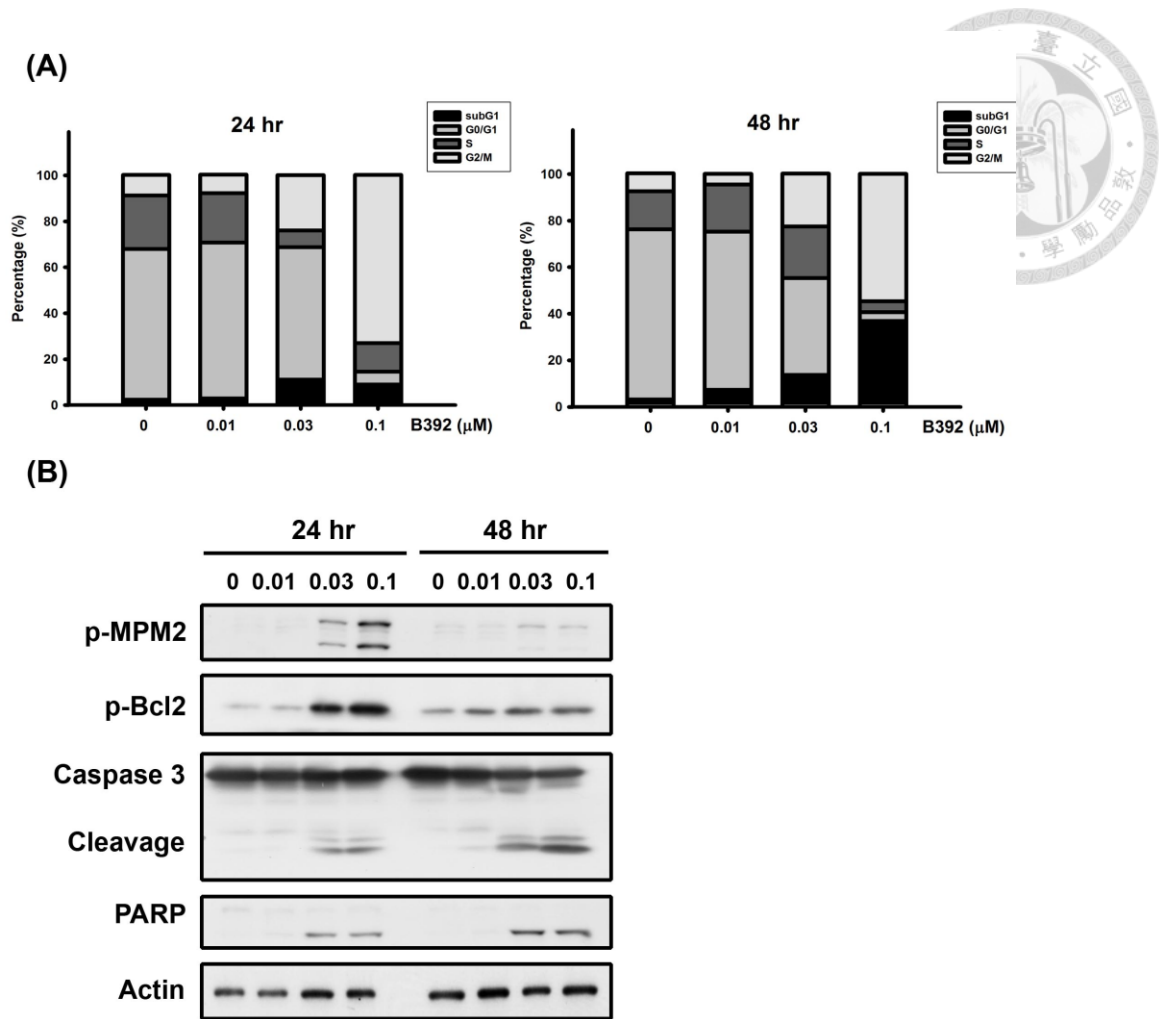
**Supplementary Figure 4-2. The effect of B392 on MOLT-4 cell line.**

MOLT-4 cells were incubated with B392 (0.01, 0.03, 0.1μM) for 24 and 48 h, then cells were harvested for (A) cell cycle analysis and (B) detection of the p-MPM2, p-Bcl-2, caspase 3 and PARP expression by western blot analysis.
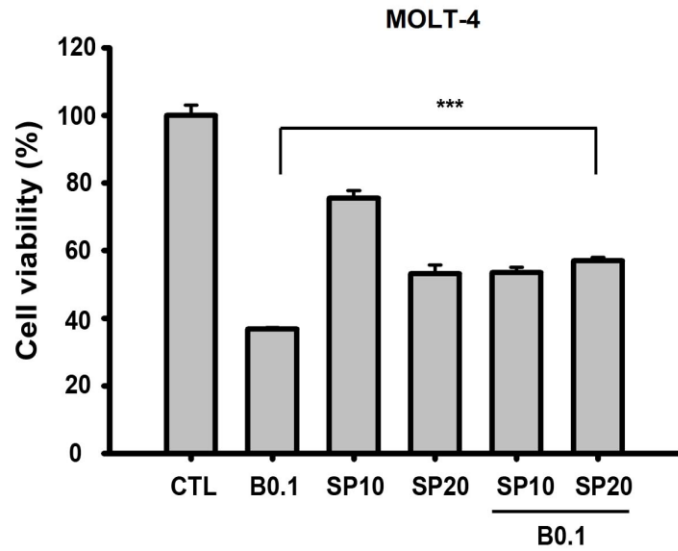
**Supplementary Figure 4-3. B392 induced MOLT-4 apoptosis also though JNK activation.**

Cell viability of MOLT-4 cells after treatment with B392 at dose of 0.1μM for 48 h in the absence or presence of SP600125 (10, 20 μM). SP: SP600125, JNK inhibitor. *** $P < 0.001$

# Chapter 5

# 探討 eIF4E binding protein 1 的表現量和人類大腸直腸癌的臨床參數之相關性

# eIF4E binding protein 1 expression is associated with clinical survival outcomes in colorectal cancer patients

# 中文摘要

eIF4E binding protein 1 (4E-BP1) 在 cap-dependent 和 independent 的轉譯過程中扮演重要角色，也因此控制了蛋白質的生合成。本篇是第一次發現 4E-BP1 蛋白的表現量和人類大腸直腸癌的進程具有相關性。和正常的大腸上皮細胞比較，4E-BP1 在大腸直腸癌細胞及病人的組織中有高度表現；此外，統計結果發現 4E-BP1 高表現量的病患其預後也較差。缺氧一直被認為是癌症治療上的障礙，根據我們之前已發表的研究，發現小穗苧麻素衍生物 YXM110 經由抑制 4E-BP1 而具有抗癌作用；因此，我們進一步去探討在缺氧情況之下，YXM110 是否也具有抑制蛋白生合成的作用。由結果顯示，在缺氧情況之下，YXM110 能夠顯著的抑制 4E-BP1 的表現，推測 YXM110 在無氧狀態下能抑制 cap-independent 的轉譯作用；除此之外，YXM110 可以藉由抑制 hypoxia-inducible factor 1α (HIF-1α) 進而影響其下游 vascular endothelial growth factor (VEGF) 蛋白的表現。綜合以上的發現，4E-BP1 在大腸直腸癌中，不僅可以作為有發展潛力的生物標記，也是一個重要的治療標的物，而 YXM110 則期能成為治療大腸直腸癌的新穎藥物。

# Abstract

eIF4E binding protein 1 (4E-BP1), is critical for cap-dependent and cap-independent translation. This study is the first to demonstrate that 4E-BP1 expression correlates with colorectal cancer (CRC) progression. Compared to its expression in normal colon epithelial cells, 4E-BP1 was upregulated in CRC cell lines and was detected in patient tumor tissues. Furthermore, high 4E-BP1 expression was statistically associated with poor prognosis. Hypoxia has been considered as an obstacle for cancer therapeutics. Our previous data showed that YXM110, a cryptopleurine derivative, exhibited anticancer activity via 4E-BP1 depletion. Here, we investigated whether YXM110 could inhibit protein synthesis under hypoxia. 4E-BP1 expression was notably decreased by YXM110 under hypoxic conditions, implying that cap-independent translation could be suppressed by YXM110. Moreover, YXM110 repressed hypoxia-inducible factor 1α (HIF-1α) expression, which resulted in decreased downstream vascular endothelial growth factor (VEGF) expression. These observations highlight 4E-BP1 as a useful biomarker and therapeutic target, indicating that YXM110 could be a potential CRC therapeutic drug.
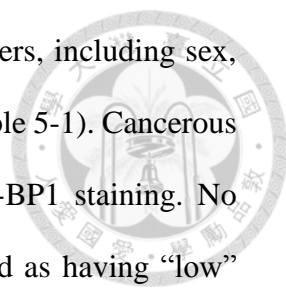
# 5-1 Results

**4E-BP1 is upregulated in the CRC cell lines and in a CRC tissue microarray**

To elucidate the mechanistic link between 4E-BP1 and CRC, we assessed the basal levels of 4E-BP1 in 6 colon cancer cell lines (SW480, SW620, Colo205, Caco-2, HCT116, and HT-29) and 1 normal colon cell line, CCD-18co, under normoxia and hypoxia. The lowest basal protein expression levels of 4E-BP1 were observed in normal CCD-18co colon cells compared to colon cancer cell lines, under normoxic and hypoxic conditions (Fig. 5-1A, 1B and Supplementary Fig. 5-1A). In addition, the expression of 4E-BP1 was dramatically increased under hypoxic conditions, especially in the CRC cells, compared to its expression under normoxic conditions. This indicates that 4E-BP1 might mediate hypoxia-induced drug resistance (Fig. 5-1C). Notably, the expression levels of 4E-BP1 in SW480, SW620, and Colo205 cells, derived from Duke's B-, C-, and D-type CRC, respectively, appeared to be elevated depending on disease progression. Caco-2 is a well-differentiated colon cancer cell line. However, 4E-BP1 levels in these cells were only slightly higher than in normal CCD-18co cells.

4E-BP1 expression in CRC tissues was also evaluated, and 4E-BP1 was more highly expressed in cancerous colon and rectal tissue sections than in the corresponding non-cancerous sections (Fig. 5-2A, 2B). The liver is the predominant metastatic site for CRC patients. Therefore, we also assessed 4E-BP1 expression levels in the liver in rectum metastases patients. Liver tissue from non-metastatic CRC patients expressed lower levels of 4E-BP1 than liver tissue from metastatic CRC patients. Taken together, the above results suggest that 4E-BP1 expression and tumor progression are related.

**Association of 4E-BP1 expression with clinical parameters for 192 CRC patients**

The association between 4E-BP1 and several clinical parameters, including sex, age, TNM, and cancer stage, was analyzed in 192 CRC patients (Table 5-1). Cancerous and non-cancerous tissues were sectioned into four parts for 4E-BP1 staining. No positive sections or only one positively stained section was defined as having "low" expression of 4E-BP1, and the presence of at least two positively stained sections was classified as "high" expression (Fig. 5-3C). Table 5-1 indicates that 4E-BP1 expression in CRC patients does not correlate with age, gender, T factor (the size of the original tumor) or M factor (distant metastasis). However, we observed a significant statistical correlation with the N factor (lymph node invasion; $p = 0.029$) and 4E-BP1 expression. It is noteworthy that 4E-BP1 expression was more prevalent in patients diagnosed at a late stage (stages III and IV; $p = 0.027$).

**Survival analysis**

The correlation between 4E-BP1 expression and clinical outcome was corroborated by a survival analysis. The patients enrolled in this study did not receive any chemotherapy before surgical resection. A Kaplan-Meier analysis showed that patients with negative results for 4E-BP1 expression exhibited longer survival times (Fig. 5-3A) and longer time to recurrence (Fig. 5-3B; $p = 0.028$ and 0.003, respectively). Taken together, these results indicate that the expression levels of 4E-BP1 directly correlate with CRC progression, patient survival, and recurrence. Therefore, 4E-BP1 could be a prognostic indicator and potential therapeutic target.

**YXM110 inhibits 4E-BP1 expression under hypoxic conditions**

Hypoxia is regarded as an obstacle to effective cancer therapy. It can cause a switch from cap-dependent to cap-independent translation (Braunstein, Karpisheva et al.

2007), a process controlled mainly by 4E-BP1. As shown in Fig. 5-1C, 4E-BP1 is upregulated in cancer cells under hypoxia, and YXM110 has been shown to inhibit its expression (Lai, Pan et al. 2013). Therefore, we assessed the ability of YXM110 to decrease 4E-BP1 protein expression under hypoxic conditions. We observed that 4E-BP1 was significantly repressed by YXM110 under hypoxia, but this was not mediated by mTOR inhibition (Fig. 5-4A). This implies that cap-independent translation is inhibited by YXM110. We confirmed that YXM110 suppressed cap-independent translation when 4E-BP1 was overexpressed using a bicistronic vector harboring cap-dependent firefly luciferase and cap-independent Renilla luciferase genes (Fig. 5-4B). Compared to paclitaxel, HCT116 cells under hypoxic conditions demonstrated increased sensitivity to YXM110 (Lai, Pan et al. 2013). These results suggest that YXM110-induced 4E-BP1 depletion reduces the survival of cancer cells under oxygen-deprivation by making them more sensitive to anticancer agents.

**YXM110 inhibits HIF-1α translation**

The HIF-1 protein activates adaptive responses to hypoxic conditions (Brocato, Chervona et al. 2014). During hypoxia, cap-dependent translation can switch to cap-independent (IRES-dependent) translation of HIF-1α mRNA (Silvera, Formenti et al. 2010). Therefore, mRNA and protein levels of HIF-1α were examined after YXM110 treatment under normoxia and hypoxia. We showed that HIF-1α mRNA expression is indeed increased during hypoxia (Fig. 5-5). However, protein expression of HIF-1α was not detectable by western blot analysis (Fig. 5-5B), suggesting that the translation process was blocked. Pretreatment with the proteasome inhibitor, MG132 could not reverse YXM110 mediated HIF-1α downregulation (Fig. 5-5C). However,

HIF-1β protein levels were also decreased after YXM110 treatment (Supplementary Fig. 5-2), including HIF-1β without IRES-dependent translation. There may be other mechanisms that facilitate YXM110 mediated HIF-1β downregulation. These results suggest that hypoxia-activated cap-independent translation is inhibited by YXM110.

**YXM110 inhibits HRE-luciferase activity and VEGF transcription and translation**

HIF-1 is a known transcription factor for dozens of hypoxia induced target genes (Harris 2002, Semenza 2003, Ziello, Jovin et al. 2007, Brocato, Chervona et al. 2014). HIF-1 regulates transcription at the hypoxia-responsive element (HRE) domain of the promoter. Therefore, we measured the transcriptional activity of HIF-1 via the expression of the downstream target gene *VEGF*. HCT116 cells were transfected with a reporter plasmid containing five copies of HRE with the luciferase promoter gene. The transcriptional activity of HIF-1 in hypoxic cells was approximately 3,000 fold higher than in normoxic cells. However, YXM110 effectively inhibited the hypoxia-induced transcriptional activity of HIF-1 (Fig. 5-6A), and the transcription of hypoxia-increased VEGFA mRNA expression (Fig. 5-6B). Furthermore, the levels of secreted VEGF decreased with YXM110 treatment (Fig. 5-6C). Taken together, the results indicate that YXM110 inhibited HIF-1α translation and its transcriptional activity.
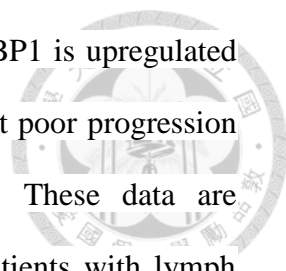
# 5-2 Discussion
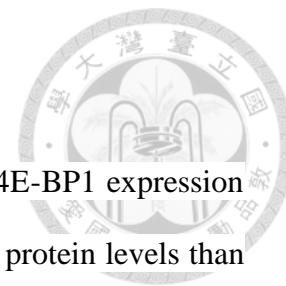
The aim of this study was to demonstrate the importance of 4E-BP1 expression in CRC. All colon cancer lines evaluated exhibited higher 4E-BP1 protein levels than normal cells under normoxia and hypoxia, and a tissue microarray confirmed this result in tumors. Moreover, 4E-BP1 expression positively correlated with poor prognosis. YXM110, a new phenanthroquinolizidine, notably suppressed 4E-BP1 expression under hypoxia, with concomitant inhibition of HIF-1$\alpha$-regulated VEGFA transcription and translation. Therefore, we contend that 4E-BP1 could be a valuable target for CRC treatment.

Translational regulation is crucial in cancer development and progression and can initiate tumor cell survival, angiogenesis, invasion, and metastasis. Translation of mRNAs is controlled by dual mechanisms at the level of initiation: cap-dependent and cap-independent (IRES-dependent) translation (Silvera, Formenti et al. 2010). Substantial evidence has shown that global protein synthesis, which is mostly regulated by cap-dependent translation, promotes tumor cell growth and survival. In cap-dependent translation, the rate-limiting step of initiation is controlled by eIF4E, the 5′ cap-binding protein, 4E-BP1, and the eIF4E-binding protein. Therefore, the roles of the interaction and expression of eIF4E and 4E-BP1 in cancer progression has been widely examined. mTOR hyperphosphorylated 4E-BP1 is inactive and unable to bind to eIF4E in the steady state, indicating that eIF4E can initiate mRNA translation. Therefore, p-4E-BP1 is regarded as a proto-oncogene and even as a "funnel factor" in human cancers (She, Halilovic et al. 2010). Many diverse oncogenic signals, such as Her2, Ras-Raf, and PI3K-Akt converge at 4E-BP1, affecting cancer cell proliferation,

invasion, and metastasis (Martineau, Azar et al. 2013). Studies have shown that in breast cancer, p-4E-BP1 is mainly expressed in poorly differentiated tumors, and correlates with tumor size, lymph node metastasis, and recurrence (Armengol, Rojo et al. 2007, Rojo, Najera et al. 2007). The ratio of 4E-BP1 to eIF4E is an indicator of rapamycin sensitivity (Dilling, Germain et al. 2002, Hsu, Lin et al. 2015) in cancer cells. Increasing evidence indicates that dephosphorylation of 4E-BP1 can serve as a clinical biomarker, and mimetic compounds of 4E-BP1 have recently been developed (Wang, Ye et al. 2014).

However, cap-dependent mRNA translation is inhibited and cap-independent translation is enhanced in response to a variety of cell stressors, including growth arrest, nutrient deprivation, mitosis, hypoxia, and apoptosis (Seton-Rogers 2008, Silvera, Formenti et al. 2010). This suggests that cap-independent translation also plays an important role in cancer. Several studies have demonstrated that 4E-BP1 expression is elevated in human breast, prostate, head and neck, and some gastrointestinal cancers (Martin, Perez et al. 2000, Ray, Yang et al. 2004, Kremer, Klein et al. 2006). Furthermore, mTOR-independent 4E-BP1 expression and phosphorylation have been reported as a mechanism of primary resistance to mTOR kinase inhibitors (Zhang and Zheng 2012, Karlsson, Perez-Tenorio et al. 2013, Ducker, Atreya et al. 2014). Reports have shown that colon cell origin is a strong predictor for mTOR inhibitor resistance (Zhang and Zheng 2012, Ducker, Atreya et al. 2014). In addition, 4E-BP1 overexpression is associated with poor prognosis and endocrine resistance in breast cancer (Karlsson, Perez-Tenorio et al. 2013).
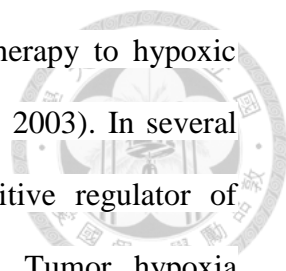
As shown in Fig. 5-1, compared to the normal colon cell line, all cancer cell lines tested had increased 4E-BP1 levels under both normoxic and hypoxic conditions. The

IHC staining of patient tumors provided strong evidence that 4E-BP1 is upregulated in cancerous tissues (Fig. 5-2). Cell line analysis demonstrated that poor progression of CRC is associated with increased 4E-BP1 protein levels. These data are corroborated by the analysis of clinical pathology parameters. Patients with lymph node metastasis had statistically significant high 4E-BP1 expression, which correlated with late-stage CRC (Table 5-1). This was also associated with survival and recurrence time, as patients with low 4E-BP1 expression had better clinical outcomes (Fig. 5-3).

We also determined the expression levels of eIF4E and p-4E-BP1 in colorectal cancer cell lines and normal cells. As shown in supplementary Fig.5-1B and 1D, eIF4E and p-4E-BP1 were upregulated in most colorectal cancer cells under normoxia and hypoxia. However, it is noteworthy that the expression levels of eIF4E and p-4E-BP1 were decreased in hypoxia compared to normoxia in most colorectal cells except for SW480 and SW620 cells, which suggest a role for eIF4E and p-4E-BP1 in cap-dependent translation. Moreover, the analysis of clinical CRC tumor tissues indicates that there is a positive association between 4E-BP1 and eIF4E protein expression (Supplementary table 5-1), suggesting that eIF4E may have a similar role as 4EBP in CRC tumorigenesis. Since the loss of 4E-BP1 or eIF4E overexpression can promote tumorigenesis, the ratio of 4E-BP1 to eIF4E in colorectal cancer cells was also evaluated. Supplementary Fig. 5-1C shows that the ratio of 4E-BP1 to eIF4E dramatically increased in cancer cells, especially under hypoxia.

Tumor hypoxia is considered as an obstacle to efficient cancer treatment with radiotherapy and chemotherapy because it acts as a barrier in the tumor region. Recent evidence has shown that tumor hypoxia is associated with more malignant phenotypes

and poor prognosis. Therefore, developing selectively targeted therapy to hypoxic cells is an ongoing area of research (Kizaka-Kondoh, Inoue et al. 2003). In several reported studies, 4E-BP1 has been demonstrated to be a positive regulator of cap-independent mRNA translation under hypoxic conditions. Tumor hypoxia induced 4E-BP1, decreases cap-dependent translation and activates cap-independent translation of mRNAs encoding HIF1α and VEGFA, which contributes to cell survival and angiogenesis (Braunstein, Karpisheva et al. 2007). YXM110 significantly depleted 4E-BP1 expression without mTOR inhibition, decreased 4E-BP1 mediated cap-independent translation HIF-1α translation and its transcriptional activity under hypoxia (Figs. 5-4-6). These results suggest that YXM110 represses hypoxia-activated cap-independent translation.

Based on the findings described in Table 5-1, we concluded that 4EBP1 expression is associated with N factor, which indicates that nearby (regional) lymph nodes are involved in CRC progression, as well as TNM stage. It has been reported that soluble VEGF-A was associated with lymphangiogenensis (Soubrane, Mouawad et al. 2006). Moreover, the expression VEGF-A and VEGF-C was significantly elevated in CRCs, and tumors with lymph node metastases had significantly higher levels of VEGF-A compared with non-metastatic tumors (George, Tutton et al. 2001, Pringels, Van Damme et al. 2012). We therefore evaluated the expression levels of VEGF-A and VEGF-C after YXM110 treatment and showed that YXM110 depleted VEGF-A and VEGF-C expression at the transcriptional level (Fig. 5-6 and Supplementary Fig. 5-3). However, it was found that hypoxia induces VEGF-C expression via a HIF-1α-independent translation-mediated mechanism (Morfoisse, Kuchnio et al. 2014). We speculated that VEGF-C translational downregulation might

be due to YXM110 mediated cap-independent inhibition rather than a 4E-BP1-HIF-1$\alpha$ pathway.

Akt/mTOR signaling is known to regulate protein synthesis. YXM110 was proved to have an ability to inhibit protein synthesis even that YXM110 induced mTOR signaling activation (Fig. 5-4A) (Lai, Pan et al. 2013). It was also shown that extracellular signals activate mTOR, which in turns triggers HIF-1$\alpha$ induction though transcriptional regulation (Demidenko and Blagosklonny 2011). Although HIF-1$\alpha$ mRNA was induced after treatment with YXM110, HIF-1$\alpha$ protein was profoundly suppressed by YXM110 in a translational manner (Fig. 5-5). Hypoxia can cause cell cycle arrest and simultaneously suppresses conversion from proliferative arrest to cellular senescence (Leontieva, Natarajan et al. 2012). (Sullivan, Pare et al. 2008). Nonetheless, inhibition of 4E-BP1 can sensitize cells, which is hypoxia tolerance and radioresistance, to chemotherapy and irradiation (Dubois, Magagnin et al. 2009). We recently reported that compared to anticancer drugs, YXM110 can reduce the survival of cancer cells during hypoxia (Lai, Pan et al. 2013). These combined observations strongly suggest that YXM110, an inhibitor of 4E-BP1, may be an effective agent for treating drug-resistant CRC.

In conclusion, to the best of our knowledge, this study is the first to demonstrate the significance of 4E-BP1 in CRC through clinical data. Although 4E-BP1 expression is paradoxically elevated in some tumors and can act as a tumor suppressor or proto-oncogene, we emphasize that, in this study, the expression of 4E-BP1 is associated with poor prognosis in CRC. Here we provide a novel mechanism of action for the cryptopleurine derivative, YXM110. We show that it significantly depletes 4E-BP1 expression and subsequently induces the suppression of cap-independent

translation with the inhibition of HIF-1α-regulated VEGFA transcription under hypoxia, which facilitates drug resistance. Therefore, from a therapeutic perspective, 4E-BP1 could be a promising prognostic marker and an excellent drug target for treatment of CRC. Accordingly, YXM110 is a potential lead therapeutic compound, particularly for treatment of drug-resistant CRC.

| Parameters | 4E-BP1 | | p value |
|---|---|---|---|
| | Low | High | |
| | (n = 98) (%) | (n = 94) (%) | p value |
| Age (years) | | | |
| ≤65 | 51 (52.0) | 43 (45.7) | |
| >65 | 47 (48.0) | 51 (54.2) | 0.391 |
| Gender | | | |
| Female | 39 (39.8) | 51 (54.3) | |
| Male | 59 (60.2) | 43 (45.7) | 0.060 |
| T factor | | | |
| 1 | 5 (5.1) | 2 (2.1) | |
| 2 | 15 (15.3) | 13 (13.8) | |
| 3 | 55 (56.1) | 55 (58.5) | |
| 4 | 23 (23.5) | 24 (25.5) | 0.713 |
| N factor | | | |
| 0 | 50 (51.0) | 33 (35.1) | |
| 1+2 | 48(49.0) | 61 (64.9) | **0.029** |
| M factor | | | |
| 0 | 83 (84.7) | 76 (80.9) | |
| 1 | 15 (15.3) | 18 (19.1) | 0.567 |
| Stage | | | |
| I | 13 (13.3) | 10 (10.6) | |
| II | 33 (33.7) | 20 (21.3) | |
| III | 36 (36.7) | 46 (48.9) | |
| IV | 16 (16.3) | 18 (19.1) | 0.184 |
| Stage | | | |
| Early | 46 (46.9) | 29 (30.9) | |
| Late | 52 (53.1) | 65 (69.1) | **0.027** |

No positive or only one positively stained section was defined as "low" expression of 4E-BP1, and the presence of at least two positively stained sections was classified as "high" expression. ($N = 192$).

**Table 5-1: Association of 4E-BP1 expression and clinical parameters in tumor tissues of colorectal cancer patients**

TNM classificationis a cancer staging system which describes the stage of solid tumor. T: the size of the original (primary) tumor; N: invasion to nearby (regional) lymph nodes; M: distant metastasis.
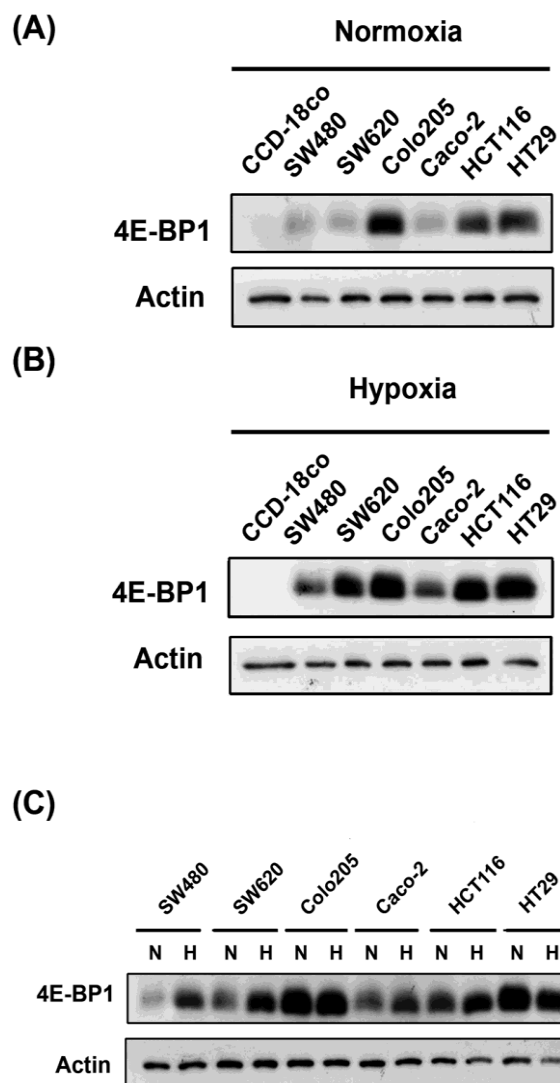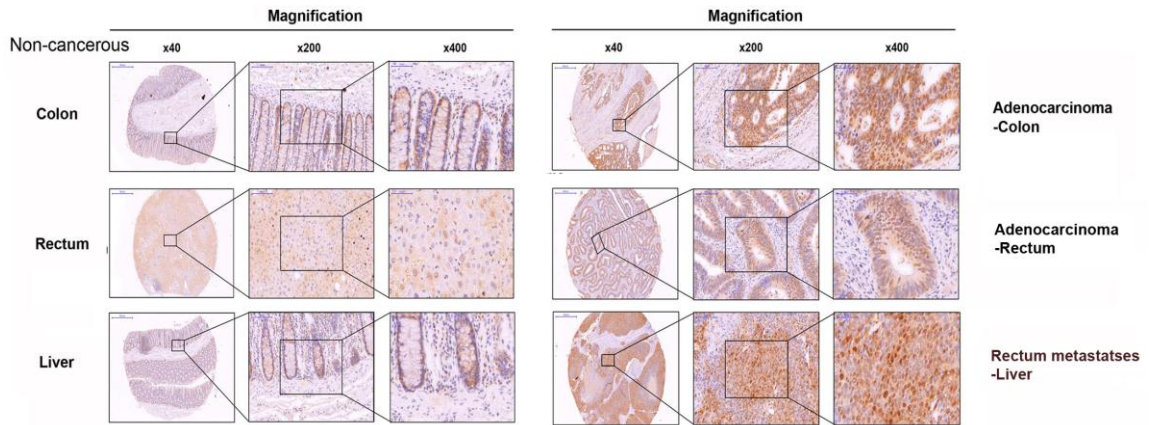
**Figure 5-1. Comparsion of 4E-BP1 expression in normal and colorectal cancer cells under normoxia and hypoxia**

The detection of 4E-BP1 expression in CCD-18co (normal colon cell), SW480, SW620, Colo205, Caco-2, HCT116, HT29 under (A) normoxia and (B) hypoxia. (C) Also camparsion of the difference of 4E-BP1 between normoxia and hypoxia in each one cell lines.
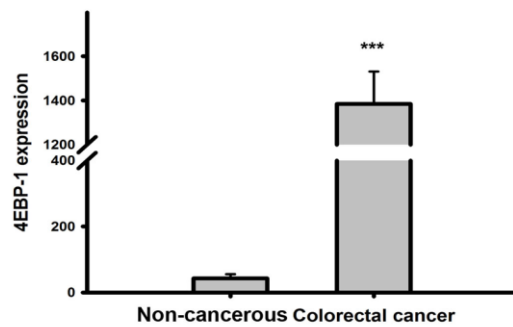
**(A)**



**(B)**



**Figure 5-2. Immnuohistochemical staining of 4E-BP1 in a tissue microarray**

(A) Representive 4E-BP1 staining of CRC specimens and corresponding non-cancerous tissues. (B) The statisitc result of 4E-BP1 expression in CRC and paired normal specimens by Image J. *** $P < 0.001$
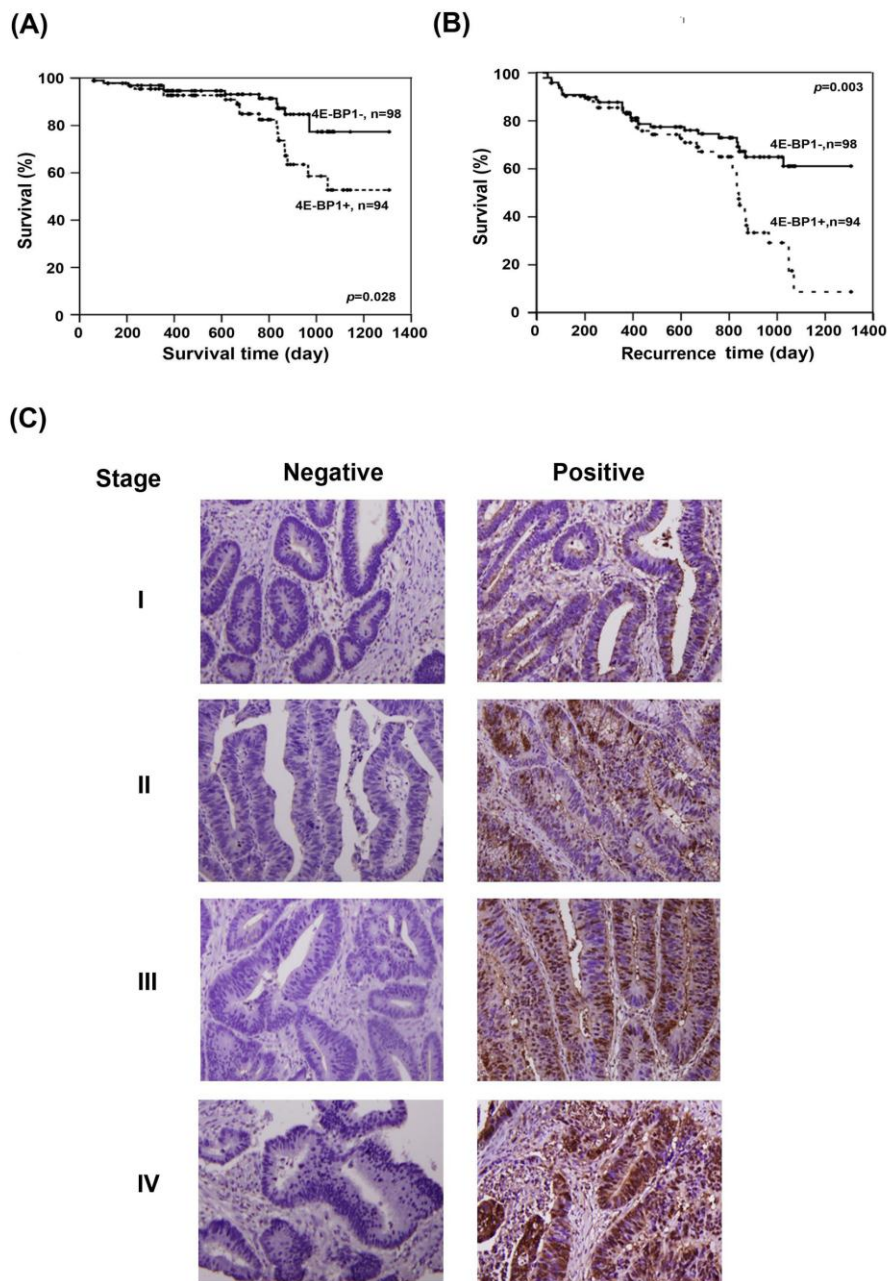
**Figure 5-3. Evaluation of the clinincal importance of 4E-BP1 expression in CRC patients**

The correlation between 4E-BP1 and (A) survival time and (B) recurrence time were analyzed by Kaplan-Meier analysis. (C) The representative of immunohistochemical staining of 4E-BP1 on different stages of sections. Left lane shows the negative staining and right lane are the positive results.
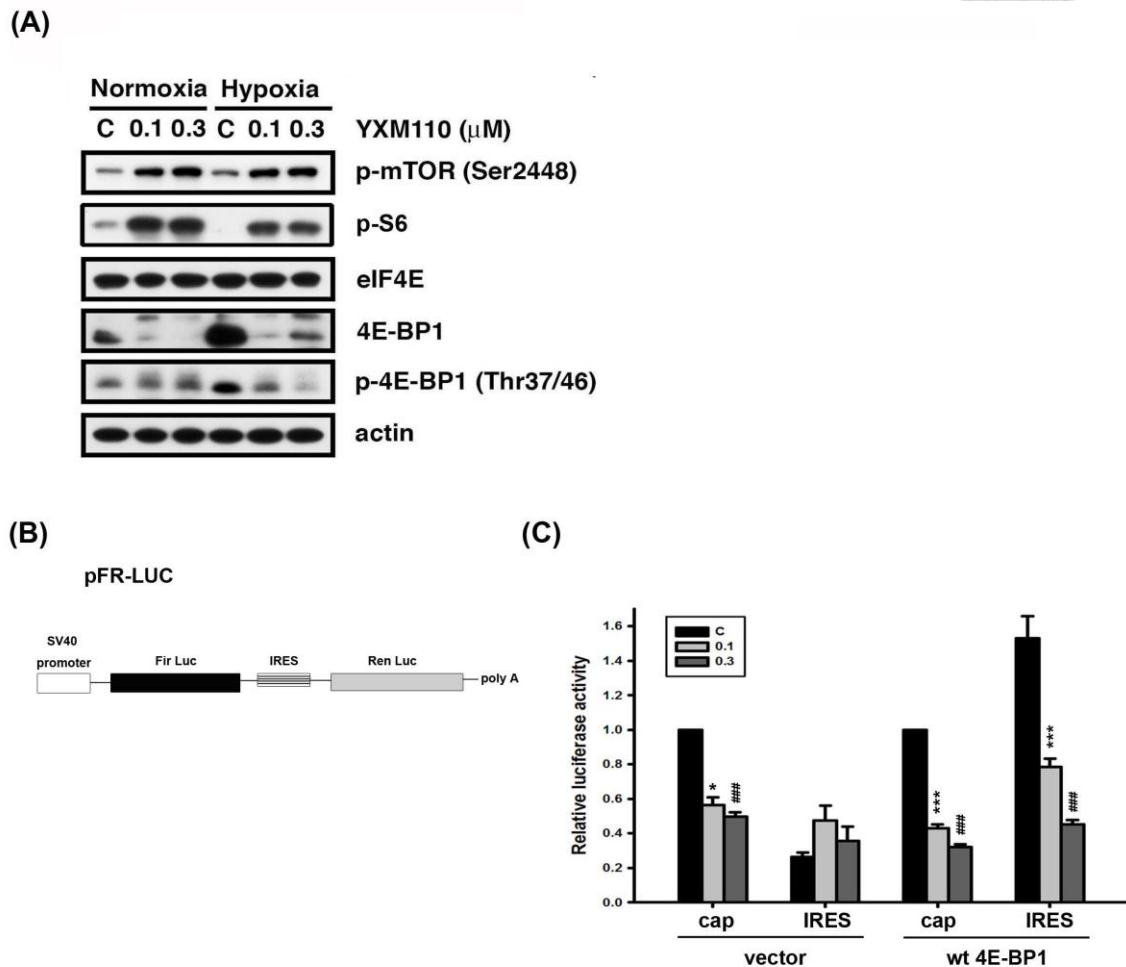
**(A)**

Normoxia  Hypoxia
C  0.1  0.3  C  0.1  0.3   YXM110 (μM)

p-mTOR (Ser2448)

p-S6

eIF4E

4E-BP1

p-4E-BP1 (Thr37/46)

actin

**(B)**

pFR-LUC

SV40 promoter | Fir Luc | IRES | Ren Luc — poly A

**(C)**

Relative luciferase activity

C
0.1
0.3

cap    IRES    cap    IRES
vector          wt 4E-BP1

**Figure 5-4. YXM110 suppresses cap-independent translation through 4E-BP1 deletion.**

(A) HCT116 cells were treated with vehicle (0.1% DMSO) or YXM110 (0.1 or 0.3 μM) under normoxia or hypoxia conditions for 24 h. The cells were then harvested for detection of p-mTOR (Ser2448), eIF4E, 4E-BP1, p-4E-BP1 (Thr37/46), p-S6 (Ser240/244) and actin by western blot analysis. (B) Bicistronic luciferase vector (pFR-Luc) contains a cap-dependent firefly (Fir) and cap-independent Renilla (Ren) luciferase. (C) HCT116 cells were cotransfected bicistronic vector and wt 4E-BP1 for testing the effect of YXM110 on cap-dependent and cap-independent translation by using a dual Luciferase reporter system. * $P < 0.05$; *** $P < 0.001$; [###] $P < 0.001$
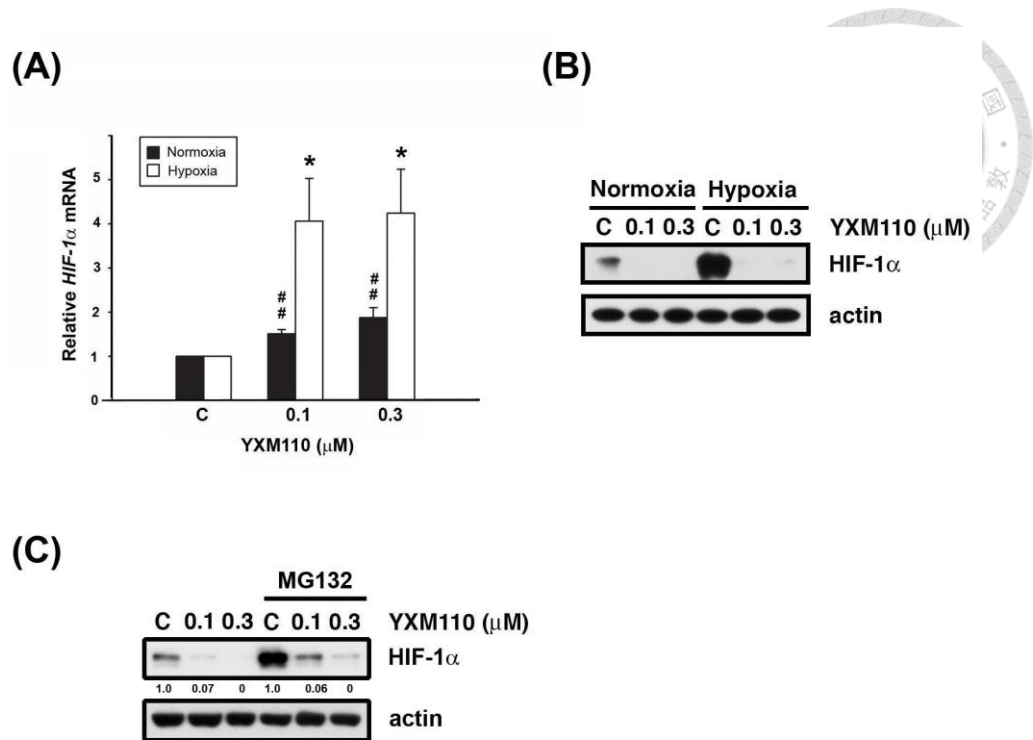
134

**Figure 5-5. YXM110 inhibits HIF-1α translation**

(A) HIF-1α mRNA was analyzed with quantitative real-time RT-PCR after 6 h treatment of YXM110 (0.1 or 0.3 μM) under normoxia or hypoxia conditions. (B) HCT116 cells were treated with vehicle (0.1% DMSO) or YXM110 (0.1 or 0.3 μM) under normoxia or hypoxia conditions for 24 h or (C) pretreated with vehicle or 10 μM MG132 and then incubated with vehicle or YXM110 (0.1 or 0.3 μM) for 24h under hypoxia. The cells were then harvested for detection of HIF-1α and actin by western blot analysis. $* P < 0.05;$ $^{##} P < 0.01$
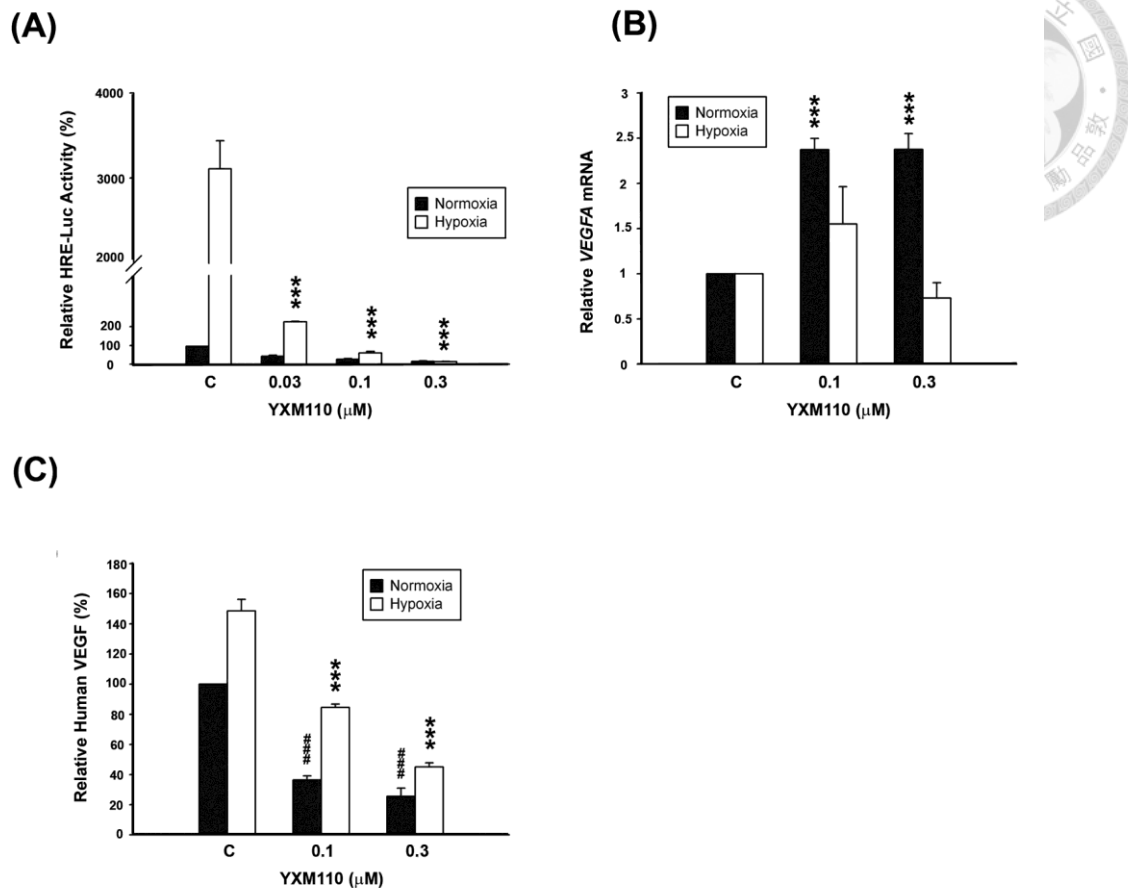
**Figure 5-6. YXM110 inhibits HRE-Luciferases activity and VEGF transcription and translation**

(A) HCT116 cells transiently transfected with 5-HRE-Luciferase reporter were treated with YXM110 under normoxia or hypoxia conditions for 24 h. Data have shown represented luciferase activity relative to the control. (B) VEGFA mRNA was analyzed with quantitative real-time RT-PCR after 6 h treatment of YXM110 (0.1 or 0.3 μM) under normoxia or hypoxia conditions. (C) VEGF levels in culture medium were determined using Human VEGF Quantikine ELISA Kit. *** $P < 0.001$; ### $P < 0.001$

|  | 4EBP1 | | |
| --- | --- | --- | --- |
|  | Low | High | |
|  | (n=30) | (n=30) | p value |
| eIF4E | | | |
| Low (n=35) | 25 | 10 | |
| High (n=25) | 5 | 20 | <0.0001 |

**Supplementary Table 5-1. The correlation of 4EBP1 and eIF4E expression in tumor tissues of CRC.**

No positive or only one positively stained section was defined as "low" expression of 4E-BP1 or eIF4E, and the presence of at least two positively stained sections was classified as "high" expression. (N = 60)
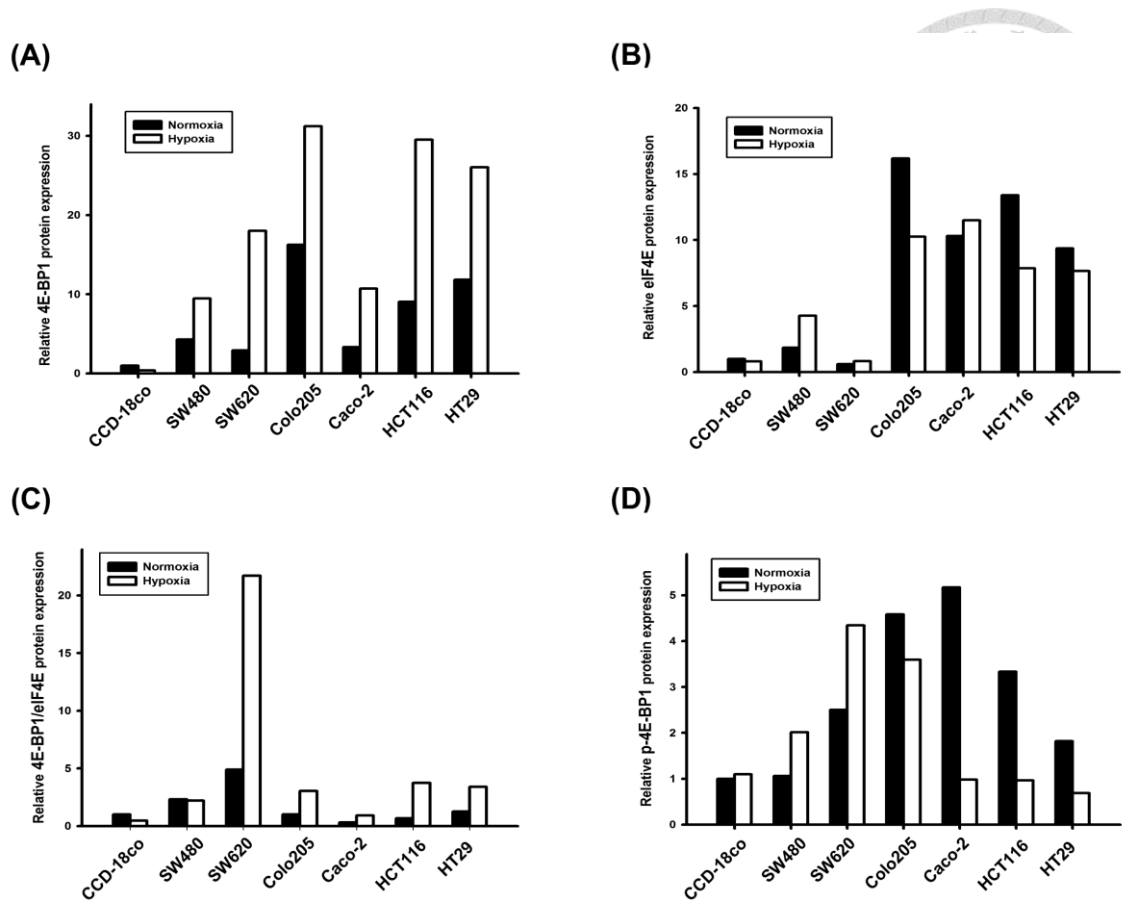
**Supplementary Figure 5-1. Comparison of basal expression of 4E-BP1, eIF4E and p-4E-BP1 in normal colon cell line and colorectal cancer cells under normoxia and hypoxia.**

The quantitative results of (A) 4E-BP1, (B) eIF4E, and (D) p-4E-BP1 expression and (C) the ratio of 4E-BP1:eIF4E in normal colon cell line and colorectal cancer cells under normoxia and hypoxia.
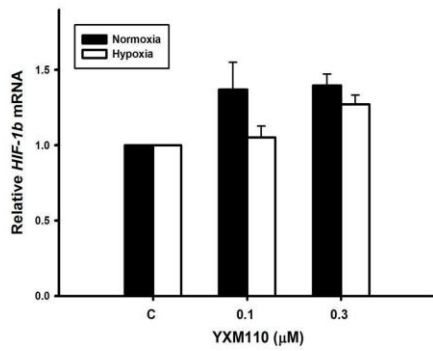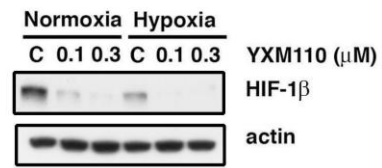
**Supplementary Figure 5-2. YXM110 inhibits HIF-1β protein levels.**

(A) HIF-1β mRNA was analyzed with quantitative real-time RT-PCR after 6 h treatment of YXM110 (0.1 or 0.3 μM) under normoxia or hypoxia conditions. (B) HCT116 cells were treated with vehicle (0.1% DMSO) or YXM110 (0.1 or 0.3 μM) under normoxia or hypoxia conditions for 24 h. The cells were then harvested for detection of HIF-1β and actin by western blot analysis.
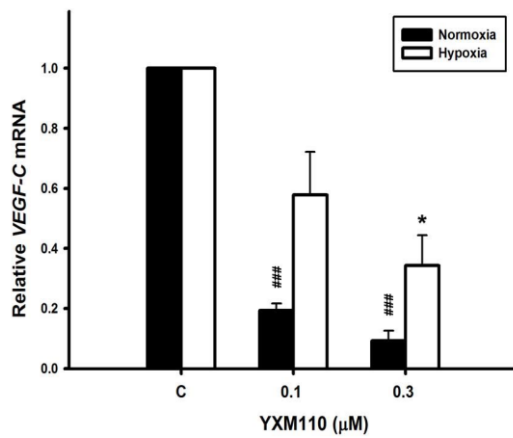
**Supplementary Figure 5-3. YXM110 suppresses VEGF-C transcriptional level.**

VEGF-C mRNA was analyzed with quantitative real-time RT-PCR after 6 h treatment of YXM110 (0.1 or 0.3 μM) under normoxia or hypoxia conditions.. * $P < 0.01$; ### $P < 0.001$

# Chapter 6 Conclusion and Perspectives

Cancer has been a life-threatening disease over the past few decades and always is the leading causes of mortality and morbidity worldwide, including Taiwan. The major causes of cancers in the great majority of cancers are due to environmental factors, such as tobacco (smoking), diet (or obesity), radiation, infections and chemical reagents. Only a small part of reasons came from inherited genetics. Amounts of researches are focusing on the pathology of carcinogenesis and learning how to fight cancer more efficiently, decrease the possibility of drug-resistances and prolong or improve the life of patients.

There are many types of cancer treatment, such as surgery, traditional systemic chemotherapy, radiation therapy, targeted therapy, immunotherapy, stem cell transplant, hyperthermia so on. Selecting proper therapeutic strategy against different characteristic cancers is the most important lessons we have to learn. In this thesis, we studied three different treatment approaches (combination therapy, improved chemotherapy by a new microtubule-targeting agent and identifying a key factor in tumorgenesis to develop targeted therapy) to show their underlying anticancer mechanisms (Fig 6-1).

ALL (acute lymphoblastic leukemia) is a complicated disease which usually needs with various combined chemotherapy for treatment in avoidance of recurrence and resistance. Moreover, the side effects from multiple drug combinations also could not be ignored. Therefore, to achieve this goal, we combined vorinostat, which has extensive action on anticancer but fewer side effects, has been used in clinical treatment of cutaneous T cell lymphoma, with vincristine on ALL cell lines. The synergic effect

with combination treatment was far better than each alone though the changes of microtubule dynamics and the same combined result also found *in vivo* animal model without toxicity. Moreover, we found vincristine and vorinostat combined effect as the same as vincristine-HDAC6 inhibitors (tubastatin A and ACY1215). Consequently, we conclude that the settings of vincristine and vorinostat combination (or vincristine-HDAC6 inhibitor) will be a new clinical therapeutic testing in acute lymphoblastic leukemia

Conventional chemotherapy therapy remains playing an essential role in present anti-leukemic therapy. However, annoying side effects, potency as well as drug resistance are still obstacles for achieving the best clinical response. In the second study, we examined whether MPT0B392 deserves as a developmental anticancer agent. From the results, MPT0B392, an oral microtubule destabilizing agent, exhibited better antitumor effect than vincristine *in vivo* xenograft model without affecting mice body weight. Moreover, another benefit of MPT0B392 is that MPT0B392 is not a P-gp substrate, which differs from many other chemotherapeutic agents, such as paclitaxel and vincristine. Furthermore, it can overcome sirolimus-resistant leukemic cells. All in all, MPT0B392 is a valuable anticancer agent against acute leukemia.

There has been an increased focus in the past few years on individualized therapy for cancer treatment. The development of prognostic and predictive markers would be helpful for the development of targeted therapeutics. Recently, several valuable molecular markers have been discovered for colorectal cancer. Here, in the third study, we identified a translational protein, 4E-BP1 as a prognostic factor in colorectal cancer. 4E-BP1 was upregulated both in colon cancer cell lines as well as patients cancerous tissues. The expression of 4E-BP1 has positive correlation with

survival and recurrence time. In hypoxia, HIF-1$\alpha$-regulated VEGFA cap-independently translation was suppressed by YXM110 through 4E-BP1 inhibition.

In virtue of the heterogeneity and variation of cancer, evaluating clinical patients' situations and selecting proper therapeutic approaches are crucial for clinical outcome of cancer treatment. Through the research and discussion of vincristine-vorinostat combination therapy, improved MPT0B392 mono-chemotherapy and 4E-BP1 targeted therapy, we hope to provide distinct aspects of treatment method and idea to bring new insights of basic research and drug discovery.
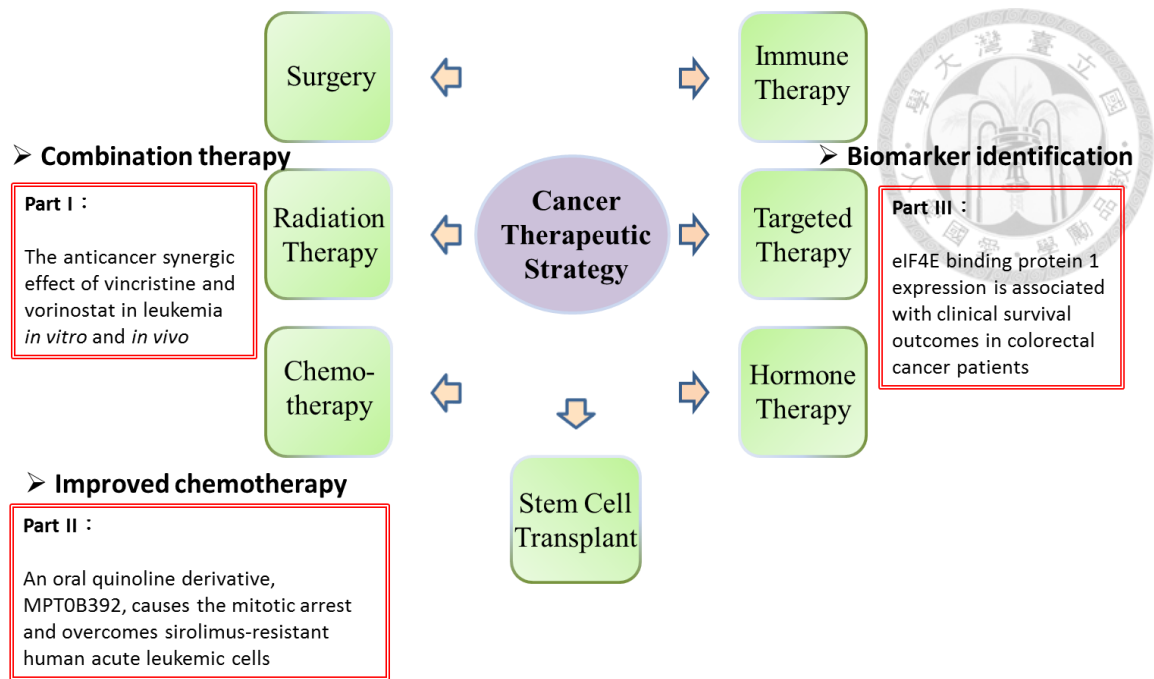
**Figure 6-1. Summary of different anticancer treatment strategies in this study.**

# Publication

1. **Chao MW**, Wang LT, Lai CY, Yang XM, Cheng YW, Lee KH, Pan SL, Teng CM. eIF4E binding protein 1 expression is associated with clinical survival outcomes in colorectal cancer. Oncotarget. 2015 Jun 29. [Epub ahead of print]

2. **Chao MW**, Lai MJ, Liou JP, Chang YL, Wang JC, Pan SL, Teng CM. The synergic effect of vincristine and vorinostat in leukemia in vitro and in vivo. J Hematol Oncol. 2015 Jul 10; 8:82.

3. **Chao MW**, Chen CH, Chang YL, Teng CM, Pan SL. α-Tomatine-mediated anti-cancer activity in vitro and in vivo through cell cycle- and caspase-independent pathways. PLoS One. 2012;7(9):e44093.

# References

Aldana-Masangkay, G. I. and K. M. Sakamoto (2011). "The role of HDAC6 in cancer." <u>J Biomed Biotechnol</u> **2011**: 875824.

Ali, I. K., L. McKendrick, S. J. Morley and R. J. Jackson (2001). "Truncated initiation factor eIF4G lacking an eIF4E binding site can support capped mRNA translation." <u>EMBO J</u> **20**(15): 4233-4242.

Armengol, G., F. Rojo, J. Castellvi, C. Iglesias, M. Cuatrecasas, B. Pons, J. Baselga and S. Ramon y Cajal (2007). "4E-binding protein 1: a key molecular "funnel factor" in human cancer with clinical implications." <u>Cancer Res</u> **67**(16): 7551-7555.

Bacus, S. S., A. V. Gudkov, M. Lowe, L. Lyass, Y. Yung, A. P. Komarov, K. Keyomarsi, Y. Yarden and R. Seger (2001). "Taxol-induced apoptosis depends on MAP kinase pathways (ERK and p38) and is independent of p53." <u>Oncogene</u> **20**(2): 147-155.

Bali, P., M. Pranpat, J. Bradner, M. Balasis, W. Fiskus, F. Guo, K. Rocha, S. Kumaraswamy, S. Boyapalle, P. Atadja, E. Seto and K. Bhalla (2005). "Inhibition of histone deacetylase 6 acetylates and disrupts the chaperone function of heat shock protein 90: a novel basis for antileukemia activity of histone deacetylase inhibitors." <u>J Biol Chem</u> **280**(29): 26729-26734.

Bali, P., M. Pranpat, R. Swaby, W. Fiskus, H. Yamaguchi, M. Balasis, K. Rocha, H. G. Wang, V. Richon and K. Bhalla (2005). "Activity of suberoylanilide hydroxamic Acid against human breast cancer cells with amplification of her-2." <u>Clin Cancer Res</u> **11**(17): 6382-6389.

Blagosklonny, M. V., R. Robey, D. L. Sackett, L. Du, F. Traganos, Z. Darzynkiewicz, T. Fojo and S. E. Bates (2002). "Histone deacetylase inhibitors all induce p21 but differentially cause tubulin acetylation, mitotic arrest, and cytotoxicity." <u>Mol Cancer Ther</u> **1**(11): 937-941.

Bloom, J. and F. R. Cross (2007). "Multiple levels of cyclin specificity in cell-cycle

control." <u>Nat Rev Mol Cell Biol</u> **8**(2): 149-160.

Bots, M. and R. W. Johnstone (2009). "Rational combinations using HDAC inhibitors." <u>Clin Cancer Res</u> **15**(12): 3970-3977.

Boyault, C., K. Sadoul, M. Pabion and S. Khochbin (2007). "HDAC6, at the crossroads between cytoskeleton and cell signaling by acetylation and ubiquitination." <u>Oncogene</u> **26**(37): 5468-5476.

Braunstein, S., K. Karpisheva, C. Pola, J. Goldberg, T. Hochman, H. Yee, J. Cangiarella, R. Arju, S. C. Formenti and R. J. Schneider (2007). "A hypoxia-controlled cap-dependent to cap-independent translation switch in breast cancer." <u>Mol Cell</u> **28**(3): 501-512.

Breuninger, L. M., S. Paul, K. Gaughan, T. Miki, A. Chan, S. A. Aaronson and G. D. Kruh (1995). "Expression of multidrug resistance-associated protein in NIH/3T3 cells confers multidrug resistance associated with increased drug efflux and altered intracellular drug distribution." <u>Cancer Res</u> **55**(22): 5342-5347.

Brocato, J., Y. Chervona and M. Costa (2014). "Molecular responses to hypoxia-inducible factor 1alpha and beyond." <u>Mol Pharmacol</u> **85**(5): 651-657.

Bruggemann, E. P., S. J. Currier, M. M. Gottesman and I. Pastan (1992). "Characterization of the azidopine and vinblastine binding site of P-glycoprotein." <u>J Biol Chem</u> **267**(29): 21020-21026.

Brunelle, J. K. and A. Letai (2009). "Control of mitochondrial apoptosis by the Bcl-2 family." <u>J Cell Sci</u> **122**(Pt 4): 437-441.

Bulinski, J. C., J. E. Richards and G. Piperno (1988). "Posttranslational modifications of alpha tubulin: detyrosination and acetylation differentiate populations of interphase microtubules in cultured cells." <u>J Cell Biol</u> **106**(4): 1213-1220.

Castedo, M., J. L. Perfettini, T. Roumier, K. Andreau, R. Medema and G. Kroemer (2004). "Cell death by mitotic catastrophe: a molecular definition." <u>Oncogene</u> **23**(16): 2825-2837.
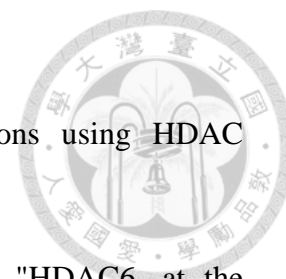
Chen, L., W. Fischle, E. Verdin and W. C. Greene (2001). "Duration of nuclear NF-kappaB action regulated by reversible acetylation." Science **293**(5535): 1653-1657.

Choi, J. H., H. J. Kwon, B. I. Yoon, J. H. Kim, S. U. Han, H. J. Joo and D. Y. Kim (2001). "Expression profile of histone deacetylase 1 in gastric cancer tissues." Jpn J Cancer Res **92**(12): 1300-1304.

Chou, T. C. (2006). "Theoretical basis, experimental design, and computerized simulation of synergism and antagonism in drug combination studies." Pharmacol Rev **58**(3): 621-681.

Crazzolara, R., A. Cisterne, M. Thien, J. Hewson, R. Baraz, K. F. Bradstock and L. J. Bendall (2009). "Potentiating effects of RAD001 (Everolimus) on vincristine therapy in childhood acute lymphoblastic leukemia." Blood **113**(14): 3297-3306.

Demidenko, Z. N. and M. V. Blagosklonny (2011). "The purpose of the HIF-1/PHD feedback loop: to limit mTOR-induced HIF-1alpha." Cell Cycle **10**(10): 1557-1562.

Dhillon, A. S., S. Hagan, O. Rath and W. Kolch (2007). "MAP kinase signalling pathways in cancer." Oncogene **26**(22): 3279-3290.

Dilling, M. B., G. S. Germain, L. Dudkin, A. L. Jayaraman, X. Zhang, F. C. Harwood and P. J. Houghton (2002). "4E-binding proteins, the suppressors of eukaryotic initiation factor 4E, are down-regulated in cells with acquired or intrinsic resistance to rapamycin." J Biol Chem **277**(16): 13907-13917.

Dowling, M., K. R. Voong, M. Kim, M. K. Keutmann, E. Harris and G. D. Kao (2005). "Mitotic spindle checkpoint inactivation by trichostatin a defines a mechanism for increasing cancer cell killing by microtubule-disrupting agents." Cancer Biol Ther **4**(2): 197-206.

Dubois, L., M. G. Magagnin, A. H. Cleven, S. A. Weppler, B. Grenacher, W. Landuyt, N. Lieuwes, P. Lambin, T. A. Gorr, M. Koritzinsky and B. G. Wouters (2009). "Inhibition of 4E-BP1 sensitizes U87 glioblastoma xenograft tumors to irradiation by decreasing hypoxia tolerance." Int J Radiat Oncol Biol Phys **73**(4): 1219-1227.

Ducker, G. S., C. E. Atreya, J. P. Simko, Y. K. Hom, M. R. Matli, C. H. Benes, B. Hann, E. K. Nakakura, E. K. Bergsland, D. B. Donner, J. Settleman, K. M. Shokat and R. S. Warren (2014). "Incomplete inhibition of phosphorylation of 4E-BP1 as a mechanism of primary resistance to ATP-competitive mTOR inhibitors." Oncogene **33**(12): 1590-1600.

Dumontet, C. and M. A. Jordan (2010). "Microtubule-binding agents: a dynamic field of cancer therapeutics." Nat Rev Drug Discov **9**(10): 790-803.

Easton, J. B. and P. J. Houghton (2006). "mTOR and cancer therapy." Oncogene **25**(48): 6436-6446.

Edwards, M. S., S. D. Chadda, Z. Zhao, B. L. Barber and D. P. Sykes (2012). "A systematic review of treatment guidelines for metastatic colorectal cancer." Colorectal Disease **14**(2): e31-e47.

Eichhorn, J. M., N. Sakurikar, S. E. Alford, R. Chu and T. C. Chambers (2013). "Critical role of anti-apoptotic Bcl-2 protein phosphorylation in mitotic death." Cell Death Dis **4**: e834.

Eot-Houllier, G., G. Fulcrand, L. Magnaghi-Jaulin and C. Jaulin (2009). "Histone deacetylase inhibitors and genomic instability." Cancer Lett **274**(2): 169-176.

Eot-Houllier, G., G. Fulcrand, Y. Watanabe, L. Magnaghi-Jaulin and C. Jaulin (2008). "Histone deacetylase 3 is required for centromeric H3K4 deacetylation and sister chromatid cohesion." Genes Dev **22**(19): 2639-2644.

Faivre, S., G. Kroemer and E. Raymond (2006). "Current development of mTOR inhibitors as anticancer agents." Nat Rev Drug Discov **5**(8): 671-688.

Fojo, A. T. and M. Menefee (2005). "Microtubule targeting agents: basic mechanisms of multidrug resistance (MDR)." Semin Oncol **32**(6 Suppl 7): S3-8.

Gascoigne, K. E. and S. S. Taylor (2008). "Cancer cells display profound intra- and interline variation following prolonged exposure to antimitotic drugs." Cancer Cell **14**(2): 111-122.

Gascoigne, K. E. and S. S. Taylor (2009). "How do anti-mitotic drugs kill cancer cells?" J Cell Sci **122**(Pt 15): 2579-2585.

George, M. L., M. G. Tutton, F. Janssen, A. Arnaout, A. M. Abulafi, S. A. Eccles and R. I. Swift (2001). "VEGF-A, VEGF-C, and VEGF-D in colorectal cancer progression." Neoplasia **3**(5): 420-427.

Halkidou, K., L. Gaughan, S. Cook, H. Y. Leung, D. E. Neal and C. N. Robson (2004). "Upregulation and nuclear recruitment of HDAC1 in hormone refractory prostate cancer." Prostate **59**(2): 177-189.

Harris, A. L. (2002). "Hypoxia--a key regulatory factor in tumour growth." Nat Rev Cancer **2**(1): 38-47.

Heinicke, U. and S. Fulda (2014). "Chemosensitization of rhabdomyosarcoma cells by the histone deacetylase inhibitor SAHA." Cancer Letters **351**(1): 50-58.

Holohan, C., S. Van Schaeybroeck, D. B. Longley and P. G. Johnston (2013). "Cancer drug resistance: an evolving paradigm." Nat Rev Cancer **13**(10): 714-726.

Hsu, H. S., M. H. Lin, Y. H. Jang, T. T. Kuo, C. C. Liu and T. H. Cheng (2015). "The 4E-BP1/eIF4E ratio is a determinant for rapamycin response in esophageal cancer cells." J Thorac Cardiovasc Surg **149**(1): 378-385.

Huang, L., Q. Ao, Q. Zhang, X. Yang, H. Xing, F. Li, G. Chen, J. Zhou, S. Wang, G. Xu, L. Meng, Y. Lu and D. Ma (2010). "Hypoxia induced paclitaxel resistance in human ovarian cancers via hypoxia-inducible factor 1alpha." J Cancer Res Clin Oncol **136**(3): 447-456.

Hubbert, C., A. Guardiola, R. Shao, Y. Kawaguchi, A. Ito, A. Nixon, M. Yoshida, X. F. Wang and T. P. Yao (2002). "HDAC6 is a microtubule-associated deacetylase." Nature **417**(6887): 455-458.

Huisman, M. T., A. A. Chhatta, O. van Tellingen, J. H. Beijnen and A. H. Schinkel (2005). "MRP2 (ABCC2) transports taxanes and confers paclitaxel resistance and both processes are stimulated by probenecid." Int J Cancer **116**(5): 824-829.

Inoki, K., M. N. Corradetti and K. L. Guan (2005). "Dysregulation of the TSC-mTOR pathway in human disease." <u>Nat Genet</u> **37**(1): 19-24.

Jordan, M. A., D. Thrower and L. Wilson (1992). "Effects of vinblastine, podophyllotoxin and nocodazole on mitotic spindles. Implications for the role of microtubule dynamics in mitosis." <u>J Cell Sci</u> **102 ( Pt 3)**: 401-416.

Kang, J. and H. Yu (2009). "Kinase signaling in the spindle checkpoint." <u>J Biol Chem</u> **284**(23): 15359-15363.

Kang, J. and H. Yu (2009). "Kinase Signaling in the Spindle Checkpoint." <u>Journal of Biological Chemistry</u> **284**(23): 15359-15363.

Karlsson, E., G. Perez-Tenorio, R. Amin, J. Bostner, L. Skoog, T. Fornander, D. C. Sgroi, B. Nordenskjold, A. L. Hallbeck and O. Stal (2013). "The mTOR effectors 4EBP1 and S6K2 are frequently coexpressed, and associated with a poor prognosis and endocrine resistance in breast cancer: a retrospective study including patients from the randomised Stockholm tamoxifen trials." <u>Breast Cancer Res</u> **15**(5): R96.

Keen, N. and S. Taylor (2009). "Mitotic drivers--inhibitors of the Aurora B Kinase." <u>Cancer Metastasis Rev</u> **28**(1-2): 185-195.

Kim, R., M. Emi and K. Tanabe (2006). "Role of mitochondria as the gardens of cell death." <u>Cancer Chemotherapy and Pharmacology</u> **57**(5): 545-553.

Kizaka-Kondoh, S., M. Inoue, H. Harada and M. Hiraoka (2003). "Tumor hypoxia: a target for selective cancer therapy." <u>Cancer Sci</u> **94**(12): 1021-1028.

Kramer, O. H., S. Mahboobi and A. Sellmer (2014). "Drugging the HDAC6-HSP90 interplay in malignant cells." <u>Trends Pharmacol Sci</u> **35**(10): 501-509.

Kremer, C. L., R. R. Klein, J. Mendelson, W. Browne, L. K. Samadzedeh, K. Vanpatten, L. Highstrom, G. A. Pestano and R. B. Nagle (2006). "Expression of mTOR signaling pathway markers in prostate cancer progression." <u>Prostate</u> **66**(11): 1203-1212.

Kufe, D. W. and J. F. Holland (2006). <u>Holland-Frei cancer medicine</u>. London, BC

Decker.
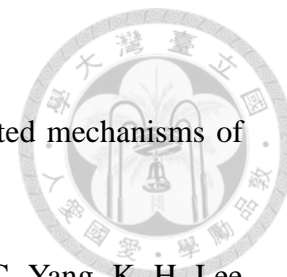
Kurmasheva, R. T., S. Huang and P. J. Houghton (2006). "Predicted mechanisms of resistance to mTOR inhibitors." Br J Cancer **95**(8): 955-960.

Lai, C. Y., S. L. Pan, X. M. Yang, L. H. Chang, Y. L. Chang, P. C. Yang, K. H. Lee and C. M. Teng (2013). "Depletion of 4E-BP1 and regulation of autophagy lead to YXM110-induced anticancer effects." Carcinogenesis **34**(9): 2050-2060.

Laird, P. W. (2005). "Cancer epigenetics." Hum Mol Genet **14 Spec No 1**: R65-76.

Lang, K. J., A. Kappel and G. J. Goodall (2002). "Hypoxia-inducible factor-1alpha mRNA contains an internal ribosome entry site that allows efficient translation during normoxia and hypoxia." Mol Biol Cell **13**(5): 1792-1801.

Leontieva, O. V., V. Natarajan, Z. N. Demidenko, L. G. Burdelya, A. V. Gudkov and M. V. Blagosklonny (2012). "Hypoxia suppresses conversion from proliferative arrest to cellular senescence." Proc Natl Acad Sci U S A **109**(33): 13314-13318.

Li, Y., G. D. Kao, B. A. Garcia, J. Shabanowitz, D. F. Hunt, J. Qin, C. Phelan and M. A. Lazar (2006). "A novel histone deacetylase pathway regulates mitosis by modulating Aurora B kinase activity." Genes Dev **20**(18): 2566-2579.

Lin, R. J., T. Sternsdorf, M. Tini and R. M. Evans (2001). "Transcriptional regulation in acute promyelocytic leukemia." Oncogene **20**(49): 7204-7215.

Loong, H. H. and W. Yeo (2014). "Microtubule-targeting agents in oncology and therapeutic potential in hepatocellular carcinoma." Onco Targets Ther **7**: 575-585.

Luo, J., F. Su, D. Chen, A. Shiloh and W. Gu (2000). "Deacetylation of p53 modulates its effect on cell growth and apoptosis." Nature **408**(6810): 377-381.

Martin, M. E., M. I. Perez, C. Redondo, M. I. Alvarez, M. Salinas and J. L. Fando (2000). "4E binding protein 1 expression is inversely correlated to the progression of gastrointestinal cancers." Int J Biochem Cell Biol **32**(6): 633-642.

Martineau, Y., R. Azar, C. Bousquet and S. Pyronnet (2013). "Anti-oncogenic

potential of the eIF4E-binding proteins." Oncogene **32**(6): 671-677.

Martinez-Balbas, M. A., U. M. Bauer, S. J. Nielsen, A. Brehm and T. Kouzarides (2000). "Regulation of E2F1 activity by acetylation." EMBO J **19**(4): 662-671.

Matson, D. R. and P. T. Stukenberg (2011). "Spindle poisons and cell fate: a tale of two pathways." Mol Interv **11**(2): 141-150.

Matsuyama, A., T. Shimazu, Y. Sumida, A. Saito, Y. Yoshimatsu, D. Seigneurin-Berny, H. Osada, Y. Komatsu, N. Nishino, S. Khochbin, S. Horinouchi and M. Yoshida (2002). "In vivo destabilization of dynamic microtubules by HDAC6-mediated deacetylation." EMBO J **21**(24): 6820-6831.

Mollinedo, F. and C. Gajate (2003). "Microtubules, microtubule-interfering agents and apoptosis." Apoptosis **8**(5): 413-450.

Morfoisse, F., A. Kuchnio, C. Frainay, A. Gomez-Brouchet, M. B. Delisle, S. Marzi, A. C. Helfer, F. Hantelys, F. Pujol, J. Guillermet-Guibert, C. Bousquet, M. Dewerchin, S. Pyronnet, A. C. Prats, P. Carmeliet and B. Garmy-Susini (2014). "Hypoxia induces VEGF-C expression in metastatic tumor cells via a HIF-1alpha-independent translation-mediated mechanism." Cell Rep **6**(1): 155-167.

Muller, A., C. Zang, C. Chumduri, B. Dorken, P. T. Daniel and C. W. Scholz (2013). "Concurrent inhibition of PI3K and mTORC1/mTORC2 overcomes resistance to rapamycin induced apoptosis by down-regulation of Mcl-1 in mantle cell lymphoma." Int J Cancer **133**(8): 1813-1824.

Nagata, K., A. Puls, C. Futter, P. Aspenstrom, E. Schaefer, T. Nakata, N. Hirokawa and A. Hall (1998). "The MAP kinase kinase kinase MLK2 co-localizes with activated JNK along microtubules and associates with kinesin superfamily motor KIF3." EMBO J **17**(1): 149-158.

Noh, E. J. and J. S. Lee (2003). "Functional interplay between modulation of histone deacetylase activity and its regulatory role in G2-M transition." Biochem Biophys Res Commun **310**(2): 267-273.

Nowak, S. J. and V. G. Corces (2004). "Phosphorylation of histone H3: a balancing

act between chromosome condensation and transcriptional activation." <u>Trends Genet</u> **20**(4): 214-220.

Park, S., N. Chapuis, J. Tamburini, V. Bardet, P. Cornillet-Lefebvre, L. Willems, A. Green, P. Mayeux, C. Lacombe and D. Bouscary (2010). <u>Role of the PI3K/AKT and mTOR signaling pathways in acute myeloid leukemia</u>.

Petroulakis, E., Y. Mamane, O. Le Bacquer, D. Shahbazian and N. Sonenberg (2006). "mTOR signaling: implications for cancer and anticancer therapy." <u>British Journal of Cancer</u> **94**(2): 195-199.

Pringels, S., N. Van Damme, B. De Craene, P. Pattyn, W. Ceelen, M. Peeters and J. Grooten (2012). "Clinical procedure for colon carcinoma tissue sampling directly affects the cancer marker-capacity of VEGF family members." <u>BMC Cancer</u> **12**: 515.

Ray, M. E., Z. Q. Yang, D. Albertson, C. G. Kleer, J. G. Washburn, J. A. Macoska and S. P. Ethier (2004). "Genomic and expression analysis of the 8p11-12 amplicon in human breast cancer cell lines." <u>Cancer Res</u> **64**(1): 40-47.

Richon, V. M., J. Garcia-Vargas and J. S. Hardwick (2009). "Development of vorinostat: current applications and future perspectives for cancer therapy." <u>Cancer Lett</u> **280**(2): 201-210.

Risinger, A. L., F. J. Giles and S. L. Mooberry (2009). "Microtubule dynamics as a target in oncology." <u>Cancer Treat Rev</u> **35**(3): 255-261.

Rojo, F., L. Najera, J. Lirola, J. Jimenez, M. Guzman, M. D. Sabadell, J. Baselga and S. Ramon y Cajal (2007). "4E-binding protein 1, a cell signaling hallmark in breast cancer that correlates with pathologic grade and prognosis." <u>Clin Cancer Res</u> **13**(1): 81-89.

Ruvolo, P. P., X. Deng and W. S. May (2001). "Phosphorylation of Bcl2 and regulation of apoptosis." <u>Leukemia</u> **15**(4): 515-522.

Sandor, V., A. Senderowicz, S. Mertins, D. Sackett, E. Sausville, M. V. Blagosklonny and S. E. Bates (2000). "P21-dependent g(1)arrest with downregulation of cyclin D1 and upregulation of cyclin E by the histone deacetylase inhibitor FR901228." <u>Br J</u>

Cancer **83**(6): 817-825.
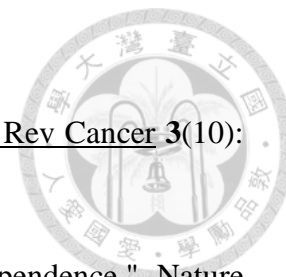
Semenza, G. L. (2003). "Targeting HIF-1 for cancer therapy." <u>Nat Rev Cancer</u> **3**(10): 721-732.

Seton-Rogers, S. (2008). "Translation - Switching to cap-independence." <u>Nature Reviews Cancer</u> **8**(1).

She, Q. B., E. Halilovic, Q. Ye, W. Zhen, S. Shirasawa, T. Sasazuki, D. B. Solit and N. Rosen (2010). "4E-BP1 is a key effector of the oncogenic activation of the AKT and ERK signaling pathways that integrates their function in tumors." <u>Cancer Cell</u> **18**(1): 39-51.

Sherr, C. J. and J. M. Roberts (1999). "CDK inhibitors: positive and negative regulators of G1-phase progression." <u>Genes Dev</u> **13**(12): 1501-1512.

Sherrill, K. W., M. P. Byrd, M. E. Van Eden and R. E. Lloyd (2004). "BCL-2 translation is mediated via internal ribosome entry during cell stress." <u>J Biol Chem</u> **279**(28): 29066-29074.

Shitashige, M., M. Toi, T. Yano, M. Shibata, Y. Matsuo and F. Shibasaki (2001). "Dissociation of Bax from a Bcl-2/Bax heterodimer triggered by phosphorylation of serine 70 of Bcl-2." <u>J Biochem</u> **130**(6): 741-748.

Shtil, A. A., S. Mandlekar, R. Yu, R. J. Walter, K. Hagen, T. H. Tan, I. B. Roninson and A. N. Kong (1999). "Differential regulation of mitogen-activated protein kinases by microtubule-binding agents in human breast cancer cells." <u>Oncogene</u> **18**(2): 377-384.

Siegel, R. L., K. D. Miller and A. Jemal (2015). "Cancer statistics, 2015." <u>CA: A Cancer Journal for Clinicians</u> **65**(1): 5-29.

Silvera, D., S. C. Formenti and R. J. Schneider (2010). "Translational control in cancer." <u>Nat Rev Cancer</u> **10**(4): 254-266.

Simms-Waldrip, T., A. Rodriguez-Gonzalez, T. Lin, A. K. Ikeda, C. Fu and K. M. Sakamoto (2008). "The aggresome pathway as a target for therapy in hematologic

malignancies." Mol Genet Metab **94**(3): 283-286.

Soubrane, C., R. Mouawad, V. Sultan, J. Spano, D. Khayat and O. Rixe (2006). "Soluble VEGF-A and lymphangiogenesis in metastatic malignant melanoma patients." J Clin Oncol (Meeting Abstracts) **24**(18_suppl): 8049-.
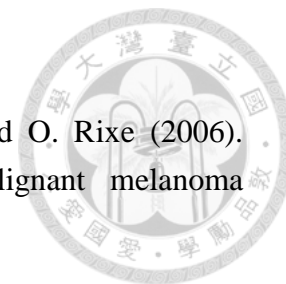
Stone, A. A. and T. C. Chambers (2000). "Microtubule inhibitors elicit differential effects on MAP kinase (JNK, ERK, and p38) signaling pathways in human KB-3 carcinoma cells." Exp Cell Res **254**(1): 110-119.

Sullivan, R., G. C. Pare, L. J. Frederiksen, G. L. Semenza and C. H. Graham (2008). "Hypoxia-induced resistance to anticancer drugs is associated with decreased senescence and requires hypoxia-inducible factor-1 activity." Mol Cancer Ther **7**(7): 1961-1973.

Tasian, S. K., D. T. Teachey and S. R. Rheingold (2014). "Targeting the PI3K/mTOR Pathway in Pediatric Hematologic Malignancies." Front Oncol **4**: 108.

Teachey, D. T., S. A. Grupp and V. I. Brown (2009). "mTOR Inhibitors and Their Potential Role in Therapy in Leukemia and Other Haematologic Malignancies." British journal of haematology **145**(5): 569-580.

Vu, C. and D. A. Fruman (2010). "Target of Rapamycin Signaling in Leukemia and Lymphoma." Clinical Cancer Research **16**(22): 5374-5380.

Vu, C. and D. A. Fruman (2010). "Target of rapamycin signaling in leukemia and lymphoma." Clin Cancer Res **16**(22): 5374-5380.

Wada, T. and J. M. Penninger (0000). "Mitogen-activated protein kinases in apoptosis regulation." Oncogene **23**(16): 2838-2849.

Walther, A., E. Johnstone, C. Swanton, R. Midgley, I. Tomlinson and D. Kerr (2009). "Genetic prognostic and predictive markers in colorectal cancer." Nat Rev Cancer **9**(7): 489-499.

Wang, J., Q. Ye and Q. B. She (2014). "New insights into 4E-BP1-regulated translation in cancer progression and metastasis." Cancer Cell Microenviron **1**(5).

Wang, T. H., D. M. Popp, H. S. Wang, M. Saitoh, J. G. Mural, D. C. Henley, H. Ichijo and J. Wimalasena (1999). "Microtubule dysfunction induced by paclitaxel initiates apoptosis through both c-Jun N-terminal kinase (JNK)-dependent and -independent pathways in ovarian cancer cells." J Biol Chem **274**(12): 8208-8216.

Wang, T. H., H. S. Wang, H. Ichijo, P. Giannakakou, J. S. Foster, T. Fojo and J. Wimalasena (1998). "Microtubule-interfering agents activate c-Jun N-terminal kinase/stress-activated protein kinase through both Ras and apoptosis signal-regulating kinase pathways." J Biol Chem **273**(9): 4928-4936.

Weaver, B. A. and D. W. Cleveland (2005). "Decoding the links between mitosis, cancer, and chemotherapy: The mitotic checkpoint, adaptation, and cell death." Cancer Cell **8**(1): 7-12.

Wertz, I. E., S. Kusam, C. Lam, T. Okamoto, W. Sandoval, D. J. Anderson, E. Helgason, J. A. Ernst, M. Eby, J. Liu, L. D. Belmont, J. S. Kaminker, K. M. O'Rourke, K. Pujara, P. B. Kohli, A. R. Johnson, M. L. Chiu, J. R. Lill, P. K. Jackson, W. J. Fairbrother, S. Seshagiri, M. J. Ludlam, K. G. Leong, E. C. Dueber, H. Maecker, D. C. Huang and V. M. Dixit (2011). "Sensitivity to antitubulin chemotherapeutics is regulated by MCL1 and FBW7." Nature **471**(7336): 110-114.

West, A. C. and R. W. Johnstone (2014). "New and emerging HDAC inhibitors for cancer treatment." J Clin Invest **124**(1): 30-39.

Wilson, A. J., D. S. Byun, N. Popova, L. B. Murray, K. L'Italien, Y. Sowa, D. Arango, A. Velcich, L. H. Augenlicht and J. M. Mariadason (2006). "Histone deacetylase 3 (HDAC3) and other class I HDACs regulate colon cell maturation and p21 expression and are deregulated in human colon cancer." J Biol Chem **281**(19): 13548-13558.

Witzig, T. E., S. M. Geyer, I. Ghobrial, D. J. Inwards, R. Fonseca, P. Kurtin, S. M. Ansell, R. Luyun, P. J. Flynn, R. F. Morton, S. R. Dakhil, H. Gross and S. H. Kaufmann (2005). "Phase II trial of single-agent temsirolimus (CCI-779) for relapsed mantle cell lymphoma." J Clin Oncol **23**(23): 5347-5356.

Xu, W. S., G. Perez, L. Ngo, C. Y. Gui and P. A. Marks (2005). "Induction of polyploidy by histone deacetylase inhibitor: a pathway for antitumor effects." Cancer

Res **65**(17): 7832-7839.

Yamamoto, K., H. Ichijo and S. J. Korsmeyer (1999). "BCL-2 Is Phosphorylated and Inactivated by an ASK1/Jun N-Terminal Protein Kinase Pathway Normally Activated at G(2)/M." Molecular and Cellular Biology **19**(12): 8469-8478.
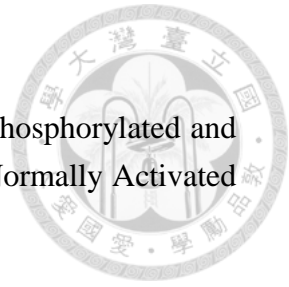
Zhang, Y., N. Li, C. Caron, G. Matthias, D. Hess, S. Khochbin and P. Matthias (2003). "HDAC-6 interacts with and deacetylates tubulin and microtubules in vivo." EMBO J **22**(5): 1168-1179.

Zhang, Y. and X. F. Zheng (2012). "mTOR-independent 4E-BP1 phosphorylation is associated with cancer resistance to mTOR kinase inhibitors." Cell Cycle **11**(3): 594-603.

Zhang, Z., H. Yamashita, T. Toyama, H. Sugiura, Y. Omoto, Y. Ando, K. Mita, M. Hamaguchi, S. Hayashi and H. Iwase (2004). "HDAC6 expression is correlated with better survival in breast cancer." Clin Cancer Res **10**(20): 6962-6968.

Zhu, P., E. Martin, J. Mengwasser, P. Schlag, K. P. Janssen and M. Gottlicher (2004). "Induction of HDAC2 expression upon loss of APC in colorectal tumorigenesis." Cancer Cell **5**(5): 455-463.

Ziello, J. E., I. S. Jovin and Y. Huang (2007). "Hypoxia-Inducible Factor (HIF)-1 regulatory pathway and its potential for therapeutic intervention in malignancy and ischemia." Yale J Biol Med **80**(2): 51-60.